Validation of an Internal Measurement Unit to Measure Knee Kinematics and ACL Fatigue in Cadaveric Specimens During Simulated One-Legged Landing

by

Mirel Ajdaroski

A thesis submitted in partial fulfillment
of the requirements for the degree of
Master of Science in Engineering
(Bioengineering)
in the University of Michigan-Dearborn
2020

Master's Thesis Committee:

Assistant Professor Amanda Esquivel, Chair
Professor Alan Argento
Assistant Professor Samir Rawashdeh

Acknowledgements

There are several people I would wish to acknowledge for helping me complete this work. First and foremost, I would like to thank my advisor Dr. Amanda Esquivel, Ph.D., Assistant professor, Department of Mechanical Engineering at the University of Michigan-Dearborn who gave me invaluable guidance throughout both my undergraduate and graduate pursuits. She allowed me to freely work on this paper but gave important suggestions and support whenever I needed. Without her guidance and support, it would've been impossible to complete this study.

Additionally, I would like to sincerely thank the Ann Arbor team for allowing us to participate in their ongoing study. Dr. James Ashton-Miller, Dr. Mélanie L. Beaulieu and doctoral student So Young Baek. Their interest in our study and their kind and welcoming attitudes made working together one of the most enjoyable experiences of my life. I look forward to working together with them in future studies.

I would also like to thank my thesis committee: Dr. Alan Argento, Ph.D., Professor, Department of Mechanical Engineering, Director of Bioengineering Program and Dr. Samir Rawashdeh, Ph.D., Assistant Professor, Department of Electrical and Computer Engineering for their comments and suggestions during the defense of this thesis. Their words allowed for the refinement of my paper.

And last by not least, I would like to thank all my lab mates and friends. Grant Baker, Lorraine "Ronnie" Nichols and Nada Saghir. Their willingness to read sections of this paper and give suggestions were invaluable. Their supportive, motivational and friendly words throughout working on this study helped immensely.

Table of Contents

List of Figures

List of Tables

List of Abbreviations

$^{\circ}/s$: Degrees Per Second

.h5 : hierarchical data format

Abs % Error : Absolute Percent Error

ACL : Anterior Cruciate Ligament

ALB : Anterolateral Bundle

AMB : Anteromedial Bundle

aTT : Anterior Tibial Translations

BA Plot : Bland-Altman Plot

BH : Body Height

BW : Body Weight

COD : Change of Direction

cm : centimeter

dMCL : Deep Medial Collateral Ligament

EMG : Electromyography

FATC : Femur-ACL-Tibia Complex

g : gravitational force

Hz : Hertz

IMU : Internal Measurement Unit

lb : Avoirdupois Pound

LCL : Lateral Collateral Ligament

LoA : Limits of Agreement

$\frac{m}{s^2}$: Meters Per Second

MCL : Medial Collateral Ligament

mm : millimeter

ms : millisecond

N : Newton

Nmm : Newton-millimeters

PCL : Posterior Cruciate Ligament

PLB : Posterolateral Bundle

PMB : Posteromedial Bundle

Q Angle : Quadriceps Angle

QL : Quadriceps Loading

R : Correlation Coefficient

R^2 : coefficient of determination

$\frac{rad}{s}$: Radians Per Second

RMSD : Root Mean Square Deviation

RMSE : Root Mean Square Error

sMCL : Superficial Medial Collateral Ligament

Std : Standard Deviation

SS : Standing Start

yrs :years old

Abstract

Participation in sports has been on the rise in the last few years, and while regular activity in sports has many benefits, there is always an associated risk of injury. Sport related injury can happen in any part of an athlete's body, however the most common of these injuries occur in the lower limbs with of the most devastating injuries being damage to a ligament. Among ligament damage, a rupture in the Anterior Cruciate Ligament is most common. While there are several different mechanisms for Anterior Cruciate Ligament tears, fatigue induced non-contact injuries are the most trackable. The purpose of this research was to correlate the data obtained through a commercially available IMU to that obtained through cadaveric testing to determine whether the selected IMU is valid for field testing and tracking potential fatigue levels of the ACL. Using 10 cadaveric specimens, regression models were developed and RMSE and abs % error values were calculated in addition to BA plots being constructed between aspects of both systems. Very strong correlations were observed between linear acceleration and force, with strong correlations in nearly all others compared aspects. Additionally, nearly all constructed models produced an abs % error of less than 10%. And while we recognize there to be several limitations with our study, we ultimately conclude that APDM Opal might be viable for on-field usage. However, additional laboratory studies to account for different actions and artifact motion that may be experienced by the IMU may be required before on-field usage begins.

Chapter 1: Introduction

1.1. Background

In the United States, the average participation rate in sports has risen in the last few years, from just under 16% in 2003 to nearly 20% in 2015.[1] While participation in sports can be beneficial for those who regularly engage in them, there is always an associated risk of injury. Nearly 30 million people are injured every year while participating in some sport.[2] And while a sports related injury can happen in any part of an athlete's body, the most common of these injuries occur in the lower limbs. Injuries to the lower limbs can entail such things as ankle sprains, stress fractures, etc., but of these injuries, one of the most devastating is damage to a ligament. A rupture in the Anterior Cruciate Ligament (ACL) is the most common ligament tear of the lower limbs, with some 100,000 to 200,000 ACL ruptures reported every year in the United States alone.[3,4]

There are two mechanisms for ACL injury. The first are contact in nature and occur as the result of direct impact with another player/equipment and primarily originate from a singular event. Unfortunately, contact injuries are unpredictable in nature and the only means to help prevent these types of injuries from occurring is to either introduce new rules or new protective equipment. The second category are non-contact ACL injuries. Non-contact ACL injuries can either be a single event (acute) or the result of repetitive, high stress/strain inducing activities (fatigue). Studies have shown the correlation between fatigue of the ligament and increasing risk of injury.[5] Nearly 75% of all reported ACL injuries are the result of noncontact, either acute or fatigue in nature.[6,7]

But unlike contact injuries, some noncontact injuries- particularly those induced by ligament fatigue- may be prevented without changes to a game by allowing "at risk" players time to rest and recover. The only thing needed is a means through which this fatigue could be tracked. If there were a device that could accurately monitor the kinematics of the knee during games/practices, correlate it to potential ACL fatigue levels and relay that information, then coaches, trainers and players would know when rest is needed.

Traditionally, monitoring knee kinematics has been performed under laboratory settings using camera-based motion capture systems. However, this method cannot be used to track movements in the field. In recent years, wearable sensors have emerged as an alternative to monitoring knee kinematics as they can be used outside the laboratory. Internal measurement units (IMUs), a particular type of wearable technology, are small devices designed to track the kinematics of the body segment they are fixed to, providing linear accelerations and angular velocities, while also not encumbering a subject's range of motion. Various studies have looked into the correlations between such aspects as linear acceleration and force and between angular velocity and moment, finding low to strong associations.[8-11] Additionally, the relationship between force and moment to ACL stress/strain has been study in-depth.[5,12] This implies that IMUs may be able to track ACL fatigue levels through linear acceleration and angular velocity.

Therefore, the purpose of this research was to correlate the data obtained through a commercially available IMU to that obtained through cadaveric testing to determine whether the selected IMU is valid for tracking potential fatigue levels of the ACL and implementation into field testing. By attaching IMUs to the tibial and femoral portions of the knee, kinematic data regarding those sections were obtained. Taking various aspects of the IMU readings, we can correlate them to those obtained through cadaveric testing that have been observed to potentially cause fatigue induced ACL failures.[5] Based on those results, the validity of the sensor was commented upon. But before delving into the methodology of the experiments and results obtained, it is important to have a brief overview of the knee structure, ligaments of the knee (specifically the ACL), as well as a brief overview of IMUs.

1.2. The Knee

The knee is a complex structure, comprised of three bones (femur, patella, and tibia), two distinct joints (tibiofemoral joint and the patellofemoral joint), and whose primary functions are to support the upper body and aid in motion. But this complexity brings with it an inherent instability. Unlike other joints in the human body, the knee joint does not have a bony stability adding structure; such as the acetabulum that is present within the hip joint or the mortise socket formed by the tibia and fibula that is observed in the ankle. With this lack of a stability structure, the knee bones, by themselves, would be insecure and collapse under the needs placed on it by

the body. To compensate for this lack of stability, the knee joint incorporates the use of many ligaments that greatly increase its stability and functionality.

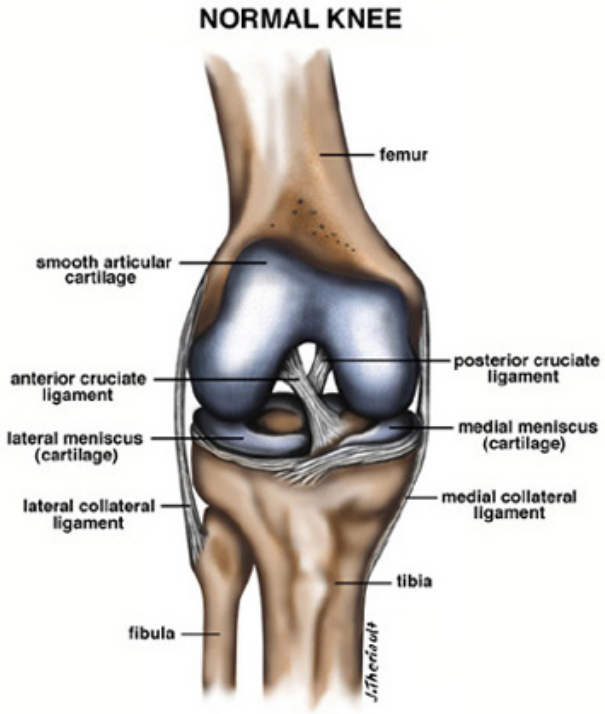

Figure 1 | Normal Knee Joint [13]

In biology, a ligament is defined as dense bands of collagenous fibers, whose function is to connect one bone with another.[14] In addition to connecting one bone to another, ligaments also serve to purpose of restricting the type of motion that may be experienced by a joint, stabilize a joint from external/internal forces, and, due to the presence of mechanoreceptors, aid joint proprioception.[14] Ligaments are not unique to the knee, as they are found throughout the body in all joints, though the shapes and sizes vary greatly depending on function and location as does the method of attachments.[14,15] The point at which a ligament is anchored upon a bone is known as the sight of insertion, the point of insertion, or the enthesis and usually involves unique, or misshaped landmarks on the bones.[16] In terms of biochemical composition of a typical ligament, nearly two-thirds is composed of water with the rest made up of organic solids; this high abundance of water in a ligament's composition contributes to its viscoelastic behavior.[17]

1.2.1. Viscoelasticity and Ligaments

Viscoelasticity is a combination of both elastic and viscous properties, and is caused by the high water content of tissue in addition to its structure.[17,18] Substances with a viscoelastic behavior will exhibit traits associated with elastic and viscous materials when undergoing deformation, such as slow deformation when exposed to a load (viscous) or returning to its original state after removal of the load (elastic). [17,18] Also, because of the exhibition of differing properties, viscoelastic substances are dependent on the rate of mechanical strain rather than load or stress. The viscoelastic behavior of ligaments also results in atypical mechanical properties such as: hysteresis; stress relaxation; creep.[19]

Energy dissipation, or hysteresis, is an observable mechanical property of both ligaments and tendons. During a loading-unloading cycle, it can be observed that stress-strain curve generated during loading differs greatly from that generated during unloading.[19] The difference between these two curves is the energy that is dissipated during the loading-unloading cycle, or the hysteresis of the system.[19] When the ligament/tendon is exposed to another loading-unloading cycle, the hysteresis curve differs, and this differing continues upon multiple cycles until several cycles in, at which point the stress-strain curve begins to stabilize and thereby becomes much more reproducible.[19] This changing of the stress-strain curve in response to multiple loading cycles is representative of the pseudo-elasticity behavior of ligaments/tendons and is an indicator of the nonlinearity that is typical of the tissue's stress-strain relationship.[19,20] Ligaments also exhibit creep, which is an increasing of deformation when subject to a constant load; this property is actually in direct contrast to elastic materials, which, when subject to a constant load, do not experience any continued deformation.[19] Stress relaxation is that ability of a ligament/tendon to experience a reduction in stress when subject to a constant deformation.

Another interesting aspect of ligaments/tendons is the stress-strain curve. Within this stress-strain curve, three distinct regions can be observed: the toe region; the linear region; the yield/failure region.[19] The first region, the toe region, represents the ligament/tendon when the collagenous fibers are crimped.[21] *Crimp,* when referring to the collagen fibrils, is the naturally occurring slack within the tissue when in a relaxed state; this slack takes up a portion of the stress when applied to the tissue.[21] This ability to withstand some of the applied stress results in these fibers straightening, the processes of which is referred to as *uncrimping*. This process of

uncrimping the fibers allows for approximately 2% deformation in the ligament/tendon with no change to tissue's structure.[19,21] Beyond this 2% deformation, the ligament/tendon enters the linear region. Within this region, the now uncrimped collagen fibers begin to stretch. If this deformation is less than 4%, the ligament/tendon will exhibit a linear behavior and return to its original state when unloaded.[21] If on the other hand, the deformation exceeds this 4% linear limit, the tissue begins to experience microscopic failures as the cross-links between the collagenous fibers begin to fail.[21] These microscopic tears persist from 4% until approximately 8% deformation.[19,21] Past 8% deformation, failures in the tissue become much more macroscopic in scale, until ultimate failure is reached, at which point a rupture of the ligament/tendon occurs.[19,21]

In addition to the viscoelastic properties of a typical tendon/ligament, a low vascularity has also been noted, though a much more vascular outer layer has been observed on many (though not all) ligaments; this outer, vascular layer that may be present on ligaments is termed the *epiligament*.[22] It is this low level of vascularity which inhibits a ligaments ability to heal naturally, and why injury to a ligament can be so devastating.[19,21]

1.2.2. Ligaments of the Knee

The motion required of the knee, in conjunction with its construct, opens the joint to being inherently unstable. To compensate for this instability, four major ligaments are present within the knee, adding stability and ensuring natural movement. They are the medial collateral ligament, lateral collateral ligament, posterior cruciate ligament and anterior cruciate ligament.

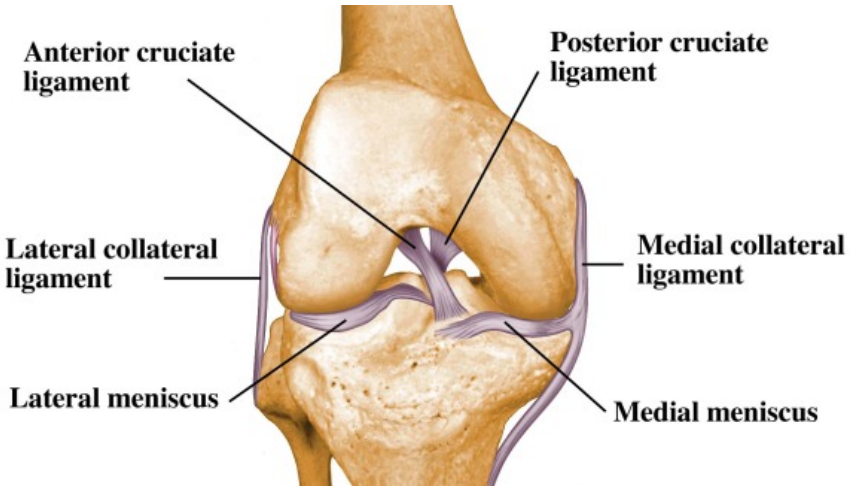

Figure 2 | Ligaments of the knee [23]

The medial collateral ligament (MCL) is found on the medial aspect of the knee and is the largest structure on the medial side.[24] The MCL is subdivided into 2 parts: a superficial medial collateral ligament (sMCL) and a deep medial collateral ligament (dMCL).[24] The sMCL is also referred to as the tibiofemoral ligament as it is the ligament of the tibiofemoral joint.[24] The sMCL has two tibial insertions and an origin located on the femur.[24] The femoral origin of the sMCL is located on the femoral medial epicondyle while the proximal tibial insertion fuses with the semimembranosus tendon.[24] The distal tibial insertion of the sMCL attaches to the posteromedial crest of the tibia.[24] The dMCL has also been referred to as the mid-third capsular ligament.[25] The dMCL is further divided into two parts: the meniscofemoral dMCL and the meniscotibial dMCL.[25] The origin for the meniscofemoral dMCL is slightly distal from the origin site of the sMCL and inserts into the medial menisci.[25] The thicker, shorter meniscotibial dMCL has its insertion on the distal aspect of the articular cartilage atop the tibial plateau and its origins on the medial meniscus.[24,25] The main function attributed to the entire MCL structure is to act as a static stabilizer of the knee; assisting in passive stabilization of the joint.[26] In addition, the MCL limits the hyperextension and anterior movement of the tibia.[26] Proprioceptors are also found within the MCL; when extended to a certain limit or when exposed to an excessive load, feedback within the ligament causes muscles to contract and reduce stress on the MCL.[14] The sMCL is responsible in resisting valgus loads across all flexion degrees of the knee with the dMCL aiding as a secondary source of resistance.[26] A more in-depth study discovered that the source of valgus stabilization within the MCL to be the proximal aspect of

the sMCL.[27] The dMCL has been attributed to aiding in rotational stability in extension to slight flexion.[28]

The lateral collateral ligament (LCL), also referred to as the fibular collateral ligament, is found on the lateral aspect of the knee; when comparing to the MCL, the LCL is narrower and stretches obliquely posteriorly.[29] The origin of the LCL is the lateral epicondyle of the femur and has its insertion located on the fibula.[29] The primary purpose of the LCL is to stabilize the knee joint's lateral side; more specifically, to resist varus angles the knee may be subjected to.[29] In addition, the LCL also serves as a primary resistor of posterolateral rotation of the tibia with respect to the femur.[29] It has been observed that the LCL acts as a secondary source of stabilization to anterior and posterior tibial translation; this secondary function is more evident when the cruciate ligaments are damaged or torn.[29]

The posterior cruciate ligament (PCL) is an extra synovial but intracapsular ligament; when compared to the ACL, the PCL is thicker, thus making the PCL more robust and less prone to injury.[30] The purpose of the PCL is to prevent posterior displacement of the tibia with respect to the femur; in addition, it also serves as a limiter to prevent hyper-extension, excessive internal rotation, and excessive valgus/varus within the knee.[30] The PCL has its origins at the anterolateral aspect of the medial femoral condyle within the intercondylar notch and has its insertion on the posterior aspect of the intercondylar fossa of the tibia.[31,32] Of note is that this ligament crosses over the ACL forming a distinct cross shape between the two. The PCL is considered a two-bundle system, being comprised of the anterolateral bundle (ALB) and the posteromedial bundle (PMB).[33] The ALB constitutes approximately 65% of the total PCL and is functionally important during flexion in where the ALB is tight while the PMB is left lax.[33] In opposition, the PMB is tight during extension, thus its functional importance during extension.[33] Of note is that in a PCL reconstruction, more importance is placed on the ALB because of both the larger associated size and the functional importance of the bundle.[33]

While the MCL, LCL, and PCL are all major ligaments of the knee, special consideration was given the ACL since this ligament is the most common knee ligament to be injured in sports.

1.2.3. The Anterior Cruciate Ligament

The ACL is a two bundle extra synovial, intracapsular ligament whose primary function is to resist anterolateral displacement between the tibia and the femur.[34] It is also one of most commonly injured ligament in sports and because of its microvascular nature, surgery is needed to repair ACL injuries.[34-36] Thus, in order to prevent ACL injuries, it becomes crucial to understand its anatomy.

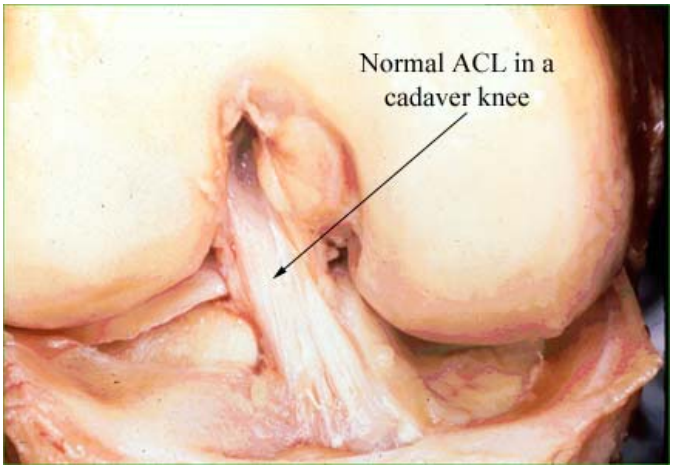

Figure 3 | Normal ACL as observed in a cadaveric specimen [37]

The ACL has its origins on the posteromedial aspect of a fossa on the lateral femoral condyle within the intercondylar notch.[38,39] The shape of this origin is semi-circular, with its anterior border straighter than the pronouncedly more curved posterior aspect.[38] The origin is fibrocartilage in nature, having four distinct zones that can easily be observed.[38] From this femoral origin, a typical ACL runs anteromedially and distally toward the tibia.[38,40] The average length of this ligament is 32mm with a width range of between 7 and 12mm.[40] At the origin site, the cross-sectional area of a typical ACL is approximately 34 mm^2.[41] The insertion of the ACL is the anterolateral aspect of the intercondylar fossa of the tibia.[41] At the site of insertion, the ACL passes underneath the transverse (anterior) mensicomeniscal ligament (a ligament that attaches the anterior horn of the lateral meniscus to the anterior horn of the medial meniscus); in some cases, the posterior fascicles of the ACL at the tibial site of attachment may mix with the posterior attachment of the lateral meniscus and become indistinguishable.[38] Like the enthesis of the origin site, the enthesis of the insertion site is also fibrocartilage in nature.[38,40] In terms of size and strength, it has been observed that the tibial site of insertion is

larger and stronger than the femoral origin site with the cross-sectional area at the site of insertion for an average ACL being approximately 42 mm^2.[41]

While the widely accepted functional model of the ACL depicts the ligament as a two-bundle system, others challenge this claim. Some studies illustrate the ACL as being a single bundle system with segments of the bundle pulled in differing direction during motion.[42] However, the widely accepted functional model of the ACL divides the ligament into two differing bundles: the anteromedial bundle (AMB) and the posterolateral bundle (PLB).[38,43] The third fascicular anatomy categorization divides the ACL into three separate portions: the AMB, the PLB, and between the two an intermediate band.[44] It should be noted that while the two-bundle system is accepted to be the best depiction of the function of the ACL, studies using MRI and 3D computer visualization observed a three-bundle system in the majority of observed cases (92%) while a clear two-bundle system was much less common.[45] Even though a three-bundle system may be more common, we will consider the ACL as a two-bundle system comprised of solely the AMB and PLB.

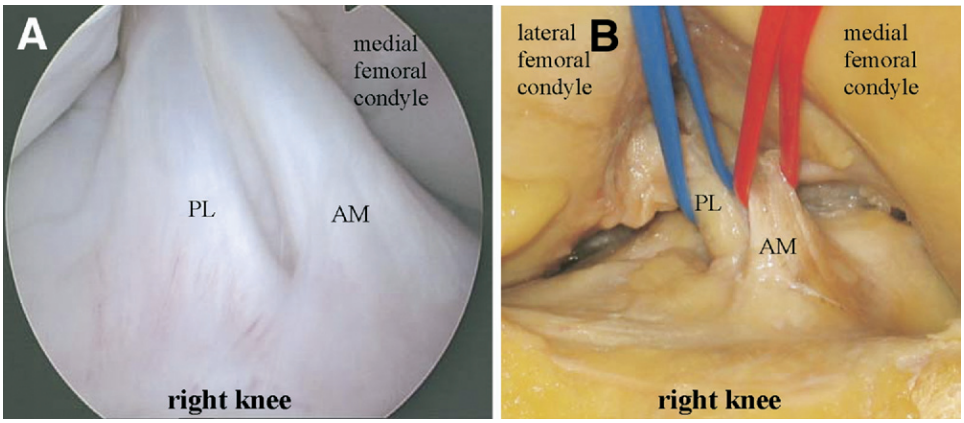

Figure 4 | AMB and PLB of an ACL [46]

The AMB is comprised of the fascicles whose origin is the proximal side of the origin of the ACL and whose insertion is the anteromedial aspect of the tibial insertion of the ligament.[44] The PLB is comprised by the fascicles whose origin is the distal aspect of the femoral origin of the ACL and whose insertion is the posterolateral aspect of the tibial insertion of the ligament.[44] Under laxed conditions, the AMB exhibits a more vertical orientation than the PLB (approximately 70° from the tibial head compared to 55°).[12] During extension more stress is placed on the PLB leaving the AMB more relaxed.[12] As the knee flexes the ACL begins to become parallel to the superior portion of the tibial head.[12] When experiencing a rotation, the

ACL tends to exhibit a greater degree of lengthening under internal rotation then during external rotation; this discrepancy between internal/external rotations is more prominent in a flexed knee.[12] While the primary function of the ACL is to resist the anteroposterior movement of the tibia with respect to the femur, it also exhibits the secondary function of resisting varus and valgus angles while the knee is under full extension; though this secondary function only plays a minor role in the knee's overall resistance to such angle types during full knee extension.[47]

While the two-bundle system used in this study is the easiest method in depicting the functional dynamics of the ACL throughout the knee's range of motion, it fails to illustrate one key point of clinical significance: because the ACL is comprised of differing fascicles, various portions of the ACL are stretched in differing directions throughout the knee's range of motion.[48] So, while the two-bundle system allows for the simplification that during flexion the AMB is functionally important and during extension the PLB is functionally important, the reality is that any position the knee assumes will exhibit some tension on portions of both the AMB and PLB.

There has been observed anatomical differences between the AMB and PLB.[38,42] In the anterior part of the AMB, the chondrocytes have been observed to be elongated rather than their typical circular morphology.[38,42] It has been thought that the appearance of the chondrocytes in this area is a functional adaptation, in response to the fact that, during extension, the AMB is in direct contact to the intercondylar fossa of the femur, which results in an impingement of the ACL and thus additional compressive stress, the elongation of these chondrocytes may aid in lessening the effect of this pinching.[38,42]

It has also been reported that both the structural and mechanical properties of the ACL are related to the age of the subject; as the age of the subject increases, the limits of the mechanical properties decrease.[49] The most important properties associated with the ACL and the femur-ACL-tibia complex (FATC) are linear stiffness, ultimate load, ultimate deformation, and the energy the system has absorbed at the point of failure.[50] The linear stiffness is defined as a material's ability to resist deformation when subjected to a load and can be observed as the linear region in the stress-strain curve. During a study conducted by Woo et al. on ACL specimens (22-35 years in age), the observed mean stiffness was 242 (± 28) N/mm.[49] Ultimate load is defined as the maximum possible load a material can withstand before failure occurs. Woo et al. noted that the mean ultimate load for the ACL specimens to be 2160 (± 157) N.[49]

Ultimate deformation is defined at the maximum possible deformation, in this case elongation, the material can withstand before failure occurs. It is much more difficult to determine the ultimate deformation that an average ACL can withstand primarily because of the range of possible ACL sizes. As such, Woo et al. used the percentage of strain that is experienced by the specimen before failure occurs; within their study, they found that the mean percent of strain at the point of failure was approximately 9%.[49] Energy absorbed by the ligament is defined as the area beneath the stress-strain curve before the point of failure. Woo et al found that the mean absorbed energy at failure for the specimens to be 11.6 (± 1.7) Nm.[49] Again, it should be noted that because both the structural and mechanical properties of the ligament is dependent upon the age of a subject, older subjects on average will have lower values for these important properties than younger subjects. Studies have also noted the effect that muscle activity can have on the strains and forces the ACL is subjected to. It has been observed that forces generated by the quadriceps can induce an increasing in the amount of anterior tibial translation experienced by the knee; this in turn causes an increasing in the amount of stress that is induced within the ACL.[49]

1.2.4. Mechanism of ACL Injury

Various studies have looked into the possible mechanisms that can cause an ACL injury, and have determined that all ACL injuries seem to fall into one of three distinct categories: direct contact (roughly 30% of cases); indirect contact (accounting for <1% of cases); non-contact (nearly 70% of all cases).[51-54] Direct contact injuries involve a transfer of force onto the knee from an external source, causing abnormal movements to occur or abnormally large anteroposterior movements to transpire.[51,52] In trying to prevent this movement, the ACL experiences a significant strain to the point of failure; this type of failure is typically acute in nature, occurring suddenly.[51,52] While unfortunate, direct contact is typically the result of gameplay with no means of prevention save for the addition of rules to limit such contact. Luckily direct contact is not the most prevalent type of injury, instead, non-contact injuries are drastically more common. Acute non-contact injuries follow a similar pattern but involve no external load. This also makes acute non-contact injuries difficult to prevent.

Figure 5 | Contact (Right) and non-contact (Left) ACL injuries. As explained, non-contact ACL injuries are not caused by an external force. Additionally, non-contact may be acute, or fatigue induced. [55,56]

During potential fatigue induced non-contact injuries, forces generated from an athlete's body while preforming a desired action leads to strain developing within the ligament, and studies have suggested that this may result in micro-tears, and continued performance of such action may lead to the propagation of these tears, which ultimately leads to failure.[5]

Cutting movements have been associated with these type of injuries, due to the sudden change in either, or both, the speed and direction, but rapid deceleration movements can also contribute to non-contact injuries; such movements include jumping, pivoting, and twisting.[51,52,57] While both sexes are susceptible to suffering from an ACL injury, women, on average, are 3 times more likely to be affected.[51,52] While the exact reasoning for why women are more prone to ACL injuries is still under contention, a plethora of possible explanations have been presented. One possible explanation is the smaller, slightly narrower shape of the intercondylar notch of the femur within females.[58-61] Geng et al conducted a study showing this to be a potential risk factor in female non-athletes, who were suffering from osteoarthritis; though, due to the age and predisposed condition of the subjects, this explanation may not apply to healthy female athletes.[58] A secondary explanation revolves around the wider pelvis present in females compared to males. This added width results in a greater quadriceps angle (Q angle), forcing the female femur into a greater angle towards the knee and thereby resulting in a lessening of muscular support of the knee.[59,62,63] It is also possible that due to hormonal differences present between males and females, the laxity of the ligament may differ which may lead to females being naturally more predisposed to ACL injuries.[59,64] In addition to this, there are potential external risk factors that may contribute to increasing the likelihood of injury occurring in both sexes.

While not completely understood, Olsen et al and others reported a higher risk of ACL injury occurring during games than during practices.[65,66] It is possible that athletes may perform an action more intensely during a game, resulting in a greater generation of force transpiring within the knee and ultimately the ACL. Or, in the case of direct contact injuries, the competitiveness of a game may result in players more intensely blocking, checking, or tackling an opposing player, which, when such force is applied to the knee, may result in a rupture or tear occurring. Another external risk factor that may contribute is the type of footwear worn by the players.[59,66-68] While the additional traction provided by certain shoes may improve the effectiveness of the player on field, it has to undue effect of adding additional stress to the ACL. In addition to footwear, the playing surface also seems to have an effect on injury rate.[59,66]

1.2.4.1 Non-Contact ACL Injury Mechanics

The typical biomechanics of non-contact injury is that the knee is externally rotated when under flexion of approximately 20° or less and in a slight valgus position.[59,66] The prevalent theory is, once these conditions are met and load is applied, the ACL stretches and lateral compression occurs.[59,66] This compression, in conjunction with an anterior force caused by muscle contraction, causes a displacement between the femur and the tibia; forcing the tibia to translate anteriorly and to rotate internally thus causing the ACL to rupture.[69] This theory places emphasis on the valgus angle as well as internal rotation of the knee, and, to a slightly lesser degree, the quadriceps contraction.[69] Additional conditions, or slightly differing conditions may also be present during ACL injury. For example, a more extended knee during landing activities also contributes to taxing the ACL to the point of injury, or eccentric muscle actions of the quadriceps that resist flexion during high-speed activities.[59,70]

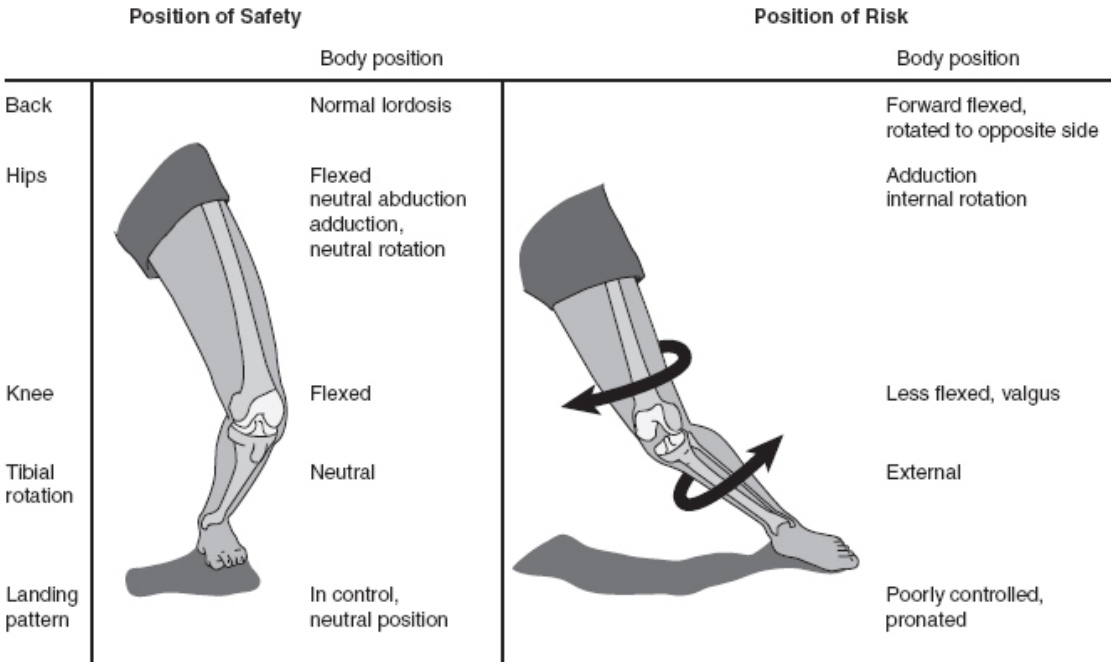

Figure 6 | Non-contact ACL injury mechanism [71]

Injury to the ACL can be categorized into 3 groups, based on the degree of severity.[72] Grade I sprains are the least severe injury. In grade I sprains, the fibers of the ACL are excessively stretched, but not to the point as to allow tearing to occur.[72] Typically, within grade I sprains, there is tenderness and slight swelling, but the knee does not feel unstable or runs the gambit of giving out during an activity.[72] The next level, grade II sprains are more severe in nature. The fibers of the ligament during grade II sprains have been stretched to a point that allows for partial tearing to occur and are typically accompanied by slight hemorrhaging.[72] Swelling, tenderness, and slight loss of function are all present within this grade.[72] Generally, the joint feels unstable and may give out during an activity.[72] Grade III sprains, the most severe, are defined by being the point at which complete tearing of the ACL has occurred; the ligament is torn into two distinct parts.[72] Tenderness and swelling are present, but the feeling of pain is limited.[72] At this degree of injury, the ACL cannot control the actions of the knee, thus the knee feels much more unstable and will give out.[72] In addition, the presence of rotational instability is apparent.[72] Hemarthrosis may also occur within a few hours of sustaining the injury.[72,73]

1.2.5. Muscles

Two major muscle groups cross over the knee, and act as the source through which knee motion is achieved; they are the quadriceps group and the hamstring group. The muscles crossing the knee are of great importance when considering non-contact ACL injuries, particularly the strength of the extensor group (quadriceps).[74] It has been observed in various studies that increased quadriceps strength compared to the hamstring greatly increases the risk of potentially suffering from an ACL injury, particularly in female athletes.[74-78] Additionally, aggressive quadriceps activity has been shown to produce significant anterior tibial translation, causing strain to develop within the ACL and increasing the risk of injury to the ligament.[79] The quadriceps group functionally acts as the main extensor of the knee joint and is located on the anterior surface of the thigh. As the name suggests, the quadriceps are a group of 4 distinct muscles: the rectus femoris; the vastus lateralis; the vastus medialis; the vastus intermedius. Of the groups, only the rectus femoris is involved in both flexion of the hip and extension of the knee as it is the only muscle of the quadriceps to cross the hip. Of note is that all the muscles of the quadriceps group envelop the patella from the respective origin sites and are anchored to the tibial tuberosity via the patellar ligament.

1.3. Internal Measurement Units (IMUs)

The last few sections have discussed, in broad, the anatomical and physiological components that needed to be considered within the study. The next few will discuss the components of the instrumentation used. As stated in the beginning, IMUs are designed to track the kinematics of whatever body segment they're affixed to. In general, IMUs consist of three distinct parts: accelerometers; gyroscopes; magnetometers.

Accelerometers allow for the measurement of linear acceleration and are generally measured in terms of either meters per second squared $\left(\frac{m}{s^2}\right)$ or in gravitational forces (g). Of note is the effect the natural gravitational acceleration has on this component. Because the accelerometer is constantly subjected to gravitational acceleration, properly calibrated IMUs should read values equivalent to earths gravitational acceleration ($9.81\ \frac{m}{s^2}$) in the appropriate direction (the appropriate direction is the axis subjected to the constant acceleration; in most systems, this is the z-axis but due to placement orientation this may be subject to change). Gyroscopes are also

an integral part of most IMUs. Able to determine rotations about an axis, gyroscopes measure the angular velocity experienced by the IMUs. The units associated with angular velocity are either radians per second $\left(\frac{rad}{s}\right)$ or, due to a conversion preprogramed into the IMU, degrees per second $(°/s)$. Magnetometers are used in the measuring of magnetic fields strength and direction; this instrumentation component can be used in conjunction with angular velocity through the implementation of various transformation matrices to provide angles between segments. The specific IMU used in this study, APDM Opal, will be discussed in depth in the next chapter, along with other equipment that were employed to carry out the experiment.

Chapter 2: Methodology

2.1. Brief Experimental Overview

Cadaveric knee specimens that were to be tested in the Biomechanics Research Laboratory at U-M Ann Arbor as part of Dr. Ashton-Miller's R01 AR054821 were utilized for this experiment. Each specimen was equipped with two wearable IMUs; one on the proximomedial aspect of the tibia and one on the distolateral aspect of the femur. Each specimen was subjected to repeated loading (up to 100 cycles) at 4x body weight (BW) at a predefined knee flexion angle with internal tibial torque. This was designed to simulate a one-legged landing from a jump. During the study, a weight limit was discovered for the testing rig. If a given subject's weight was sufficiently high (>190 lbs.), the target BW was reduced to 3x; this reduction prevented catastrophic failure of the testing rig. Linear acceleration and angular velocities of both the tibia and femur were measured using the wearable IMUs and compared to forces and moments acquired with the "gold-standard" Certus optoelectronic tracking system and load cells. Other aspects were also considered, the specifics of which will be discussed in the coming sections. In addition, an in-depth review of specimen consideration and preparation will also be discussed as will the materials used within the experiment.

2.2. Experimental Materials

There were three major pieces of equipment that were used during the experiments. The first major piece of equipment that was used was a custom-built testing rig (Table 9). This testing rig had been used and validated during previous studies.[80,81] The second was the Certus optoelectronic tracking system. Optoelectronic markers (Optotrak Certus; Northern Digital Inc, Waterloo, Ontario, Canada) were placed on the proximal tibia and distal femur in order to capture tibiofemoral kinematics. Sampling rate for this process was set to 400 Hz. A 3D digitizing wand was used to define anatomic landmarks of the knee. Through this process, changes in 3D translations and rotations of the tibia were calculated with respect to the femur.

Anterior tibial translation (aTT) and internal tibial rotation were measured compared to the base line that was established at the beginning of each testing session. Two 6-axis load cells were used to monitor the reaction forces and moments applied to the tibia and femur. Before being used, knee specimens were screened and were excluded if they had a history of surgery, trauma, or generative changes. Once they passed screening, the knees were dissected of tissue while keeping the ligamentous capsular structure intact. Attention was also paid in keeping the muscle tendons of the quadriceps, hamstrings, and gastrocnemius intact. Once prepped, the distal end of the tibia and the proximal end of the femur were potted and rigidly fixed in the testing apparatus in an inverted position (Figure 9). After the specimen was placed within the rig, calibration of the camera system occurred according to a pre-established process by the Ann Arbor team. After calibration, the quadriceps, hamstring and gastrocnemius muscles were pretensioned to 180 N, 70 N and 70 N, respectively to mimic the tensions present in real-world.

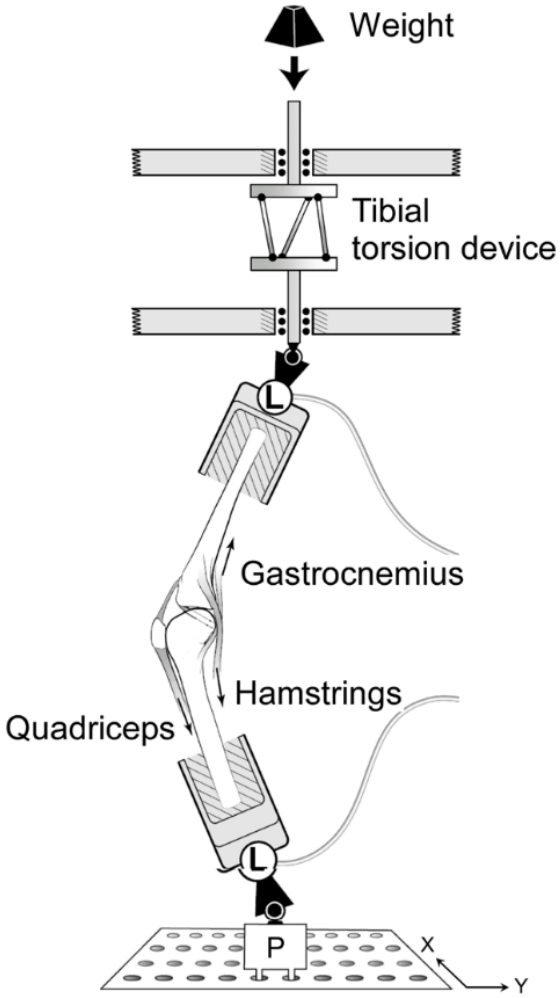

Figure 7 | Blueprint of the custom testing rig used in the experiment

2.2.1. APDM Opal

In the beginning of this thesis, the main purpose of this study was presented: to compare the data obtained through an IMU to that obtained through cadaveric testing to determine whether the selected IMU can be used to identify an injurious loading cycle.

Standing for Ambulatory Parkinson's Disease Monitoring, devices developed by APDM (APDM Inc., Portland OR) specialize in the monitoring of gait movements, specifically in those suffering from Parkinson's. Opal, a device developed by APDM, allows for the monitoring of kinematics whilst being small and relatively non-cumbersome to subjects wearing them. In addition, a long battery life (16 hours), and a high internal storage capacity (28 days' worth of data) allows for the possible integration of this device in monitoring the kinematic of players on the field. The characteristics of the internal and external components of the IMU are given in the following tables (Table 1) (Table 2). In addition, Figure 8 illustrates APDM's Opal's coordinate system for linear accelerations, as well as the interpretation of the angular velocities (Figure 8).

Figure 8 | APDM Opal's appearance and coordinate system

Table 1 | Characteristics of the internal components of APDM Opal

	Accelerometer	Gyroscope	Magnetometer
Number of Axis	3	3	3
Range	$\pm$ 2000 $\frac{m}{s^2}$	$\pm$ 2000 $\frac{rad}{s}$	$\pm$ 8 Gauss
Bandwidth	50 Hz	50 Hz	32.5 Hz

Table 2 | Characteristics of APDM Opal Unit

Dimensions (L x W x H) (mm)	43.7 x 39.7 x 13.7
Weight (g)	< 25
Material	PC-ABS Plastic, Glass
Internal Storage	8 Gb
Battery Life	16 hours*

*Only during asynchronous logging; 12 hours during synchronous logging

2.3. Experimental Procedure

APDM Opal was calibrated through the predefined calibration conditions that were implemented in the Moveo Mobility software developed by APDM. The sampling rate for APDM Opal was set to 256 Hz. Once prepped, the specimen was placed within the testing rig in accordance to the procedure developed by the Ann Arbor team. The two designated wearable IMUs (i.e., sensors corresponding to the calibrated positions of lower leg and upper leg of the appropriate side) were undocked and attached to the specimen. Before placing them, the IMUs were tightly bound in plastic wrapping and placed into a small zip-lock bag (the bag was small enough as to prevent movement of the IMU thus mitigating potential noise that this process may have caused); this process was employed as to prevent direct contact of the specimen with the IMU, thus not posing a biohazardous risk. Once placed in the protective layers of plastic, the IMUs were fixed to the appropriate segments through the usage of both Co-Flex bands and elastics ties in order to prevent, as much as possible, movement of the sensors (exact placement of the sensors was described earlier in the chapter). Once successively placed, the specimen was straightened to a fully extended position in accordance with initialization requirements of Moveo Mobility. This initialization process was used by the software to establish initial conditions and minimize the influence drift may have on data validity. Once initialized, the sensors were left recording while the Ann Arbor team pretensioned the muscles, adjusted the knee angle, and froze the patellar ligament, and was not stopped until the conclusion of testing.

After each drop trial, both the impact number and the time of impact as presented by Moveo Mobility was recorded. This recording allowed for easy filtering of the data so only genuine

impacts that were a result of a drop trial were considered. In addition to recording the number and time of each impact, any distinguishing features associated with the specimen, such as longer/shorter upper or lower leg portions, damage to knee capsule prior to testing, or other defining characteristics were noted. This was done if data obtained from a specimen appeared abnormal: as a means of potential justification for data omission or data outliers.

Drop height and weight were adjusted to match the target compressive force prior to testing based on testing conditions of previous specimens. Liquid nitrogen was used to freeze the patellar tendon and was periodically refrozen throughout the session once sufficiently thawed. Impacts were initiated by unclipping the clipped weights and allowing them to freely fall onto the tibial torsional device (Figure 9). The weights were guided to the desired impact location through the use of two parallel rods. The load applied to the knee was monitored with a load cell on the proximal femur and distal tibia. At least 5 preconditioning trials were conducted before the activation of the tibial torsional device.

The inactivation of the tibial torsional device meant that during these preconditioning trials, the specimen was only allowed to flex. This gave the benefit of adjusting the drop height as needed to match the desired compressive force without the need to account for the transformation of some of the linear force to torque. In addition, these preconditioning trials also minimized the effect hysteresis may play through the uncrimping of the fibers. Once completed, the tibial torsional device was activated as was done in previous studies.[5,80,81] Once the device was activated, the weight and drop height remained unaltered until the conclusion of the experiment. Between each trial, corrections to muscle forces and the flexion angle were made to ensure consistent starting testing conditions between each trial. Testing only concluded once 100 trials were completed or failure of the specimen occurred. Failure was clinically defined as the moment a specimen experienced 3mm of cumulative aTT during any given trial. Once the experiment concluded, the IMUs were removed from the subject, APDM recording was stopped, and the specimen was removed from the rig and sent to MRI to review the damage, if any, sustained by the ACL during the experiment.

2.4. Data Analysis

Once testing concluded, the Ann Arbor team provided the files containing the load cell data in hierarchical data format (.h5). A custom script written through MATLAB

(MATLAB_R2019b; MathWorks, Natick, MA) was developed in order to obtain maximum forces, loads on muscles, and moments experienced by the specimen from each testing trial (Script 1). Files from APDM's Opal sensors were downloaded from the individual sensors involved during testing through Moveo Mobility. These files were also downloaded in .h5 but required another custom script to interpret (Script 2). Interpretation of APDM's Opal data provided the triaxial linear accelerations and triaxial angular velocities in standard Cartesian coordinates as given in the previous sections. Impacts associated with each drop test were obtained through usage of the notes taken during the experiments. Impacts were considered to be the maximum vertical linear accelerations during an experiment; example of which can be found below (Figure 9).

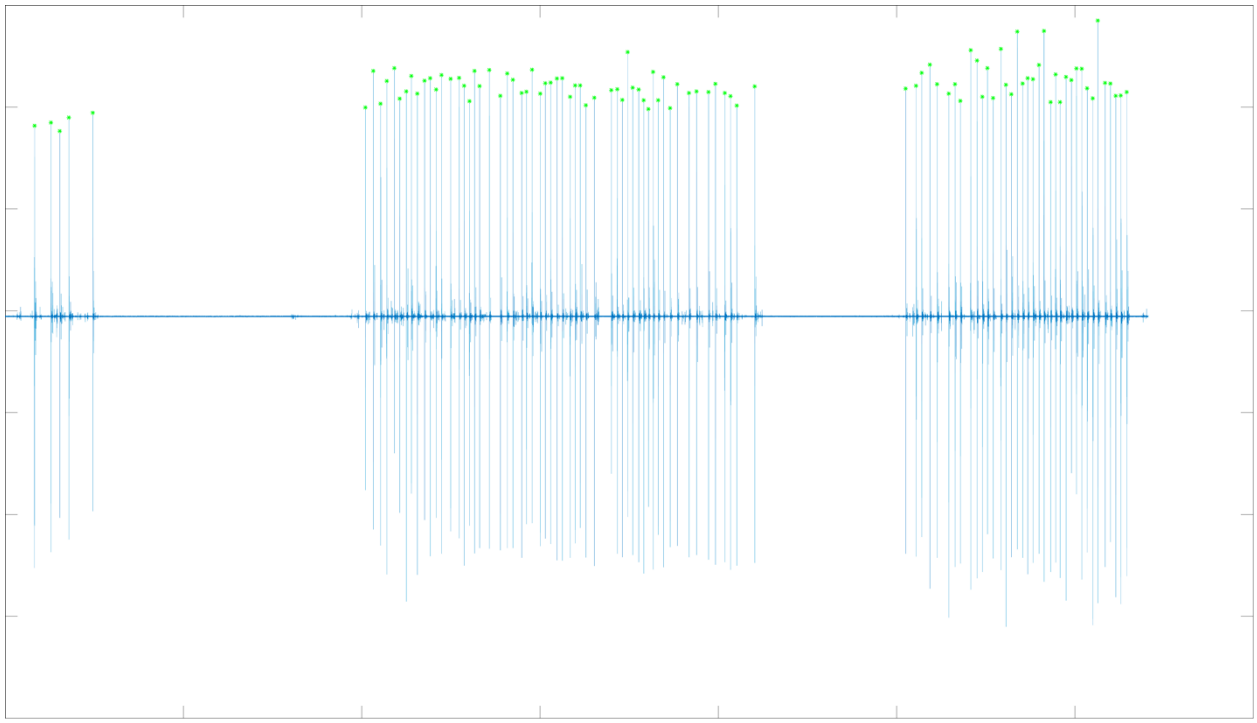

Figure 9 | Example of the process involved in selecting the moment of drop impacts; figure depicts the vertical linear acceleration of a left shank.

Figure 9 shows a typical testing period when observing linear acceleration. Each green point corresponds to a drop impact and was considered the moment the weight hit the specimen. In addition, data corresponding to 250ms prior and post impact were taken into consideration. The purpose of this time period was to account for the possibility that maximum angular velocity may not have occurred at maximum linear acceleration; continued compression of the tissues

resulting from the applied acceleration most likely causes maximum angular velocity to develop later during the trial, and this time period allowed for the consideration of this possibility. Both the linear accelerations and angular velocities were zeroed by taking the difference between their respective maximum and minimum values.

For each specimen, a trial indicating the initial, or static condition, was also added and pertained to the real-world application of the IMU. While not included in any analysis, this initial condition established proper regression models. Additionally, freezing of the quadriceps tendon presented the potential to affect the mechanical properties of the specimen during the trials pre/post freezing. Initial reviewing of these trials showed a significant change in force and angular velocity. Thus, the trials between which refreezing of the quadriceps tendon occurred were omitted from any analysis. Furthermore, any noted trial(s) in which something against the established testing protocols of either the Ann Arbor Team or ours were omitted; such trials included instances in which malfunctioning of the testing rig occurred or improper fastening of certain aspects of the rig.

Once trimmed of all points associated with freezing/improper protocol, the data was further trimmed to only include the first 30 trials. Due to the fact each testing session consisted of only one subject, an average of those first 30 trials were considered when developing regression models, but when employing the developed regression models to determine other aspects (such as absolute percent error), all trials associated with a specimen were considered.

2.4.1. Regression Analysis

After vetting all the data and applying the exclusion criteria, development of a regression model was performed between corresponding aspects of the IMU and those of the load cells/camera system. The list of these comparisons can be seen in Table 3. In latter sections, the reasoning behind there consideration will be explained in depth. All comparisons, save of angular velocity v. quadriceps force, utilized the IMU components associated with the shank (e.g. the resultant linear acceleration of the shank with respect to the force experienced) which was also established to be the independent variable of the regression models. Angular velocity v. quadriceps force utilized the angular velocity associated with the femur; this was also established as the independent variable of this particular regression model.

Table 3 | The aspects that were considered to be most important in determining whether the IMU has the ability to accurately determine the potential factors that increase stress/strain on the ACL.

		Axis of Consideration	
	Type	APDM Opal	Load Cell
Linear Acceleration V. Force	Resultant	All axis	All axis
Angular Velocity V. Moment	Valgus/Varus	Y-Axis	X-axis
	Internal/External Rotation	X-axis	Z-axis
Angular Velocity V. Quadriceps Force	Flexion/Extension (IMU only)	Z-axis	-
Linear Acceleration V. aTT	Mediolateral	Y-axis	-

Depending on the aspects being compared, differing regression models were employed. This was primarily done in response to the ($0^{\circ}/_{S}$, 0 Nmm) initial condition that was established between angular velocity and moment as well as linear acceleration and aTT, and the ($0^{\circ}/_{S}$, 180 N) initial condition that was established between angular velocity and quadriceps force. The list of employed regression models, as well as their established starting conditions can be found in Table 4.

Table 4 | The types of regression models developed for each comparison of interest along with the employed initial condition

	Applied Regression Model		Initial Condition
Linear Acceleration V Force	Linear		(9.81 $^{m}/_{s^2}$, $\frac{\sum weight}{2n}$ N)*
	Exponential		
	Power		
	Logarithmic		
Angular Velocity V Moment	Valgus/Varus	Linear	(0 $^{\circ}/_{s}$, 0 Nmm)
	Internal/External Rotation		
Angular Velocity V. Quadriceps Force	Linear		(0 $^{\circ}/_{s}$, 180 N)
	Exponential		
Linear Acceleration V aTT	Linear		(0 $^{m}/_{s^2}$, 0 mm)

In addition to the basic regression models, it was noted that moment is a function of both rotation and force, thereby meaning moment could potentially be a function of the angular velocity and linear acceleration. As such, multi-linear regression models were developed by a custom MATLAB script (Script 3). Additionally, it was also noted that, due to the sites of insertions of the muscle group, the quadriceps force may be a function of the angular velocities associated with the shank and the femur, and as such, a third multi-linear regression model was developed.

Table 5 | The parameters used in determine fit level of developed regression models

Range of R^2	Interpretation
$0.90 \leq R^2 \leq 1.00$	Very Strong Fit
$0.70 \leq R^2 \leq 0.89$	Strong Fit
$0.50 \leq R^2 \leq 0.69$	Moderate Fit
$0.30 \leq R^2 \leq 0.49$	Low Fit
$0.00 \leq R^2 \leq 0.29$	Negligible Fit

The coefficient of determinations (R^2) for each of regression model was obtained and evaluated in terms of model fit strength. The interpretation in evaluating R^2 were based on interpretation of correlation coefficients.[82] Table 5 shows the entirety of these interpretations and their associated R^2 value ranges (Table 5).

2.4.2. Absolute Percent Error and Root Mean Square Error

Once developed, the regression models were used to determine the average absolute percent error (abs % error) associated with the model as well as the root mean square error produced by each model (RMSE). In order to develop the abs % error, the absolute difference between the calculated value and those obtained through the load cell/camera system was determined, and then divided by the value obtained through the load cell/camera system (Equation 1)

Equation 1 | Absolute Percent Error

$$\boldsymbol{abs\ \%\ error} = \frac{|\boldsymbol{C} - \boldsymbol{L}|}{\boldsymbol{L}}$$

Where *C* is the values obtained through the application of the regression model and *L* is the values obtained through the load cell/camera system. From there, the average abs % error was calculated as follows (Equation 2)

Equation 2 | Average Absolute Percent Error

$$\boldsymbol{average\ abs\ \%\ error} = \frac{\sum \boldsymbol{abs\ \%\ error}}{\boldsymbol{N}}$$

Where *N* is the total number of samples considered. The abs % error measures the difference between the calculated value (as obtained through the developed regression model) and that of the true value (as obtained through the load cell/camera system). Smaller abs % error values indicate less of a difference between the systems.

RMSE was determined as the square root of the average squared difference between the systems and is presented in Equation 3 (Equation 3).

Equation 3 | Root Mean Squared Error

$$\boldsymbol{RMSE = \sqrt{\frac{\sum_{i=1}^{n}(C_i - L_i)^2}{n}}}$$

where C_i is the ith value obtained through the application of the regression model, L_i is the ith value obtained through the load cell/camera system, and n is the total number of samples considered.

In terms of what it means, the RMSE is the standard deviation of the variance between the model and true response. It is an indication of the absolute fit of the developed model. Lower RMSE values illustrate that the regression model more accurately predicts the response. Because the purpose of this study was validation of IMUs response, the RMSE value associated with each regression model was given added importance and the main criteria used when considering the model best suited for potential on-field usage.

2.4.3. Descriptive Analysis

In addition, a descriptive analysis was performed through the development of Bland-Altman (BA) plots. The framework was first present in 1981 by S. Eksborg, but the Bland-Altman measurement of agreement (BA plots) was formally developed 1983 by D.G. Altman and J.M Bland.[83-85] The BA plot is an easy way to determine the bias between two factors of measurement and visually illustrate trends that may exist with respect to variance.[86] Of note is that BA plots can be based on either unit differences or percentage differences, as such, percentage differences would allow for an easier interpretation of the variance between variables and were exclusively used.[83-86] The independent variable is the average value between the data sets, while the dependent variable is the percent difference between the data sets.

Limits of agreement (LoA) are most often established *a priori* and are used as a means of determining acceptable inaccuracies. LoAs are based on either clinical requirements, biological considerations, or researcher preference.[86] Therefore, for the purpose of this study a ±10% difference between the systems were used as the LoA. Trials falling within this range were considered to have a level of error that was acceptable. Additionally, consideration was given to points that fell within ±1% difference and were considered a negligible practical difference.

Chapter 3: Results

3.1 Subject overview

A total of 10 specimens were tested (3 females, 7 males; 2 left legs, 8 right legs). The demographics of the specimens can be observed in Table 6. Across the specimens, the average age was observed to be 29.9yrs (±5.04yrs) with an average weight of 162lbs (±33.1lbs). Only one specimen was observed to have failed during testing; specimen F90932R (failing at trial 53 according to cumulative aTT). Additionally, according to the protocol established for specimens exceeding 190lbs, specimens FUM35588L, MAR19011797R, MGOL22R and MGOL21R were all tested at 3x BW. Due to only the first 30 trials being considered, a total trial population of 300 was utilized in analysis (30 trials from each of the 10 specimens).

Table 6 | Depicts the demographic data concerning the specimens that were involved within the study. Specimens are separated based on sex, with female specimen demographics being presented first. Age, leg side, weight, total testing trials and trials analyzed after exclusion criteria are all presented.

Specimen	Sex	Age	Side	Weight (lbs.)	Total Testing Trials	Trials Analyzed
FUM35588L	F	20	L	191	100	80
F40374R	F	28	R	140	100	98
F90932R	F	30	R	181	53	50
Average (all females)		26 (±5.29)		171 (±27.0)	253	228
MSC182486L	M	39	L	120	100	96
MSC182515R	M	32	R	150	100	96
MAR19011797R	M	32	R	195	100	98
MGOL22R	M	25	R	190	100	96
MGOL21R	M	31	R	204	100	96
M91814R	M	33	R	110	100	96
M91160R	M	29	R	165	149	143
Average (all males)		31.6 (±4.24		162 (±37.1)	749	721

3.1.1. Linear Acceleration V. Force

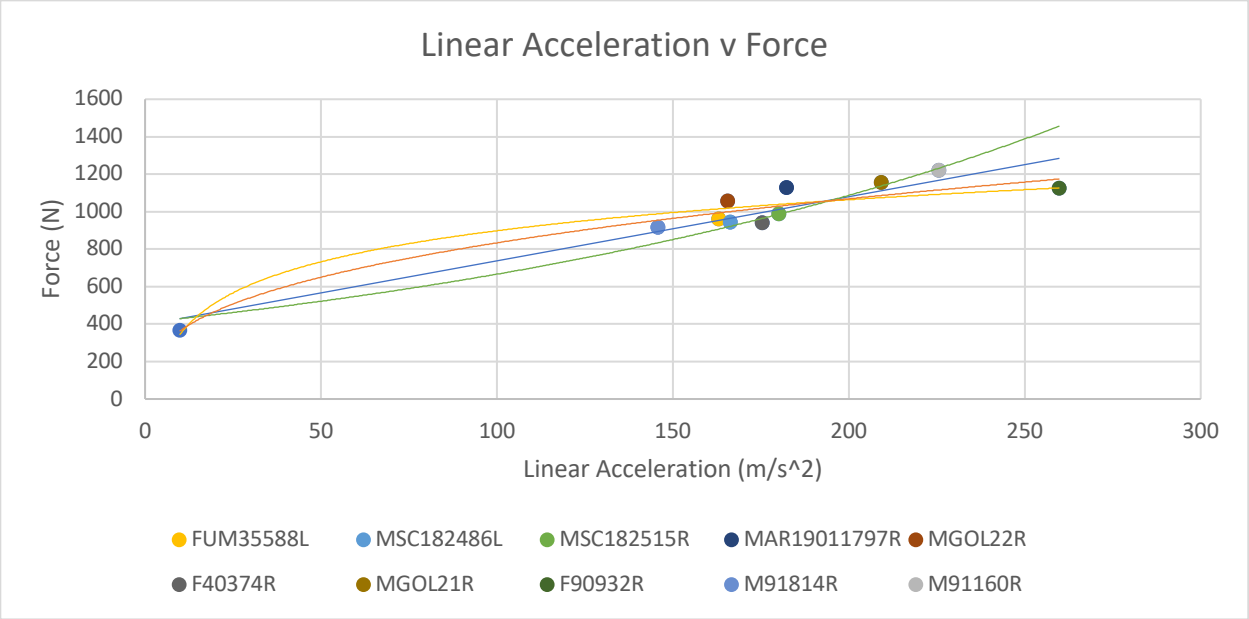

Figure 10 | Resultant linear acceleration plotted against the resultant force as obtained through the IMU and load cells respectively. The average of each specimens first 30 trials were utilized and linear (blue), exponential (green), logarithmic (yellow) and power (red) regression models were applied.

In all the applied models, a strong fit was observed in accordance to interpretation criteria of R^2 values (Table 5). The power regression model was the only model to exhibit a very strong fit (R^2=0.96) (Table 7). When examining the RMSE, 3 of the models were observed to have values lower than 90N; only the exponential model was seen to have an RMSE above 90N (RMSE=140N) (Table 7). All models where observed to exhibit abs % errors below 10%, with the abs % error associated with the power model exhibiting the smallest value (6.46% ± 3.30%) (Table 7). This observation in abs % error translated to the RMSE values in which the power model was seen to exhibit the smallest RMSE (76.4N) (Table 7).

Figure 11 shows the relationship trends between the systems when a specific regression model is applied. In both the linear and exponential regression model BA plots, an upward trend can be observed: as the average force increases the percent difference between the systems increases thereby leading to the IMU overestimating higher forces (Figure 11). While not as pronounced in the linear variant, this trend is readily observed within the exponential (Figure 11). Both the logarithmic and power regression model BA plots have no observable trends associated with them, as the data appears sporadically spread regardless of force value (Figure 11). Within Figure 11, the application of the power regression model resulted in the highest

percentage of trials falling within the LoA (88.57%), with lower values in the linear (78.9%), exponential (67.1%), and logarithmic models (76.4%) (Figure 11). When considering the percentage of trials falling within ±1% of difference, the applications of the power and linear regression models were observed to result in the same values (7.86%), while the exponential was seen to exhibit a slightly larger value (8.21%) and the logarithmic a lower value (5.00%).

Table 7 | The values associated with the regression models developed in Figure 12.

Model Type	R^2	RMSE (N)	Abs % Error (±Std)
Linear	0.88	86.9	6.49% (4.81%)
Exponential	0.87	140	9.04% (9.13%)
Power	0.96	76.4	6.46% (3.30%)
Logarithmic	0.89	83.5	7.25% (3.49%)

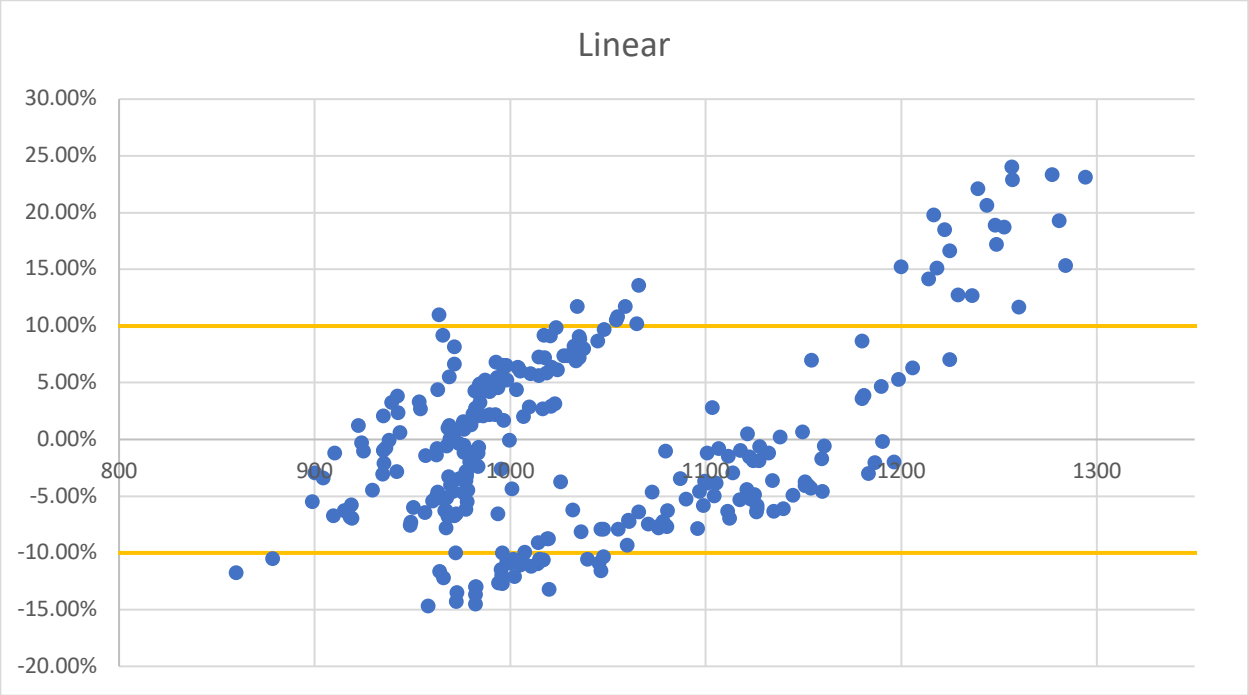

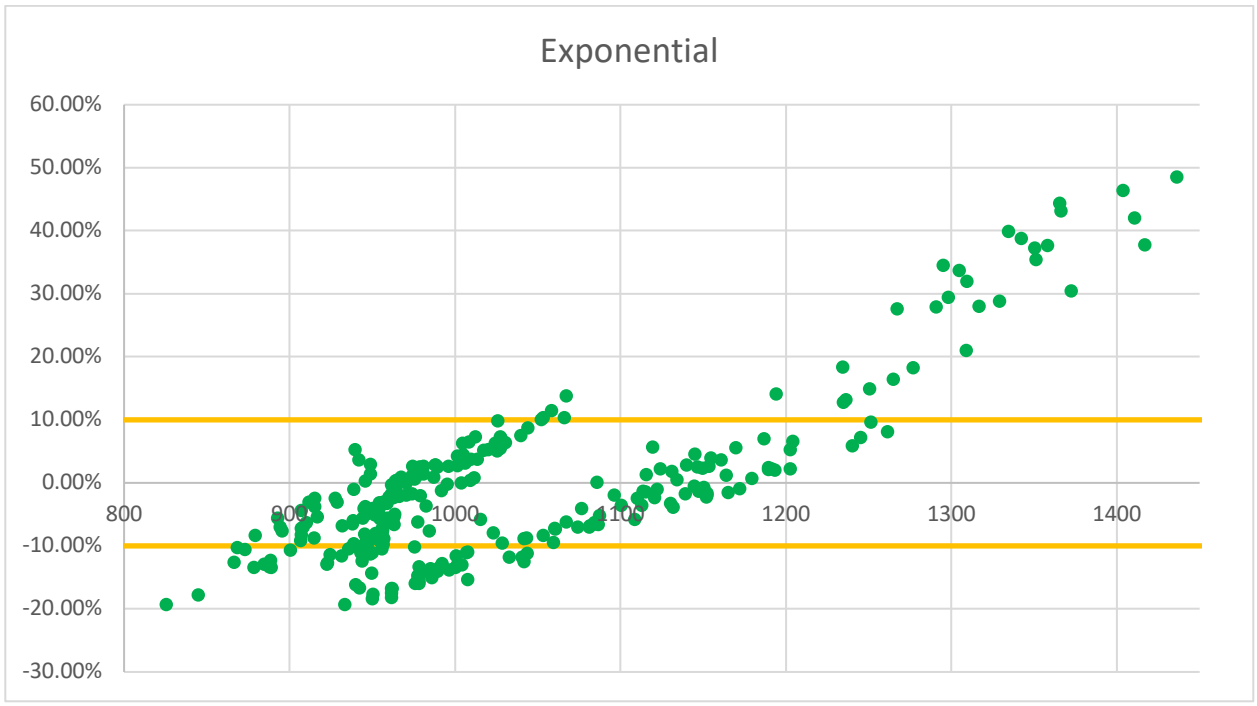
Exponential
60.00%
50.00%
40.00%
30.00%
20.00%
10.00%
0.00%
-10.00%
-20.00%
-30.00%
800
900
1000
1100
1200
1300
1400

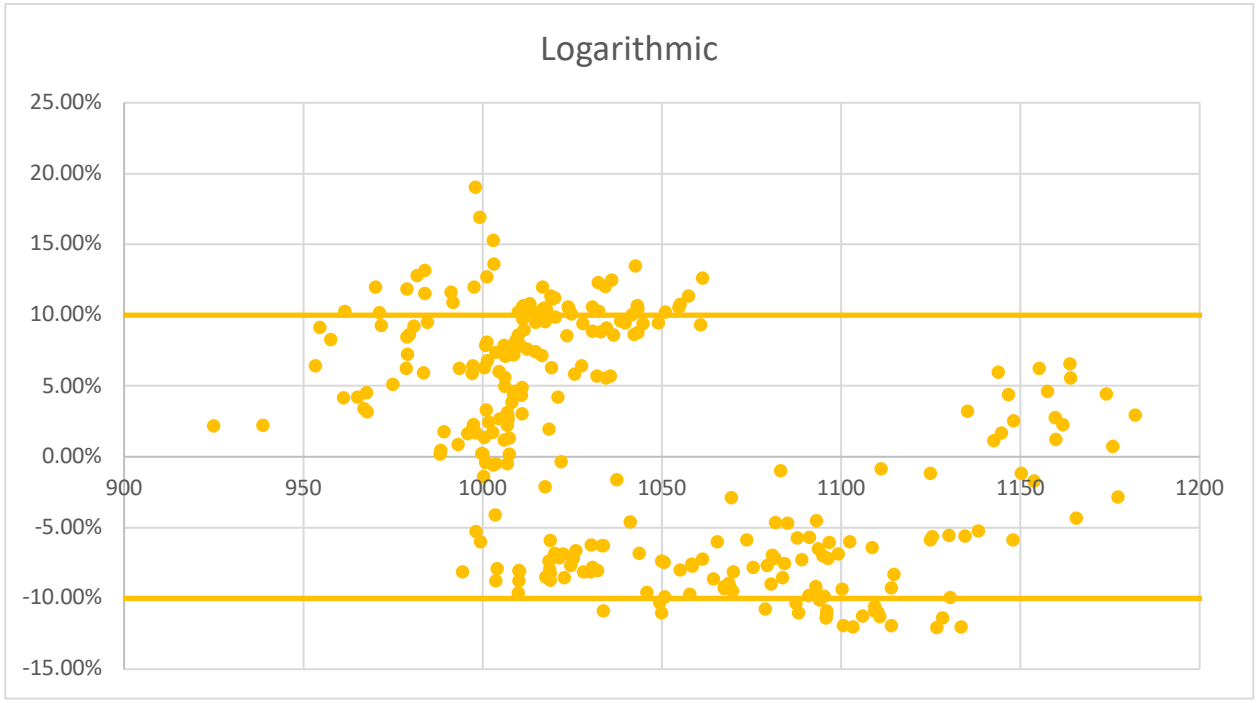
Logarithmic
25.00%
20.00%
15.00%
10.00%
5.00%
0.00%
-5.00%
-10.00%
-15.00%
900
950
1000
1050
1100
1150
1200

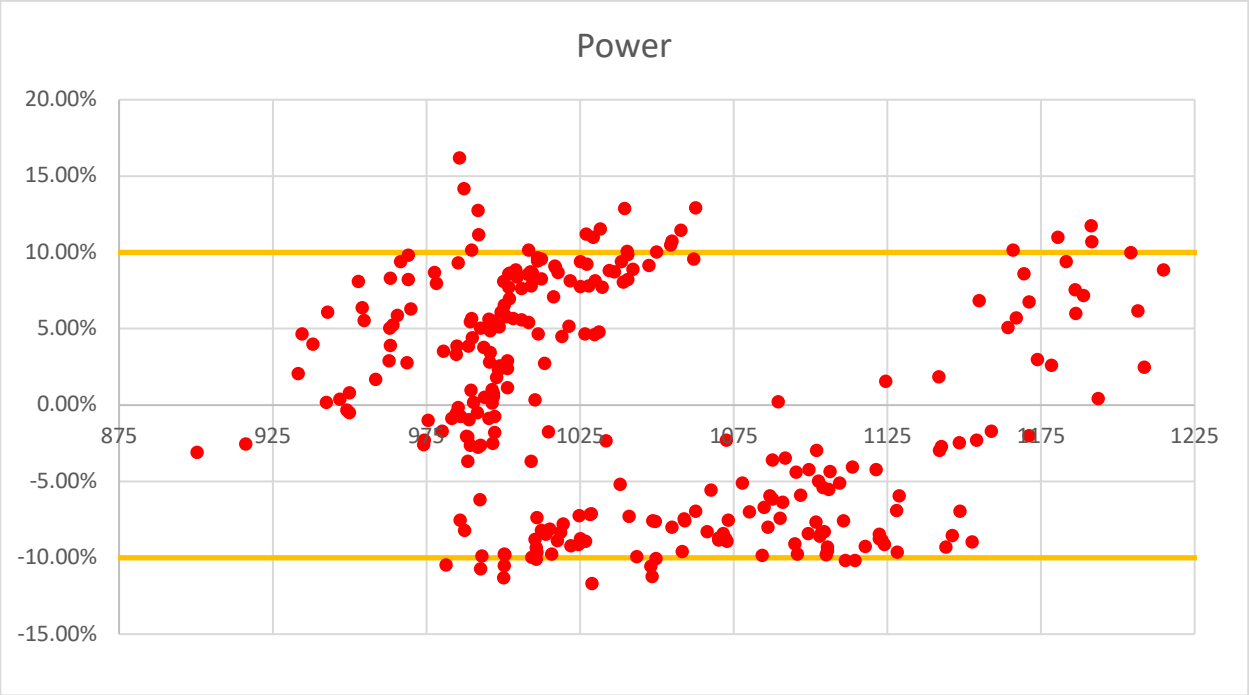

Figure 11 | BA plots associated with the application of the regression models developed in Figure 10.

3.1.2. Angular Velocity V. Moment (Valgus/Varus)

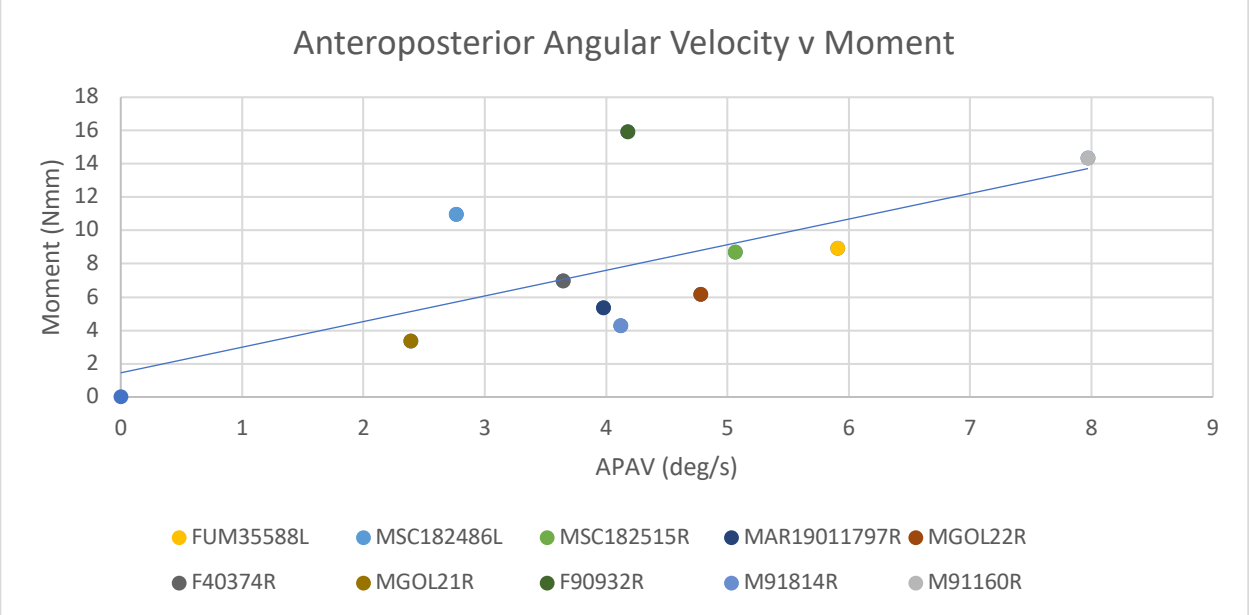

Figure 12 | Anteroposterior angular velocity plotted against the valgus/varus moment as obtained through the IMU and load cells respectively. The average of each specimens first 30 trials were utilized, and a linear regression model was applied.

The developed linear regression model was observed to have a low fit level associated with it (R^2=0.44) (Table 8). This was seen as being lower than the multi-linear regression model

which was observed to exhibit a moderate fit (R^2=0.65) (Table 8). Between the two models, the multi-linear regression model was seen as having a slightly smaller RMSE (2.93 Nmm v. 3.60 Nmm) as well as a slightly smaller abs % error (35.5% v. 36.7%) (Table 8). Though, of particular note is the standard deviation associated with abs % error, where the multi-linear regression was observed to have a larger accompanying value compared to the linear regression model (32.7% v. 28.8%).

Within Figure 14, the BA plots utilizing the regression models developed within Figure 12 and Figure 13 can be observed. While no definitive trend can be commented upon in either BA plot, it was observed that in both cases, lower average valgus/varus moments resulted in a higher degree of percent differences; below 9 Nmm the moments obtained through the application of either model resulted in larger moments as observed by larger positive percent differences (Figure 14). Further examination of the BA plots in Figure 14 revealed that the application of the linear regression model resulted in a higher percentage of trials falling within the LoA (26.8% v. 18.2%). Narrowing this consideration to trials within ±1% of difference also saw the application of the linear regression model resulting in a higher percentage within range (2.86% v. 1.43%) (Figure 14).

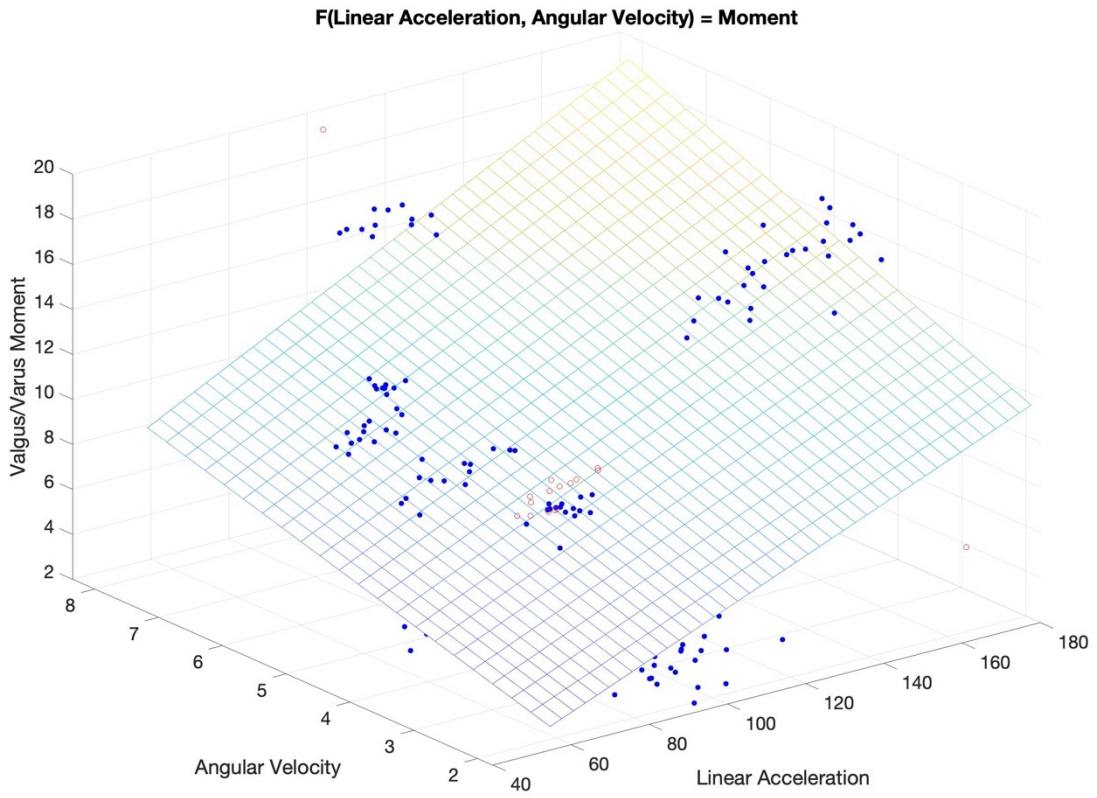

Figure 13 | Valgus/varus moment of the knee plotted against the angular velocity and linear acceleration as obtained through the load cells and IMU respectively. In order to establish a better trend, all 300 trials were utilized rather than the average. Residuals were also utilized to remove any trial considered an outlier and appear in red, while clean trials appear in blue.

Table 8 | The values associated with the regression models developed in Figures 14 and 15.

Model Type	R^2	RMSE (Nmm)	Abs % Error (±Std)
Linear	0.44	3.60	36.7% (28.8%)
Multi-Linear	0.65	2.93	35.5% (32.7%)

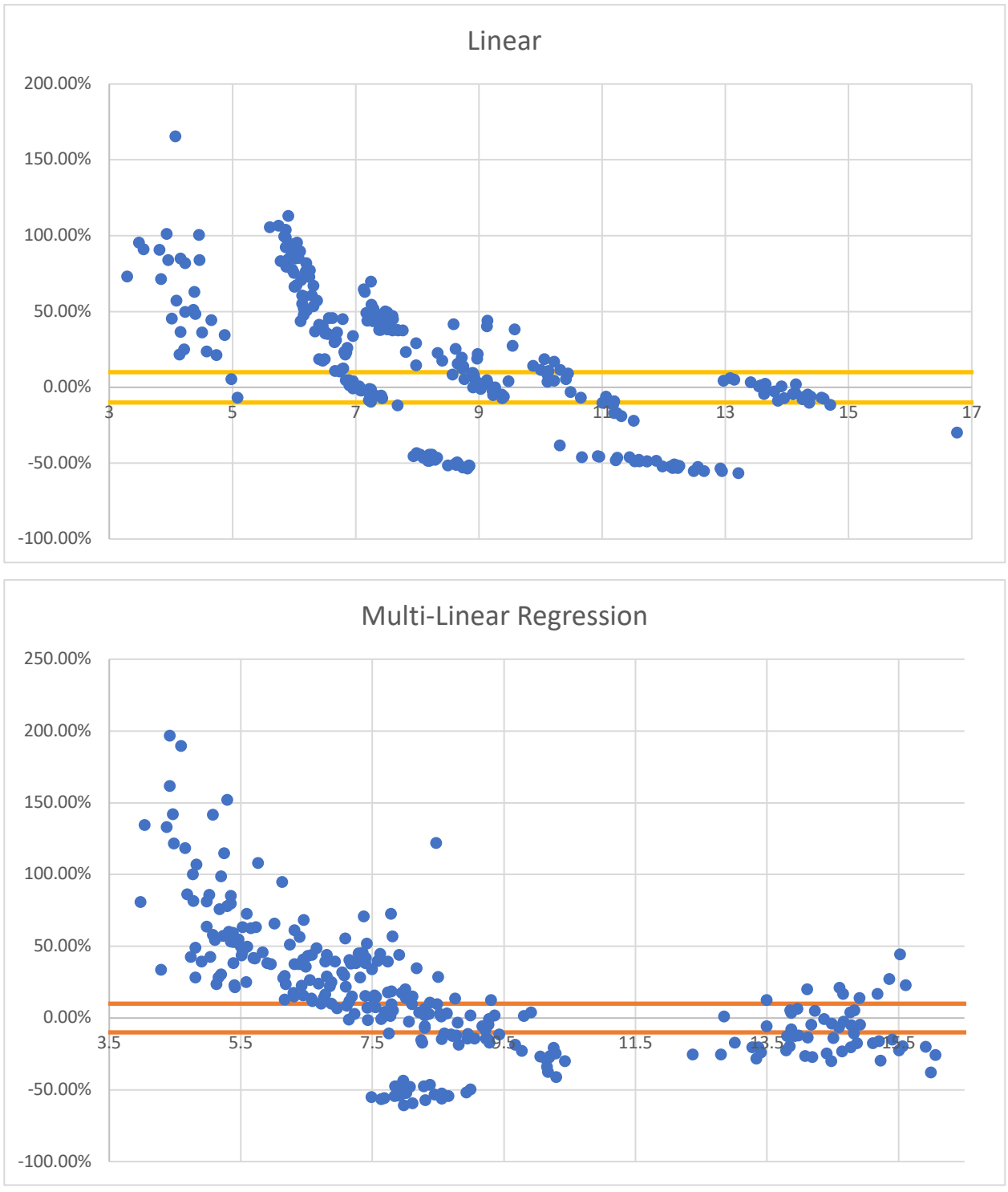

Figure 14 | BA plots associated with the linear and multi-linear regression models developed in Figures 12 and 13 respectively.

3.1.3. Angular Velocity V. Moment (Internal/External Rotation)

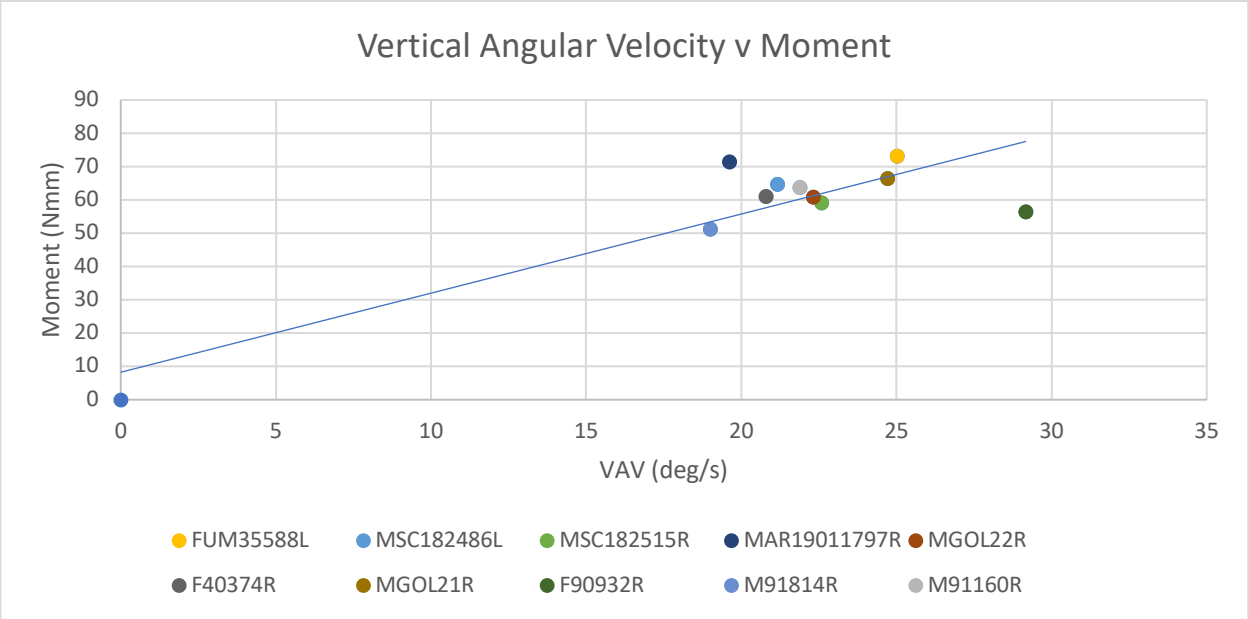

Figure 15 | Vertical angular velocity plotted against the internal/external rotational moment as obtained through the IMU and load cells respectively. The average of each specimens first 30 trials were utilized, and a linear regression model was applied.

The linear regression model developed in Figure 15 exhibited a strong fit (R^2=0.78) (Table 9). This fit was observed to be much higher than that of the multi-linear regression model that was developed in Figure 16, which was seen to exhibit a low fit (R^2=0.45) (Table 9). However, inspection of the RMSE and abs % error between the models showed that the multi-linear regression model exhibited lower values in both (RMSE: 5.10 Nmm v. 13.5 Nmm; Abs % Error: 7.05% v. 16.4%) (Table 9).

The BA plots constructed based on the models of Figure 15 and 16 showed a very slight upward trend within the linear regression model and no discernable trend within the multi-linear regression model (Figure 17). Further analysis of Figure 17 revealed a higher percentage of trials falling within the LoA when the multi-linear regression model was applied (78.2% v. 50.0%) (Figure 17). When narrowing the range to only trials with ±1% of difference, the multi-linear regression model again exhibited a higher percentage though to a much lesser extent (5.78% v. 4.29%) (Figure 17).

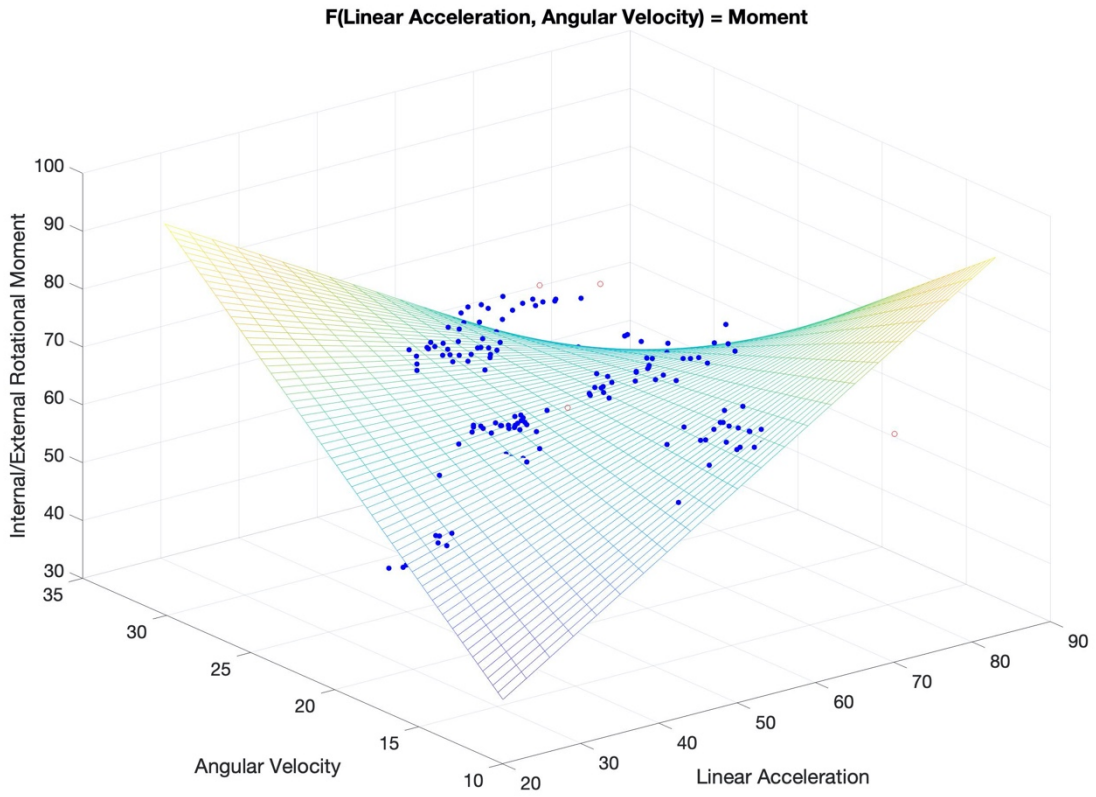

Figure 16 | Internal/external rotational moment of the knee plotted against the angular velocity and linear acceleration as obtained through the load cells and IMU respectively. In order to establish a better trend, all 300 trials were utilized rather than the average. Residuals were also utilized to remove any trial considered an outlier and appear in red, while clean trials appear in blue.

Table 9 | The values associated with the regression models developed in Figures 17 and 18

Model Type	R^2	RMSE (Nmm)	Abs % Error (±Std)
Linear	0.78	13.5	16.4% (14.0%)
Multi-Linear	0.45	5.10	7.05% (4.40%)

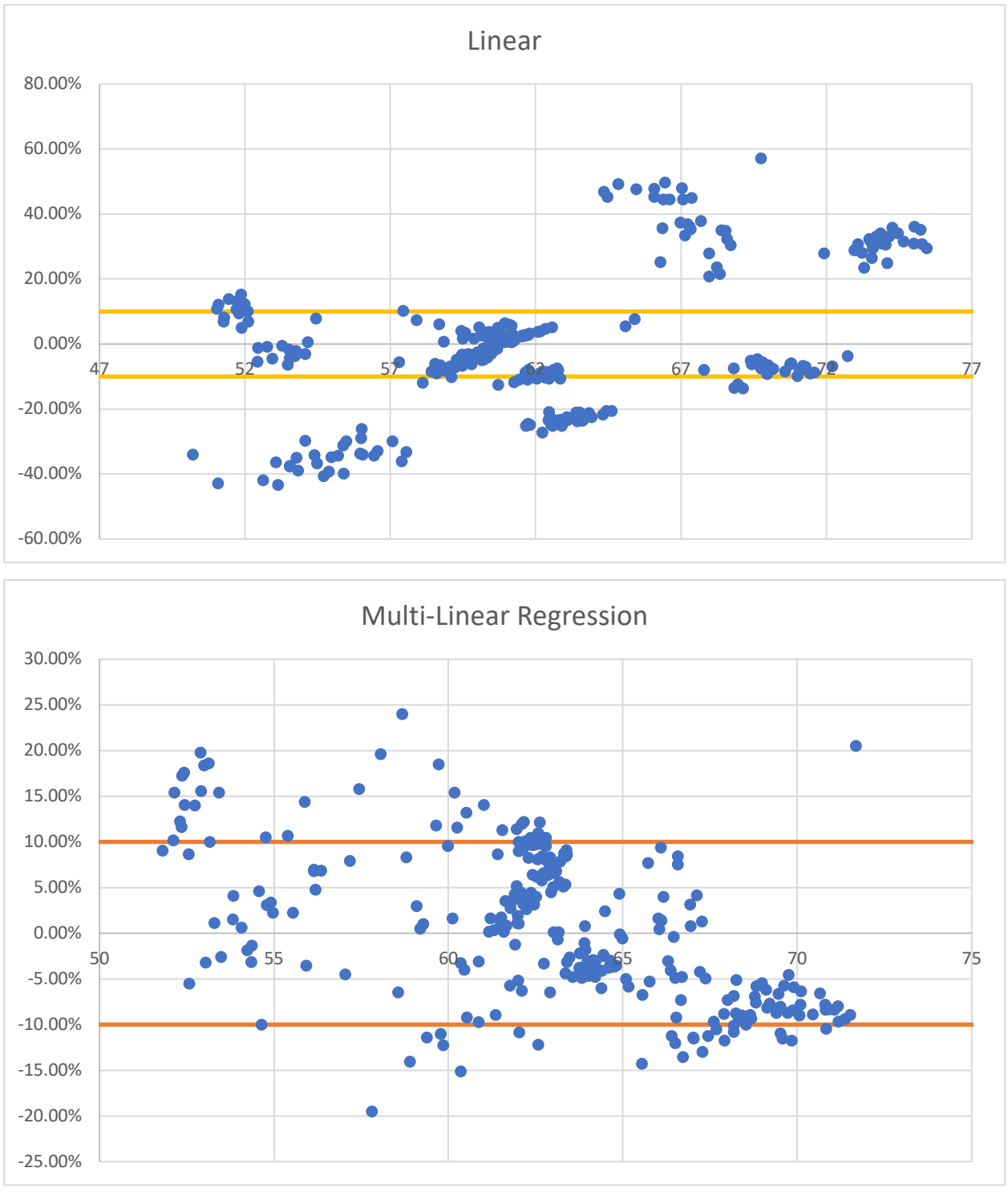

Figure 17 | BA plots associated with the linear and multi-linear regression models developed in Figures 15 and 16 respectively

3.1.4. Mediolateral Angular Velocity V. Maximum Quadriceps Force

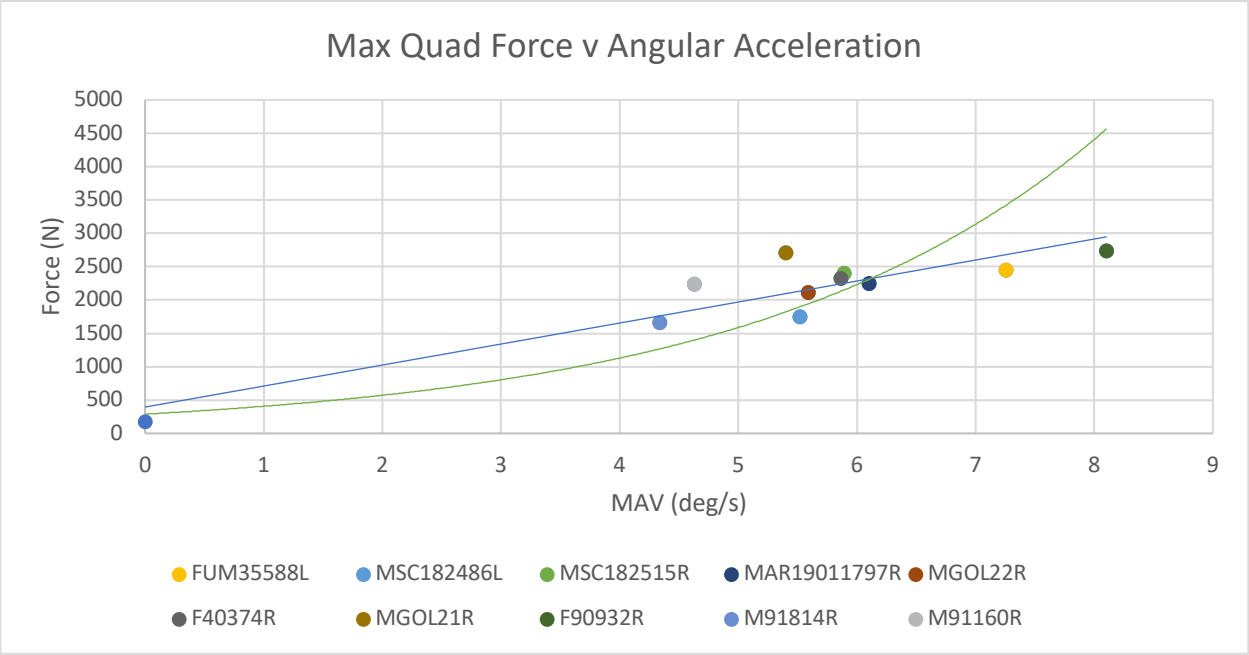

Figure 18 | Mediolateral angular velocity plotted against the maximum quadriceps force as obtained through the IMU and load cells respectively. The average of each specimens first 30 clean trials were utilized and a linear (blue) and an exponential (green) regression models were applied.

In both single variable regression models developed in Figure 19 and the multi-linear regression model developed in Figure 20, a strong fit was observed (Table 10). Among all the models, the highest fit was observed within the linear regression model (R^2=0.83), though this was only slightly higher than the multi-linear regression model, which among the three, was observed to have the lowest associated R^2 (R^2=0.79) (Table 10). Though of interest are the associated RMSE and abs % error, which were observed to be smallest within the multi-linear regression model (RMSE: 189 N; Abs % Error: 6.52%) and highest within the exponential regression model (RMSE: 800 N; Abs % Error: 24.0%) (Table 10).

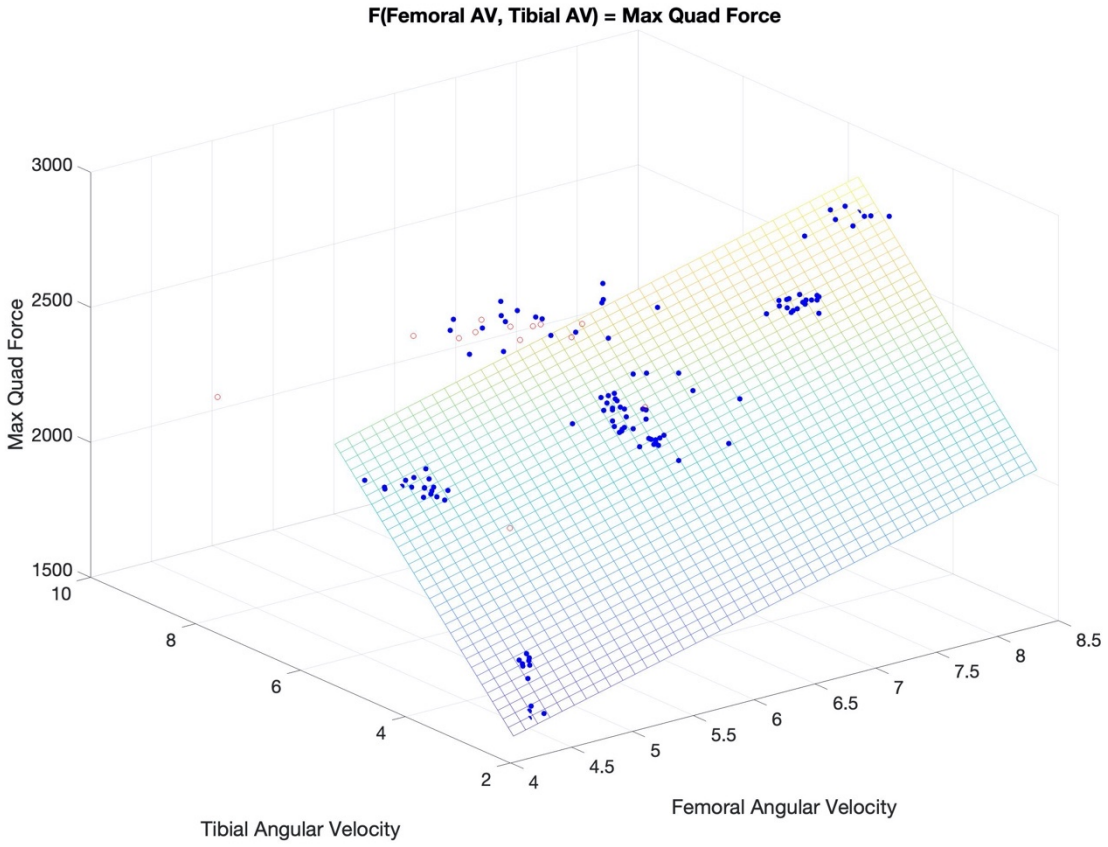

Figure 19 | Maximum quadriceps force of the specimen plotted against the tibial and femoral angular velocities as obtained through the load cells and IMU respectively. In order to establish a better trend, all 300 trials were utilized rather than the average. Residuals were also utilized to remove any trial considered an outlier and appear in red, while clean trials appear in blue.

In Figure 21, a distinct upward trend in the BA plot can be observed with the application of the developed exponential regression model (Figure 21). The BA plot associated with the multi-linear regression model showed a sporadic spread as the average force increased, thus there was no discernable trend (Figure 21). When considering the percentage of trials that fell within the LoA, the multi-linear regression model was observed to have the highest (79.3%), followed by the linear regression model (64.6%) and the exponential regression model (37.9%) (Figure 21). Observing trials with ±1% of difference again revealed the highest value associated with the multi-linear regression model (10.7%), with lower value associated with the linear and exponential regression models (6.07% and 2.14% respectively) (Figure 21).

Table 10 | The values associated with the regression models developed in Figures 20 and 21

Model Type	R^2	RMSE (N)	Abs % Error (±Std)
Linear	0.83	303	10.2% (8.58%)
Exponential	0.82	800	24.0% (20.7%)
Multi-Linear	0.79	189	6.52% (5.10%)

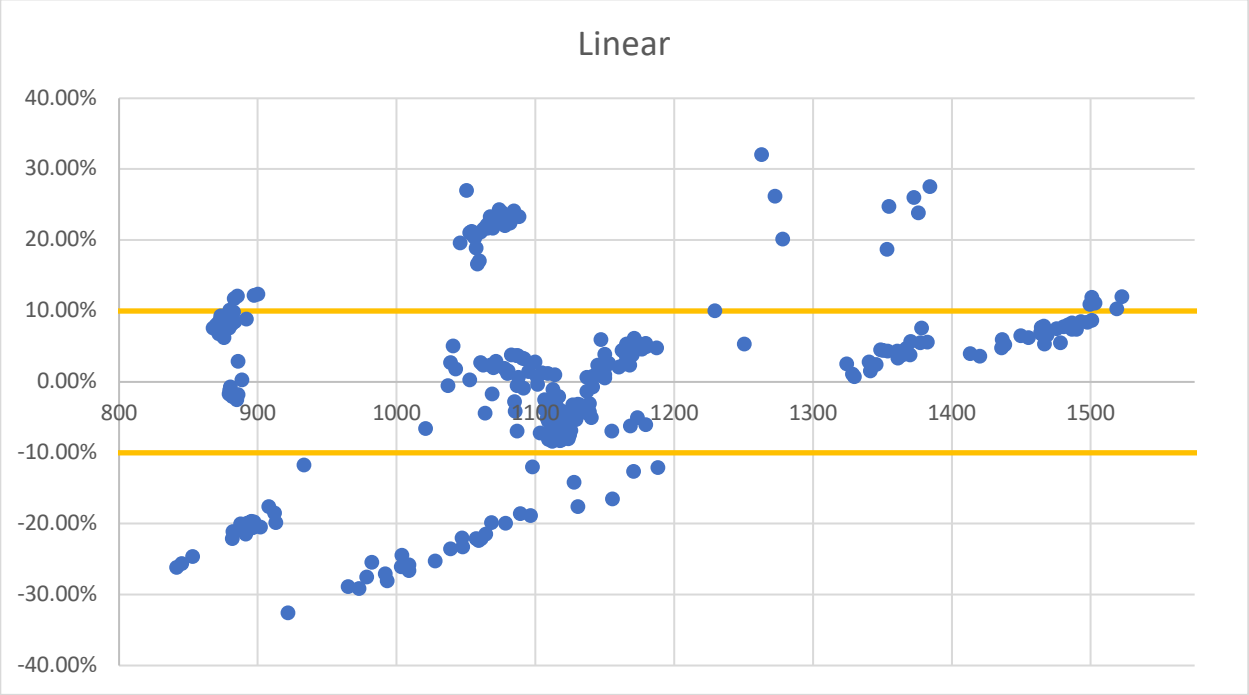

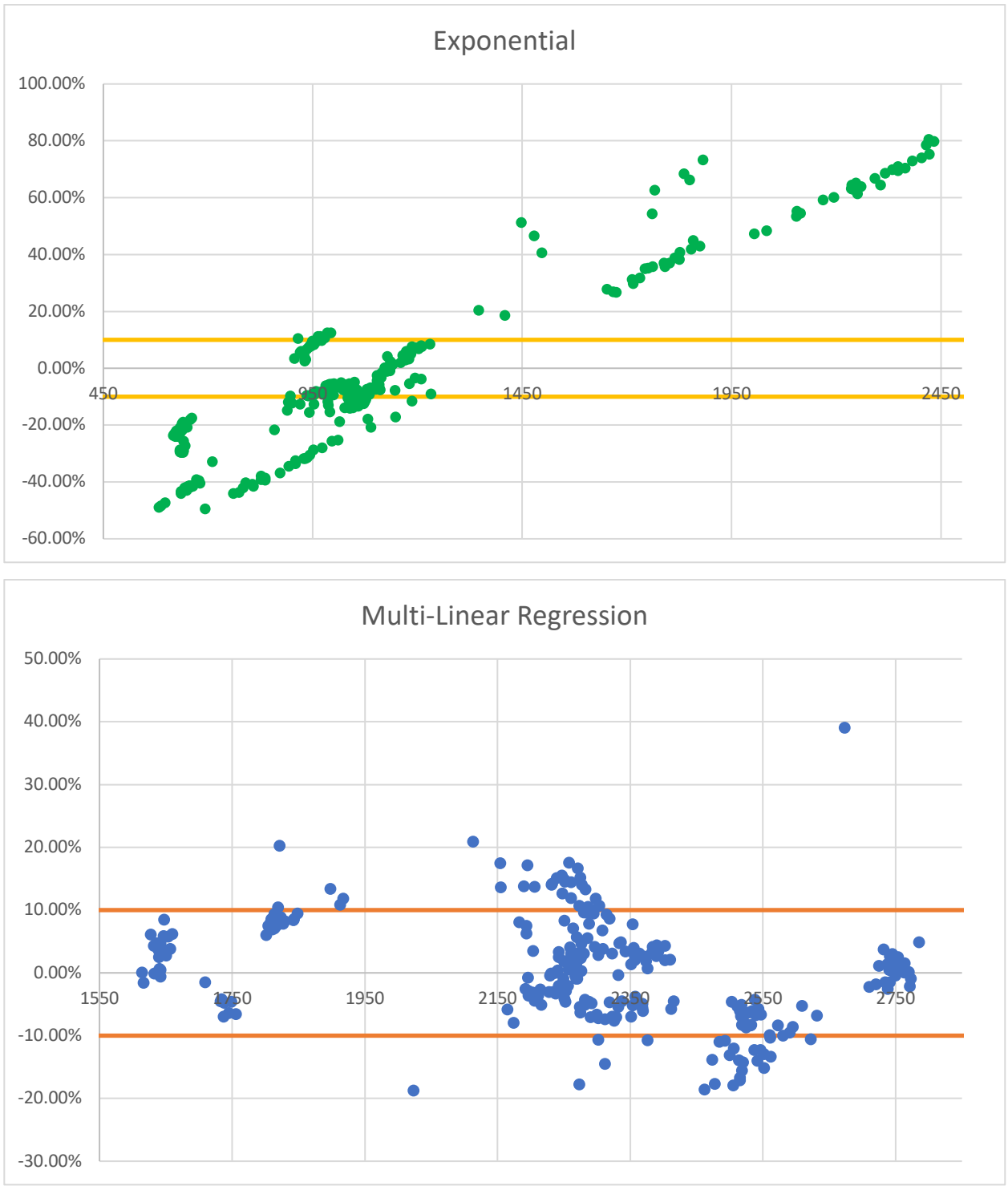

Figure 20 | BA plots associated with the linear, exponential and multi-linear regression models developed in Figures 18 and 19 respectively

3.1.5. Anteroposterior Linear Acceleration V. aTT

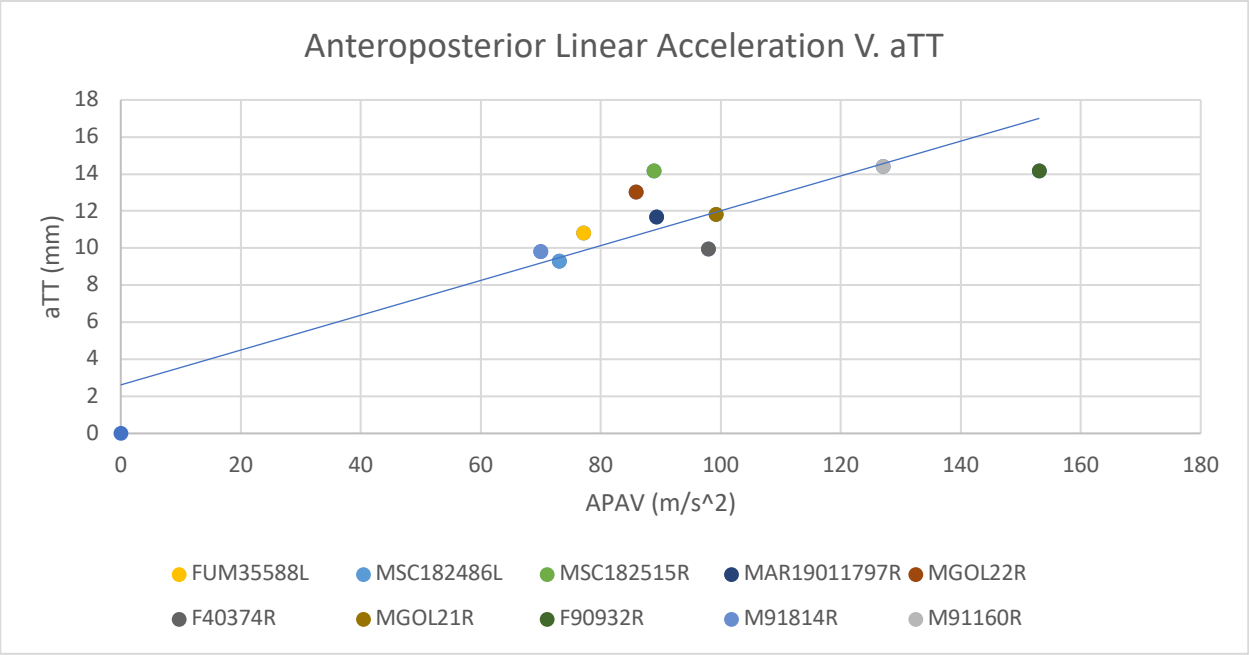

Figure 21 | Anteroposterior linear acceleration plotted against the aTT as obtained through the IMU and camera system respectively. The average of each specimens first 30 trials were utilized, and a linear regression model was applied.

The regression model developed showed a strong fit (R^2=0.78). The RMSE was 1.39 mm while the abs % error was 8.44% (±6.39%) (Table 11). The BA plot showed no discernable trend (Figure 24). However, as aTT increased in magnitude, the % difference between the systems showed a slight increase in variability.

Table 11 | The values associated with the regression model developed in Figure 23

R^2	RMSE (mm)	Abs % Error (±Std)
0.78	1.39	8.44% (6.93%)

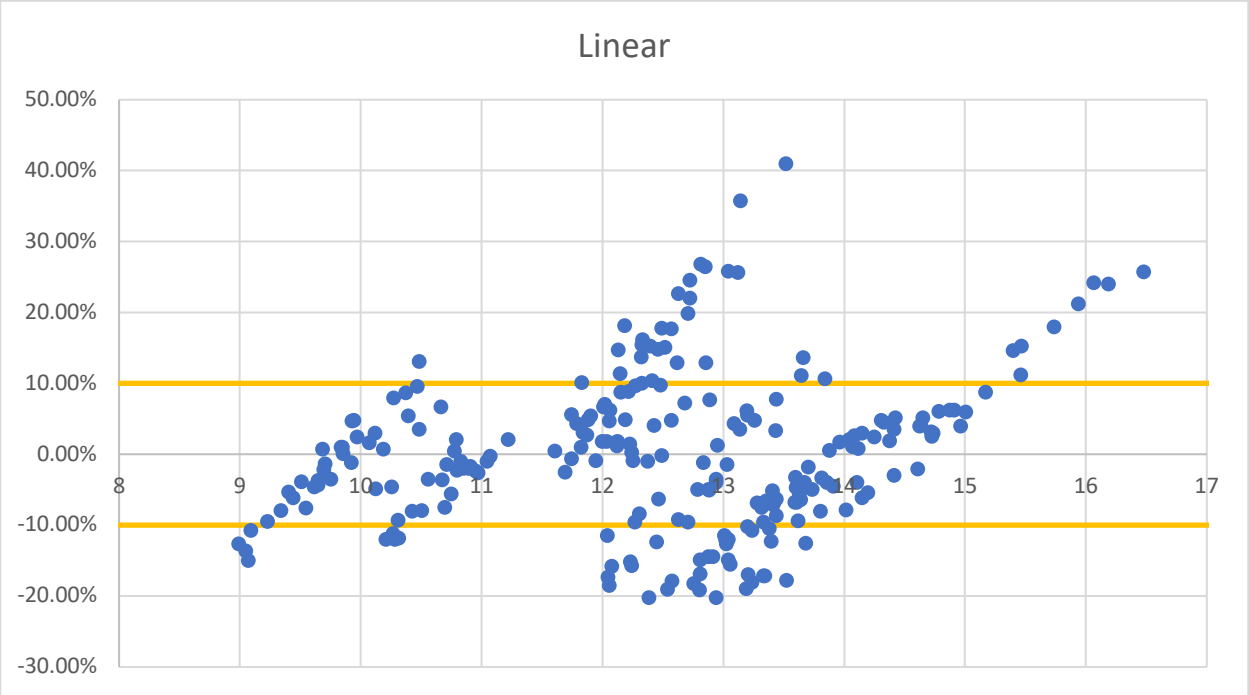

Figure 22 | BA plot associated with regression model developed in Figures 21

Chapter 4: Discussion

4.1. Overview and Interpretation of Results

The purpose of this study was to compare the data obtained through an IMU to that obtained through cadaveric testing to determine whether an IMU could be used to identify loading cycles like those that have been found to cause injury in a cadaveric model. To minimize the variables being compared, only comparisons that could potentially indicate ACL fatigue levels were observed and were presented in Table 3. Regression models were developed and RMSE and abs % error values were calculated. In addition, BA plots were constructed to determine any trends the models may exhibit.

Examining the regression models developed for linear acceleration v. force in the resultant direction, the developed power regression model was determined as being most suited for on-field testing. Among the models, not only was the power variant observed to experience the highest level of fit among the four, but the RMSE and abs % error were also seen to be lowest. Additionally, the constructed BA plots revealed no discernable trends associated with the application of the power variant, unlike the trends observed in the exponential regression model and somewhat observed in the linear regression model.

For angular velocity v. moment in the valgus/varus direction, the multi-linear regression model was the most appropriate for usage on-field. Compared directly to the linear regression model, the associated fit (R^2) and predictability (indicated by a lower RMSE) of the multi-linear regression were larger, while the average error (abs % error) was slightly lower. And while both constructed BA plots were observed to have an associated trend (higher percent differences at moments below 9 Nmm), and though the percentage of trials falling within the LoA were observed higher in the linear regression model, a greater degree of stabilization seemed to occur at higher moments within the multi-linear regression model. However, additional specimens at both greater and lesser valgus/varus moment magnitudes are needed to fully confirm this.

Among the models developed for the angular velocity v. moment pertaining to the internal/external rotation, the multi-linear regression model was considered the best for on-field

usage. While the fit level was lower within the multi-linear regression model (R^2=0.45 v. R^2=0.78), the most important aspect was the RMSE associated with each model and in that regard the multi-linear regression model exhibited a value lower than that of the linear regression model (5.10 Nmm v. 13.5 Nmm). Additionally, the abs % error was also observed to be lower with the application of the multi-linear regression model than the linear model. Also, the lack of any discernable trend associated with the multi-linear variant gives further credence that this model would be better for on-field usage.

The multi-linear regression model developed for the mediolateral angular velocity v. maximum quadriceps force was considered the most apt for on-field usage. In terms of fit, both the linear and exponential regression models showed slightly higher associated values, but RMSE linked to the application of the multi-linear regression model was observed as being considerably smaller. The abs % error within the multi-linear variant was also observed as being smaller than values observed in either the linear or exponential regression models. Further evidence to the claim that the multi-linear regression model is best suited for on-field testing can be seen within the constructed BA plots as no discernable trend can be observed within the multi-linear variant while an upward trend can be observed within the exponential variant and somewhat observed within the linear variant.

Because of the constrains associated with the anteroposterior linear acceleration v. aTT, only a linear regression model could be developed and thus is by default the best suited for on field testing. However, it should be noted that anteroposterior linear acceleration is a function of aTT and time, therefore a linear fit should be the most appropriate model. A strong linear fit and a low associated RMSE value demonstrate that the developed linear regression model may accurately predict aTT with an acceptable degree of error for practical usage through measured linear acceleration.

4.2. Linear Acceleration V. Force

The force experienced by the lower limbs of have been linked to various injuries such as patellar tendinitis, tibial stress fractures and of course ACL injuries.[5,6,69] More importantly for this study, repeated impacts at sub-maximal loading has been observed to cause micro-damage of the ACL, which from continued exposure without rest, could lead to their propagation and ultimately rupture of the ligament.[5] As such, the ability to track the force experienced by the

lower limbs are of paramount importance. Due to the understanding that a force is composed of an acceleration, the thought of correlating linear acceleration to force arose.

Other studies have also utilized this comparison but have focused on linearly modeling the data.[9,10,87] It may be possible that with the inclusion of specimens at lower testing parameters, a linear regression model would be more appropriate than a power. However, it may also be possible that other studies did not applied a power regression model to their data, or their data is comprised of specimens at lower testing parameters. Regardless, it is still possible to compare the performance of our IMU to that of others.

Most similar to our study was that conducted by Elvin et al, which sought to correlate ground reaction force to the tibial linear acceleration during a vertical landing.[9] Utilizing IMUs from ZeroPoint Technology, the study consisted of having 6 participants jump at differing heights, ranging from 50% of their maximum jump height, to 95%.[9] Standard linear least square correlation was used to determine R^2 values within their study.[9] Across all their subjects, an average R^2 value of 0.81 (range: 0.75 to 0.90) was determined.[9] This is observed as being smaller than either the linear regression model developed within this study (R^2=0.88) or the settled upon power regression model (R^2=0.96). However, several important considerations must be taken with regards to this study. Firstly, no RMSE value was reported within their study.[9] The importance of RMSE in the determination of a model's ability to predict an outcome was discussed earlier (see section 2.4.2.), and thus not reporting the value calls into question how well their model predicts a response. Secondly, the linear regression models were developed on an individual basis rather than as a group.[9] Because all trials arose from a single subject, it is likely that individual regression models would report higher coefficients of determination. Additionally, if force is correlated to linear acceleration, it would be regardless of subject consideration. The study conducted by Elvin et al utilized live subjects.[9] Within our study, cadaveric specimens were used, and while this might allow for the development of models that more accurately depict the relationship between linear acceleration and force, it also has the underlying effect of mitigating the consequences of skin laxity which would always be present in real-world applications. Thus, while the R^2 values associated with our regression models appear better by comparison to those determined by Elvin et al, it also does not consider the effect skin laxity might have on potential readings. However, in all, the study by Elvin et al shows how linear acceleration might be related to force.

Other studies have also compared linear acceleration of an IMU to force. In the study conducted by Meyer et al, two different IMUs were used (ActiGraph GT3X+ and GENEA) and various tasks such as walking, jogging, running, etc.[87] Strong to very strong correlations can be observed between the IMU's within the Meyer et al study (R=0.89 for GENEA and R=0.90 for ActiGraph GT3X+).[87] However, converting the coefficient of determination to the correlations coefficient revealed the correlations observed by Meyer et al as being lower than the linear regression model developed within our study (R = 0.93). It should be noted that the correlation coefficient (R) is a measure of linearity of the data, and therefore a comparison between the results of the Meyer et al study and our power regression model could not be made without converting the power model to a linear model. Similar concerns to those raised within the study by Elvin et al were presented within the study by Meyer et al; such as the lack of a group consideration and that added effect of skin laxity.[87] Additionally, the IMUs in the study by Meyer et al were placed on the hip rather than the tibia as were our sensors.[87] The placement of these IMUs on their subjects may have contributed to the results obtained by the team.[87] Also, of note is the reported observation by Myer et al that both IMUs consistently overestimated forces, which was not found to be true for our sensor as observed by the BA plots (Figure 11).[87]

The study conducted by Gurchiek et al used a YOST Data Logger 3-Space Sensor from YEI Technology, 15 subjects, and two distinct actions: a sprint from a standing start (SS) and a 45° change of direction task (COD).[10] Within their study, Gurchiek et al found R-values of low fit between linear acceleration and force in regard to either SS or COD tasks (R=0.49 each).[10] This is in contrast to the observations made by Meyer et al and their selected IMUs as well as that by Elvin et al and our own.[9,87] However of particular interest is that unlike any of the other studies, Gurchiek et al reported RSME values that resulted from the application of their developed models.[10] The RSME associated with SS tasks were reported by Gurchiek et al to be 466.28 N, while those linked to COD tasks were reported as being 600.41 N.[10] Either task resulted in an RMSE larger than any produced by the developed regression models in this study. Though, it should be noted that both SS and COD tasks are more dynamic than a jumping action, and this added dynamicity may have contributed to additional noise pollution which may have affected the result of their study. Additionally, similar concerns as those in other studies such as

the effect of skin laxity and individual regression model development must also be considered.[10]

4.3. Angular Velocity V. Moment (Valgus/Varus)

Various studies have shown that increases in valgus moment in conjunction with increases in antero-tibial shear, increases the stress experienced by the ACL.[12,88] Additionally, it has been observed that shear force combined with knee valgus/varus moments significantly increases the strain that the ACL sustains.[89] Markolf et al also noted that anterior shear in conjunction with a valgus/varus moment produces stress far greater than that produced by either component individually.[88] Hewett et al conducted a study to determine potential predictive factors that could be used in understanding risk factors for female athletes and found athletes that experienced an ACL injuries had a 2.5x greater knee valgus moment ($p < 0.01$).[51,52] Further investigation on the part of Hewett et al revealed that the magnitude of knee valgus moment was able to predict ACL injury status (73% specificity; 78% sensitivity).[51,52]

This information lead to the conclusion that tracking the valgus/varus moment experienced by the knee would be important in tracking ACL fatigue. Initially, the thought was to compare the anteroposterior angular velocity obtained by the IMU to the valgus/varus moment obtained by the load cells, however, further thinking revealed that a moment is comprised of a rotation as well as a force. Therefore, the thought of utilizing a multi-linear regression model in where the independent variables were the angular velocity (rotational component) and linear acceleration (force) as obtained by the IMU came about. When comparing both models, it was clear that the multi-linear regression model was more appropriate to be used for on-field testing.

However, nearly all studies that have attempted tracking valgus/varus moment through angular velocity of an IMU have utilized linear regression modeling.[8,11] It may be possible that the lower testing conditions (i.e. differing, less dynamic actions) of some studies might lead to a developed linear model being more apt for usage, or with the inclusion of specimens at lower testing parameters, might lead to the developed of a linear regression model being better suited to model our data. Although, the stark improvement in all aspects (R^2-value, RMSE, and Abs % Error) when employing the multi-linear regression model instead of a linear model leads itself to thinking valgus/varus moment should be plotted as a multiple variable function.

Similar to our study with respect to observed actions was the study conducted by Dowling et al.[8] Within their study, Dowling et al recruited 26 subjects and had them drop from a 36 cm high box as well as perform a maximum vertical high jump.[8] While not a one-legged landing as was simulated during our study, the jumping actions observed by the team is comparable. Additionally, Dowling et al made use of a combination of motion capture camera system (Qualysis; 47 marker protocol; 120Hz) and force plates (Bertec; 1200Hz) to determine knee joint kinetics through the point cluster method and inverse dynamic approach as was performed by Andriacchi et al.[8,90] These calculated knee joint kinetics were then compared to the angular velocities as obtained by an IMU (Physiolog; 240Hz).[8] Dowling et al reported a correlation coefficient (R) between the anteroposterior angular velocity and valgus/varus moment of the knee to be 0.43 ($p < 0.05$).[8] This was observed as being much smaller than the correlation coefficients associated with either the linear regression model developed within our study ($R = 0.66$) or the multi-linear regression model ($R = 0.80$) It should be noted though that the study by Dowling et al shows the potential relationship between angular velocity and moment, but it should equally be noted that a lack of a reported RMSE or abs % error gives pause to the effectiveness of their IMU ability to track valgus moments using angular velocity.[8]

Another study conducted by Konrath et al also sought to estimate knee valgus/varus moments using IMUs, but utilized actions there were less dynamic than either those examined by Dowling et al or those within our study.[11] Using IMUs (Xsens Awinda; 60Hz) and a motion capture camera system (Oqus 300 series; 53 marker protocol; 120Hz), participants in the study conducted by Konrath et al were asked to perform a stair ascent/descent as well as a sit-to-stand movement.[11] It was observed by Konrath et al that the R-value between the IMU and motion capture system ranged from strong to very strong (R-values: Stair Ascent: 0.86; Stair Descent: 0.74; Sit-to-stand: 0.98).[11] Additionally, RMSE values were reported by Konrath et al in terms of subject's body weight and body height (RMSE: Stair Ascent: 0.01; Stair Descent: 0.014; Sit-to-stand: 0.006).[11] The values reported by Konrath et al were larger than those by Dowling et al and show a very close relationship between the two aspects, however, because of the more dynamic actions associated within the Dowling et al study, it is possible that noise pollution had an effect.[8,11] Moreover, while the RMSE values associated with the Konrath et al study appear to be smaller than those within our study, noise pollution may have influenced our results as

well. However, it should be noted that the Konrath et al study utilized more elderly subjects, which would mean additional stress would be placed on the effect of skin laxity.

4.4. Angular Velocity V. Moment (Internal/External Rotation)

Studies have observed that increases in the internal rotational moment in combination with some antero-tibial shear increases the stress the ACL experiences, additionally, this mixture of loading in conjunction with a valgus moment significantly increases the experienced stress.[88] Furthermore, studies have also observed that antero-tibial shear in concurrence with internal rotation and valgus moments significantly increases the strain experienced by the ACL.[89,91] Of note are the observations reported by Shin et al in a study that sought to quantify the combined effect of valgus and internal rotational moments on ACL strain during a single-leg landing.[91] Using vivo human loading data and a previously validated simulation model of knee dynamics, Shin et al was able to predict strains an ACL would experience and reported that a combination of maximum physiological valgus and internal rotational moments produced a predicted peak strain of 0.105.[91] It was also noted by Shin et al that the reported range for ACL rupture due to strain is between 0.09-0.15.[91] Furthermore, when they increased the parameters to conditions akin to game situations, Shin et al saw predicted strains as high as 0.115.[91] Shin et al also reported that the application of either rotational moment (internal/external) caused increases in the strain experienced by the ACL, with increases of 27% when only subjected to a peak internal rotational moment, and 34% when combined with a vertical force.[91]

While a combination of internal rotational and valgus moments leads to greater stresses/strains on the ACL, in-game maneuvers that have been observed to lead to ACL failure (such as one-footed landings) are observed to produce very high valgus moments with respect to normal gameplay.[92] Additionally, while sex discrepancies exist in where females experience higher degrees of valgus and internal rotational moments, more emphasis has been placed on valgus moments, as it has been regarded as being more disruptive to the integrity of the ACL.[92,93]

However, this does not diminish the significance of internal/external rotational moment tracking when attempting to track ACL fatigue, as it clearly effects ACL strength to some degree. Originally, we thought to compare the internal/external rotational moment to the vertical angular velocity, however, as noted when constructing models for valgus/varus moments, a

moment is comprised of a rotational and a force component. As such, a multi-linear regression model was constructed in which vertical moment was plotted as a function of the IMU's vertical angular velocity and vertical linear acceleration. When comparing the models, while the fit of the linear was seen as higher, the predictive capabilities of the multi-linear regression model were vastly superior (lower RMSE) and as such, was clearly better for a real-world application.

Other studies have sought to use IMUs or IMU-like instrumentation to track the rotational moment of the knee, though they have employed differing methods than those utilized within our study.[8,94] The study conducted by Dowling et al that sought to compare angular velocities to valgus moments also sought to compare angular velocities to internal/external moments.[8] When observing the angular velocity of the shank with respect to internal/external moment of the knee, an R-value of 0.06 was reported with no significance in correlation.[8] This negligible linear correlation was drastically lower than either correlation associated with the regression models developed within this study. However, of particular note is Dowling et al reported that both thigh angular velocity and the difference between thigh and shank angular velocities were better correlated with the internal/external moment (R=0.17, R=0.20 respectively).[8] This may mean further examination between the IMU associated with femur kinematics is needed within our study. Although, given the multi-linear regression model's predictive capabilities (i.e. relatively low RMSE value) this may be unnecessary.

Karatsidis et al also sought a means to estimate the internal/external moment experienced by the knee, but utilized a full-body internal motion capture (IMC) method to do so.[94] This IMC method made use of 17 IMUs (Xsens MVN Link; 240Hz) that were mounted to various parts of the body and processed though the IMC affiliated software.[94] For the purpose of validation, an optical motion capture system was used by Karatsidis et al, the same make/model that was employed by Konrath et al (Oqus 300 series; 53 marker protocol; 240Hz).[11,94] Participants in the Karatsidis et al study were asked to perform three different walking speeds with the IMC and motion capture system running concurrently.[94] A strong correlation for internal/external rotation was reported by Karatsidis et al (R=0.82; RMSD 0.2 ± 0.1 % BW*BH), higher than that observed by Dowling et al.[8,94] This was also seen as being higher than the R-value associated with our multi-linear regression model (R = 0.67), yet lower than the our developed linear regression model (R = 0.88). However, while the IMC system does show a better correlation and a small RMSD value, it cannot be implemented into gameplay as it would

be a hindrance to athletes. Additionally, while the actions tested by Karatsidis et al range in how dynamic they are, they do not incorporate many of the cutting actions that have been observed to cause ACL failure.[92-94] Although, further investigation into improving IMC technology as to minimize/eliminate hindrance may be warranted.

4.5. Mediolateral Angular Velocity V. Maximum Quadriceps Force

Various studies have examined the effect of quadriceps contraction on ACL injury, and noted that aggressive quadriceps loading (QL) increases the stresses/strains placed on the ligament.[79,95,96] A study conducted by DeMorat et al examined the possibility that aggressive QL induces noncontact ACL injuries and reported that, in conjunction with the knee in slight flexion, increases in QL produces significant increases in aTT and ACL injuries.[79] Furthermore, DeMorat et al stated that the possible central force within noncontact ACL injuries is this QL.[79]

A study by Withrow et al sought to determine the relationship between quadriceps muscle force and ACL strain in an In Vitro simulated jump landing and is particularly interesting in that the same testing conditions/apparatus that were used with the Withrow et al study were used by the Ann Arbor team within our study.[96] Withrow et al observed that increases in ACL strain were proportional to increases in QL ($R^2 = 0.74$; $p < 0.01$), and intriguingly, also reported that impact force was not correlated with ACL strain ($R^2 = 0.009$; $p = 0.08$).[96] This observation by Withrow et al may be indicative of the importance the effect of QL has on ACL fatigue and is also supportive of the claim by DeMorat et al of QL being the central force within non-contact ACL injuries.[79,96]

Because of these observations, it became clear to us the potential importance of being able to track the quadriceps force as it pertains to ACL fatigue level. Initially, we sought if a relationship existed between angular velocity of the femur and quadriceps forces. This was considered because, during one-footed landings, the shank would remain relatively fixed as the angle decreases (knee undergoes flexion). In order to accomplish this knee flexion, some angular displacement of the femur would need to take place. Additionally, as knee flexion increases the quadriceps group (being the main extensors of this joint) would increase in force as it tries to prevent flexing. However, further examination revealed potentials problems in that the shank was not stationary.

Considering the system in terms of a simple machine, the knee joint and quadriceps group can be mapped as a class 3 lever in which the effort (contraction of the quadriceps group as the site of insertion of the patellofemoral ligament is on the tibial tuberosity) is between the fulcrum (considered to be the knee joint, which lies superior to the tibial tuberosity) and load (force experienced by distal end of the shank, or in terms or real-world, force placed on the sole of the foot). Under this consideration, emphasis is placed on the angular velocity of the shank, as any load would cause rotation about the fulcrum producing a contraction by the quadriceps group as it tries to prevent this movement. But this too was considered a poor system as the major assumption under this model is the femur is held stationary, which we have observed to be untrue due to the presence of measurable angular displacements in the femoral IMU.

Thus, both considerations needed to be considered in order to produce an accurate model, as angular displacement of either the femoral or tibial segments would produce a reactionary force within the quadriceps group. Therefore, while a linear regression model was produced for the femoral angular velocities v. quadriceps force, an additional multi-linear regression model was constructed in which the independent variables were the angular velocities of the femur and tibia. While both models were observed to have strong correlations, the RMSE and abs % error associated with the multi-linear regression model were observed to be drastically lower. This ultimately meant that the multi-linear variant was the most appropriate for real-world application.

The comparison of angular velocity from an IMU to quadriceps force and the construction of the multi-linear regression model are particularly exciting as, to our knowledge, there exists no current studies that have attempted this. This potential novel idea in tracking QL from wearable sensors means the potential tracking of ACL strain as studies have presented clear relationships between the two.[79,96] Furthermore, tracking of QL may be employed in determining potential differences between sexes during on-field testing.

A study conducted by Malinzak et al wanted to compare the knee kinematic patterns between male and female recreational athletes and utilized 20 subjects (N = 11 males; N = 9 females), a motion capture system (Motion Analysis Corporation; 240 Hz), a Myosoft system to measure surface EMG signals (Noraxon; 960 HZ) and 3 different actions: running, side-cutting, and cross-cutting.[95] Consistently across all actions, Malinzak et al reported higher quadriceps activity in females than in males, noting differences between the sex's maximum voluntary

contraction electromyograms (EMG) of up to 40%.[95] Given the importance of QL in understanding the ACL fatigue level, this heighten quadriceps activity in females may heavily contribute to understanding why females suffer a higher rate of ACL injuries. Because of the potential of the IMU to track QL in-real-world, future consideration should be given to conducting a study examining the IMUs ability to track sex differences in athlete during games/practices.

4.6. Anteroposterior Linear Acceleration V. aTT

It is commonly known that the function of the ACL is to prevent anterior displacement of the tibia with respect to the femur, and various studies have noted increases in this displacement result in increases in the strain experienced by the ligament.[79,96,97] Additionally, studies have also noted the effect quadriceps contraction and/or load on the leg has on the experienced aTT.[79,96] However, because of this dependency between aTT and other factors, few studies have placed emphasis on tracking aTT in of itself.

Although, a study conducted by Rosene et al did seek to compare differences in aTT between sexes, sports, and leg dominance in collegiate athletes.[98] Utilizing 60 collegiate athletes (N=22 males; N=38 female) and a KT-1000 knee arthrometer to measure aTT (MEDmetric Corporation), Rosene et al observed 3 different sports: volleyball; soccer; basketball.[98] The sports chosen by Rosene et al are of interest as soccer and basketball athletes have been observed to suffer the greatest instances of ACL injury. While no significant differences were observed between sports or leg dominance within the sexes, Rosene et al study did report a significant difference between sexes in terms of aTT, with females reportedly experiencing higher aTT than males ($p < 0.05$).[98] Recent studies have further corroborated the observations by Rosene et al, noting differences between the sexes pre/post ACL reconstruction.[99-101] Furthermore, the observation by Malinzak et al that females experience higher quadriceps activity and the observations by both DeMorat et al and Withrow et al linking QL with aTT, gives further evidence that females may indeed experience higher aTTs than males.[79,95,96] Therefore, the ability to track aTT would not only be a potential means to track ACL fatigue levels, but also a potential means to track differences between sexes when playing the same/similar sport(s). This may give further insight into why females suffer ACL injuries at a higher rate the males.

To our knowledge, IMUs have never been used to track aTT in either a real-world application or in cadaveric testing, indicating how innovative this idea may be. However, there was initial skepticism in the sensitivity of the IMU to be able to track aTT, given how small this displacement is. However, we continued with the construction of a linear regression model in which we linked linear acceleration in the anteroposterior direction to aTT. A strong correlation and the relatively low RMSE and abs % errors gave a good indication that aTT may in fact be a function of linear acceleration and supports the potential for APDM Opal to be able to measure aTT during on-field testing.

4.7. Limitations of Study

There are several limitations we wish to acknowledge within our study. First, the use of cadaveric specimens omits potential artifact motion due to the various tissues that would be present during on-field testing. This limitation was touched upon earlier in multiple sections, and various studies have examined its effect on data acquisition.[102,103] Because the IMUs were directly attached to bone, the natural laxity that is present within muscle/skin cannot be accounted for. This laxity in the tissue may cause noise pollution which in turn, may affect the recordings of the IMUs. However, one could argue that noise pollution is also present within our models as the IMUs were not rigidly fixed onto the bones. While the use of Co-Flex bands and elastic ties may have mitigated most of the noise, it is reasonable to assume that some was still present during the construction of our models. Although, the effect of noise pollution could be combated through the implementation of post collection filter of IMU data. Various studies have looked into potential ways to filter noise from recordings, which warrants future study into a filtering process when employing the IMU during on-field testing.[104,105]

Another limitation present within our study are the parameters that were utilized. We solely focused on forces of 3-4x BW because of its correlation to ACL injuries, however, this also means that our constructed models only account for this upper range. It is possible that, with the addition of specimens at lower forces, models other than what we have suggested may be more appropriate for on-field usage. Furthermore, the addition of these specimens at lower testing parameters may greatly alter the correlation between variables in such a way that a strong fit may become a moderate or low fit. This limitation is extremely important because, while actions like a one-legged landing may induce this high BW force and has been observed to lead

to ACL injuries, other actions such as cross-cutting have also been linked to ACL injuries and induce much lower BW forces.[51,52,57] This may mean our models are only applicable to actions that induce high BW forces and may not be apt for on-field usage. Although, it should be noted that some of the most common actions in the sports that have highest rate of ACL injuries, are these one-legged landings (basketball and soccer). So, while it may not be applicable to all sports, our models might be utilized in basketball and soccer like sports.

Akin to the parameter limitation within our study, a third limitation is the action that was observed. Our study only observed one-legged landings, which do result in ACL injuries, but are not the only cause of them. As mentioned in various sections, actions that result in rapid deceleration or change of direction also influence ACL fatigue levels and injury.[51,52,57] Furthermore, such actions may be considered more dynamic than a one-legged landing and may induce a much greater degree of noise pollution as the IMUs may be subject to additional motion. Further testing might be required in rigs that mimic actions other than a one-legged landing, or on human subjects in a laboratory setting using motion capture technology and EMGs in order to establish trends and construct additional models.

A fourth limitation is the method of regression model construction. While taking the average of the first 30 trials for each specimen is acceptable in constructing relationships between aspects, it also has the unwarranted effect of mitigating the variation that is present within each specimen. Perhaps a more appropriate method would have been to employ a linear-mixed effect model, as it would consider the variation of each specimen. However, construction of basic regression/multi-linear regression models do allow for initial viewing of potential relationships between aspects which in turn may warrant additional model construction in the form of linear-mixed effect models. Further research into the application of these linear-mixed effect models may be merited.

Chapter 5: Conclusion

The purpose of this study was to validate a set of IMUs through cadaveric testing to determine the viability for on-field usage of the device in tracking ACL fatigue levels. Regression models were developed and RMSE and abs % error values were calculated in addition to BA plots that were constructed. Very strong correlations were observed between linear acceleration and force, with strong correlations in nearly all other compared aspects. Additionally, nearly all constructed models produced an abs % error of less than 10%. And while we recognize there to be several limitations with our study, we ultimately conclude that APDM Opal might be viable for on-field usage. However, additional laboratory studies to account for different actions and artifact motion that may be experienced by the IMU may be required before on-field usage begins. But, nevertheless, APDM Opal may be a potential device that could accurately monitor knee kinematics during games/practices that affect ACL fatigue levels, relay that information to coaches and trainers, and ultimately reduce ACL injury rates by allowing players to naturally recover before a ligament rupture occurs and surgery is required.

References

1. Woods, R.A. Sports And Exercise. Labor, U.S.D.o., Ed. U.S. Bureau of Labor Statistics: Washington, D.C, 2017; pp 1-27.

2. Habelt, S.; Hasler, C.C.; Steinbruck, K.; Majewski, M. Sport injuries in adolescents. *Orthop Rev (Pavia)* **2011**, *3*, e18, doi:10.4081/or.2011.e18.

3. Alghamdi, W.; Alzahrani, A.; Alsuwaydi, A.; Alzahrani, A.; Albaqqar, O.; Fatani, M.; Alaidarous, H. Prevalence of Cruciate Logaments Injury among Physical Education Students of Umm Al-Qura University and the Relation betwen the Dominant Body Side and Ligament Injury Side in Non-Contact Injury Type. *American Journal of Medicine and Medical Sciences* **2017**, *7*, 14-19.

4. Saeed, I.O. MRI Evaluation for Post-Traumatic Knee Joint INjuries. *Journal of Nursing and Health Science* **2018**, *7*, 48-51.

5. Wojtys, E.M.; Beaulieu, M.L.; Ashton-Miller, J.A. New perspectives on ACL injury: On the role of repetitive sub-maximal knee loading in causing ACL fatigue failure. *J Orthop Res* **2016**, *34*, 2059-2068, doi:10.1002/jor.23441.

6. Boden, B.P.; Sheehan, F.T.; Torg, J.S.; Hewett, T.E. Noncontact anterior cruciate ligament injuries: mechanisms and risk factors. *J Am Acad Orthop Surg* **2010**, *18*, 520-527, doi:10.5435/00124635-201009000-00003.

7. Launay, F. Sports-related overuse injuries in children. *Orthop Traumatol Surg Res* **2015**, *101*, S139-147, doi:10.1016/j.otsr.2014.06.030.

8. Dowling, A.V.; Favre, J.; Andriacchi, T.P. The Relationship between Segment Angular Velocity and Knee Abduction Moment during a Drop Jump: Implicatoins for ACL Injury Risk Prediction. In Proceedings of 11th Annual Orthopaedic Research Society

9. Elvin, N.G.; Elvin, A.A.; Arnoczky, S.P. Correlation between ground reaction force and tibial acceleration in vertical jumping. *J Appl Biomech* **2007**, *23*, 180-189, doi:10.1123/jab.23.3.180.

10. Gurchiek, R.D.; McGinnis, R.S.; Needle, A.R.; McBride, J.M.; van Werkhoven, H. The use of a single inertial sensor to estimate 3-dimensional ground reaction force during accelerative running tasks. *J Biomech* **2017**, *61*, 263-268, doi:10.1016/j.jbiomech.2017.07.035.

11. Konrath, J.M.; Karatsidis, A.; Schepers, H.M.; Bellusci, G.; de Zee, M.; Andersen, M.S. Estimation of the Knee Adduction Moment and Joint Contact Force during Daily Living Activities Using Inertial Motion Capture. *Sensors (Basel)* **2019**, *19*, doi:10.3390/s19071681.

12. Hollis, J.M.; Takai, S.; Adams, D.J.; Horibe, S.; Woo, S.L. The effects of knee motion and external loading on the length of the anterior cruciate ligament (ACL): a kinematic study. *J Biomech Eng* **1991**, *113*, 208-214, doi:10.1115/1.2891236.

13. Anterior Cruciate Ligament (ACL) Tears. Availabe online: https://www.pinnacle-ortho.com/anterior-cruciate-ligament-acl-tears

14. Frank, C.B. Ligament structure, physiology and function. *J Musculoskelet Neuronal Interact* **2004**, *4*, 199-201.

15. Benjamin, M.; Ralphs, J.R. Tendons and ligaments--an overview. *Histol Histopathol* **1997**, *12*, 1135-1144.

16. Apostolakos, J.; Durant, T.J.; Dwyer, C.R.; Russell, R.P.; Weinreb, J.H.; Alaee, F.; Beitzel, K.; McCarthy, M.B.; Cote, M.P.; Mazzocca, A.D. The enthesis: a review of the tendon-to-bone insertion. *Muscles Ligaments Tendons J* **2014**, *4*, 333-342.

17. Mow, V.C.; Ateshian, G.A.; Spilker, R.L. Biomechanics of diarthrodial joints: a review of twenty years of progress. *J Biomech Eng* **1993**, *115*, 460-467, doi:10.1115/1.2895525.

18. Wang, J.H.; Guo, Q.; Li, B. Tendon biomechanics and mechanobiology--a minireview of basic concepts and recent advancements. *J Hand Ther* **2012**, *25*, 133-140; quiz 141, doi:10.1016/j.jht.2011.07.004.

19. Robi, K.; Jakob, N.; Matevz, K.; Matjaz, V. The Physiology of Sports Injuries and Repair Processes. 2013; 10.5772/54234pp 42-86.

20. Woo, S.L.; Debski, R.E.; Zeminski, J.; Abramowitch, S.D.; Saw, S.S.; Fenwick, J.A. Injury and repair of ligaments and tendons. *Annu Rev Biomed Eng* **2000**, *2*, 83-118, doi:10.1146/annurev.bioeng.2.1.83.

21. Killian, M.L.; Cavinatto, L.; Galatz, L.M.; Thomopoulos, S. The role of mechanobiology in tendon healing. *J Shoulder Elbow Surg* **2012**, *21*, 228-237, doi:10.1016/j.jse.2011.11.002.

22. Georgiev, G.P.; Iliev, A.; Kotov, G.; Nedialkova, V.K.; Kirkov, V.; Landzhov, B. Epiligament Tissue of the Medial Collateral Ligament in Rat Knee Joint: Ultrastructural Study. *Cureus* **2019**, *11*, e3812, doi:10.7759/cureus.3812.

23. Knee Ligament Treatment. https://www.fitnessphysio.com/knee-ligament-injury. **2020**.

24. LaPrade, R.F.; Engebretsen, A.H.; Ly, T.V.; Johansen, S.; Wentorf, F.A.; Engebretsen, L. The anatomy of the medial part of the knee. *J Bone Joint Surg Am* **2007**, *89*, 2000-2010, doi:10.2106/JBJS.F.01176.

25. Phisitkul, P.; James, S.L.; Wolf, B.R.; Amendola, A. MCL injuries of the knee: current concepts review. *Iowa Orthop J* **2006**, *26*, 77-90.

26. Chen, L.; Kim, P.D.; Ahmad, C.S.; Levine, W.N. Medial collateral ligament injuries of the knee: current treatment concepts. *Curr Rev Musculoskelet Med* **2008**, *1*, 108-113, doi:10.1007/s12178-007-9016-x.

27. Griffith, C.J.; LaPrade, R.F.; Johansen, S.; Armitage, B.; Wijdicks, C.; Engebretsen, L. Medial knee injury: Part 1, static function of the individual components of the main medial knee structures. *Am J Sports Med* **2009**, *37*, 1762-1770, doi:10.1177/0363546509333852.

28. Cavaignac, E.; Carpentier, K.; Pailhe, R.; Luyckx, T.; Bellemans, J. The role of the deep medial collateral ligament in controlling rotational stability of the knee. *Knee Surg Sports Traumatol Arthrosc* **2015**, *23*, 3101-3107, doi:10.1007/s00167-014-3095-1.

29. Recondo, J.A.; Salvador, E.; Villanua, J.A.; Barrera, M.C.; Gervas, C.; Alustiza, J.M. Lateral stabilizing structures of the knee: functional anatomy and injuries assessed with MR imaging. *Radiographics* **2000**, *20 Spec No*, S91-S102, doi:10.1148/radiographics.20.suppl_1.g00oc02s91.

30. Amis, A.A.; Gupte, C.M.; Bull, A.M.; Edwards, A. Anatomy of the posterior cruciate ligament and the meniscofemoral ligaments. *Knee Surg Sports Traumatol Arthrosc* **2006**, *14*, 257-263, doi:10.1007/s00167-005-0686-x.

31. Gali, J.C.; Oliveira, H.C.S.; Lisboa, B.C.B.; Dias, B.D.; Casimiro, F.G.; Caetano, E.B. Tibial Insertions of the Posterior Cruciate Ligament: Topographic Anatomy and Morphometric Study. *Rev Bras Ortop* **2013**, *48*, 263-267, doi:10.1016/j.rboe.2012.06.005.

32. Lopes, O.V., Jr.; Ferretti, M.; Shen, W.; Ekdahl, M.; Smolinski, P.; Fu, F.H. Topography of the femoral attachment of the posterior cruciate ligament. *J Bone Joint Surg Am* **2008**, *90*, 249-255, doi:10.2106/JBJS.G.00448.

33. Anderson, C.J.; Ziegler, C.G.; Wijdicks, C.A.; Engebretsen, L.; LaPrade, R.F. Arthroscopically pertinent anatomy of the anterolateral and posteromedial bundles of the posterior cruciate ligament. *J Bone Joint Surg Am* **2012**, *94*, 1936-1945, doi:10.2106/JBJS.K.01710.

34. Arliani, G.G.; Astur Dda, C.; Kanas, M.; Kaleka, C.C.; Cohen, M. Anterior Cruciate Ligament Injury: Treatment and Rehabilitation. Current Perspectives and Trends. *Rev Bras Ortop* **2012**, *47*, 191-196, doi:10.1016/S2255-4971(15)30085-9.

35. Nagano, Y.; Ida, H.; Akai, M.; Fukubayashi, T. Biomechanical characteristics of the knee joint in female athletes during tasks associated with anterior cruciate ligament injury. *Knee* **2009**, *16*, 153-158, doi:10.1016/j.knee.2008.10.012.

36. Bach, B.R., Jr.; Levy, M.E.; Bojchuk, J.; Tradonsky, S.; Bush-Joseph, C.A.; Khan, N.H. Single-incision endoscopic anterior cruciate ligament reconstruction using patellar tendon autograft. Minimum two-year follow-up evaluation. *Am J Sports Med* **1998**, *26*, 30-40, doi:10.1177/03635465980260012201.

37. Arthroscopic ACL Reconstruction Technique using Patellar Tendon Autograft (Diagrams).

38. Duthon, V.B.; Barea, C.; Abrassart, S.; Fasel, J.H.; Fritschy, D.; Menetrey, J. Anatomy of the anterior cruciate ligament. *Knee Surg Sports Traumatol Arthrosc* **2006**, *14*, 204-213, doi:10.1007/s00167-005-0679-9.

39. Purnell, M.L.; Larson, A.I.; Clancy, W. Anterior cruciate ligament insertions on the tibia and femur and their relationships to critical bony landmarks using high-resolution volume-rendering computed tomography. *Am J Sports Med* **2008**, *36*, 2083-2090, doi:10.1177/0363546508319896.

40. Zyl, R.v.; Schoor, A.N.v.; Toit, P.J.d.; Louw, E.M. Clinical anatomy of the anterior cruciate ligament and pre-operativeprediction of ligament length. *SA Orthopaedic Journal* **2016**, *15*, 47-52.

41. Harner, C.D.; Baek, G.H.; Vogrin, T.M.; Carlin, G.J.; Kashiwaguchi, S.; Woo, S.L.-Y. Quantitative Analysis of Human Cruciate Ligament Insertions. *The Journal of Arthroscopic and Related Surgery* **1999**, *15*, 741-749.

42. Castile, R.M.; Skelley, N.W.; Babaei, B.; Brophy, R.H.; Lake, S.P. Microstructural properties and mechanics vary between bundles of the human anterior cruciate ligament during stress-relaxation. *J Biomech* **2016**, *49*, 87-93, doi:10.1016/j.jbiomech.2015.11.016.

43. Stieven-Filho, E.; Garschagen, E.T.; Namba, M.; Silva, J.L.; Malafaia, O.; Cunha, L.A. Anatomic study of the double-bundle of the anterior cruciate ligament with the knee in 90 masculine flexion. *Rev Col Bras Cir* **2011**, *38*, 338-342.

44. Amis, A.A.; Dawkins, G.P. Functional anatomy of the anterior cruciate ligament. Fibre bundle actions related to ligament replacements and injuries. *J Bone Joint Surg Br* **1991**, *73*, 260-267.

45. Otsubo, H.; Akatsuka, Y.; Takashima, H.; Suzuki, T.; Suzuki, D.; Kamiya, T.; Ikeda, Y.; Matsumura, T.; Yamashita, T.; Shino, K. MRI depiction and 3D visualization of three anterior cruciate ligament bundles. *Clin Anat* **2017**, *30*, 276-283, doi:10.1002/ca.22810.
46. Shen, W.; Fu, F.H. Anterior cruciate ligament insertion site anatomy. *Arthroscopy* **2008**, *24*, 850-851; authhor reply 851-852, doi:10.1016/j.arthro.2008.04.069.

47. Matsumoto, H.; Suda, Y.; Otani, T.; Niki, Y.; Seedhom, B.B.; Fujikawa, K. Roles of the anterior cruciate ligament and the medial collateral ligament in preventing valgus instability. *J Orthop Sci* **2001**, *6*, 28-32, doi:10.1007/s007760170021.

48. Mommersteeg, T.J.; Kooloos, J.G.; Blankevoort, L.; Kauer, J.M.; Huiskes, R.; Roeling, F.Q. The fibre bundle anatomy of human cruciate ligaments. *J Anat* **1995**, *187 (Pt 2)*, 461-471.

49. Woo, S.L.; Hollis, J.M.; Adams, D.J.; Lyon, R.M.; Takai, S. Tensile properties of the human femur-anterior cruciate ligament-tibia complex. The effects of specimen age and orientation. *Am J Sports Med* **1991**, *19*, 217-225, doi:10.1177/036354659101900303.

50. Woo, S.L.; Wu, C.; Dede, O.; Vercillo, F.; Noorani, S. Biomechanics and anterior cruciate ligament reconstruction. *J Orthop Surg Res* **2006**, *1*, 2, doi:10.1186/1749-799X-1-2.

51. Hewett, T.E.; Ford, K.R.; Myer, G.D. Anterior cruciate ligament injuries in female athletes: Part 2, a meta-analysis of neuromuscular interventions aimed at injury prevention. *Am J Sports Med* **2006**, *34*, 490-498, doi:10.1177/0363546505282619.

52. Hewett, T.E.; Myer, G.D.; Ford, K.R. Anterior cruciate ligament injuries in female athletes: Part 1, mechanisms and risk factors. *Am J Sports Med* **2006**, *34*, 299-311, doi:10.1177/0363546505284183.

53. Myer, G.D.; Paterno, M.V.; Ford, K.R.; Quatman, C.E.; Hewett, T.E. Rehabilitation after anterior cruciate ligament reconstruction: criteria-based progression through the return-to-sport phase. *J Orthop Sports Phys Ther* **2006**, *36*, 385-402, doi:10.2519/jospt.2006.2222.

54. Paterno, M.V.; Schmitt, L.C.; Ford, K.R.; Rauh, M.J.; Myer, G.D.; Huang, B.; Hewett, T.E. Biomechanical measures during landing and postural stability predict second anterior cruciate ligament injury after anterior cruciate ligament reconstruction and return to sport. *Am J Sports Med* **2010**, *38*, 1968-1978, doi:10.1177/0363546510376053.

55. Schiable, G. Preventing The ACL Injury Epidemic with Strength & Conditioning. **2020**.

56. Are you Ready for Some Football? Tackling Orthopedic Injuries. **2016**.

57. Pfeifer, C.E.; Beattie, P.F.; Sacko, R.S.; Hand, A. Risk Factors Associated with Non-Contact Anterior Cruciate Ligament Injury: A Systematic Review. *Int J Sports Phys Ther* **2018**, *13*, 575-587.

58. Geng, B.; Wang, J.; Ma, J.L.; Zhang, B.; Jiang, J.; Tan, X.Y.; Xia, Y.Y. Narrow Intercondylar Notch and Anterior Cruciate Ligament Injury in Female Nonathletes with Knee Osteoarthritis Aged 41-65 Years in Plateau Region. *Chin Med J (Engl)* **2016**, *129*, 2540-2545, doi:10.4103/0366-6999.192771.

59. Griffin, L.Y.; Agel, J.; Albohm, M.J.; Arendt, E.A.; Dick, R.W.; Garrett, W.E.; Garrick, J.G.; Hewett, T.E.; Huston, L.; Ireland, M.L., et al. Noncontact anterior cruciate ligament injuries: risk factors and prevention strategies. *J Am Acad Orthop Surg* **2000**, *8*, 141-150, doi:10.5435/00124635-200005000-00001.

60. Smith, H.C.; Vacek, P.; Johnson, R.J.; Slauterbeck, J.R.; Hashemi, J.; Shultz, S.; Beynnon, B.D. Risk factors for anterior cruciate ligament injury: a review of the literature - part 1: neuromuscular and anatomic risk. *Sports Health* **2012**, *4*, 69-78, doi:10.1177/1941738111428281.

61. Smith, H.C.; Vacek, P.; Johnson, R.J.; Slauterbeck, J.R.; Hashemi, J.; Shultz, S.; Beynnon, B.D. Risk factors for anterior cruciate ligament injury: a review of the literature-part 2: hormonal, genetic, cognitive function, previous injury, and extrinsic risk factors. *Sports Health* **2012**, *4*, 155-161, doi:10.1177/1941738111428282.

62. McLean, S.G.; Huang, X.; van den Bogert, A.J. Association between lower extremity posture at contact and peak knee valgus moment during sidestepping: implications for ACL injury. *Clin Biomech (Bristol, Avon)* **2005**, *20*, 863-870, doi:10.1016/j.clinbiomech.2005.05.007.

63. Mountcastle, S.B.; Posner, M.; Kragh, J.F., Jr.; Taylor, D.C. Gender differences in anterior cruciate ligament injury vary with activity: epidemiology of anterior cruciate ligament injuries in a young, athletic population. *Am J Sports Med* **2007**, *35*, 1635-1642, doi:10.1177/0363546507302917.

64. O'Malley, K.; Rubinstein, A.; Postma, W. Anterior Cruciate Ligament Injury: Current Understanding of Risk Factors. *Orthopedics and Rheumatology Open Access Journal* **2015**, *1*, 1-8, doi:10.19080/OROAJ.2015.01.555565.

65. Kobayashi, H.; Kanamura, T.; Koshida, S.; Miyashita, K.; Okado, T.; Shimizu, T.; Yokoe, K. Mechanisms of the anterior cruciate ligament injury in sports activities: a twenty-year clinical research of 1,700 athletes. *J Sports Sci Med* **2010**, *9*, 669-675.

66. Olsen, O.E.; Myklebust, G.; Engebretsen, L.; Bahr, R. Injury mechanisms for anterior cruciate ligament injuries in team handball: a systematic video analysis. *Am J Sports Med* **2004**, *32*, 1002-1012, doi:10.1177/0363546503261724.

67. Carlson, V.R.; Sheehan, F.T.; Boden, B.P. Video Analysis of Anterior Cruciate Ligament (ACL) Injuries: A Systematic Review. *JBJS Rev* **2016**, *4*, doi:10.2106/JBJS.RVW.15.00116.

68. Thomson, A.; Whiteley, R.; Bleakley, C. Higher shoe-surface interaction is associated with doubling of lower extremity injury risk in football codes: a systematic review and meta-analysis. *Br J Sports Med* **2015**, *49*, 1245-1252, doi:10.1136/bjsports-2014-094478.

69. Koga, H.; Nakamae, A.; Shima, Y.; Iwasa, J.; Myklebust, G.; Engebretsen, L.; Bahr, R.; Krosshaug, T. Mechanisms for noncontact anterior cruciate ligament injuries: knee joint kinematics in 10 injury situations from female team handball and basketball. *Am J Sports Med* **2010**, *38*, 2218-2225, doi:10.1177/0363546510373570.

70. Renstrom, P.; Ljungqvist, A.; Arendt, E.; Beynnon, B.; Fukubayashi, T.; Garrett, W.; Georgoulis, T.; Hewett, T.E.; Johnson, R.; Krosshaug, T., et al. Non-contact ACL injuries in female athletes: an International Olympic Committee current concepts statement. *Br J Sports Med* **2008**, *42*, 394-412, doi:10.1136/bjsm.2008.048934.

71. Makovith, S.A.; Blauwet, C.A. Traumatic Knee Injuries. **2017**.

72. Alford, J.W.; Bernard R. Bach, J. Managing ACL tears: Evaluation and diagnosis. *The Journal of Musculoskeletal Medicine* **2004**, *21*, 381-390.

73. Souryal, T.O.; Freeman, T.R. Intercondylar notch size and anterior cruciate ligament injuries in athletes. A prospective study. *Am J Sports Med* **1993**, *21*, 535-539, doi:10.1177/036354659302100410.

74. Myer, G.D.; Ford, K.R.; Hewett, T.E. Rationale and Clinical Techniques for Anterior Cruciate Ligament Injury Prevention Among Female Athletes. *J Athl Train* **2004**, *39*, 352-364.

75. Brent, J.L.; Myer, G.D.; Ford, K.R.; Paterno, M.V.; Hewett, T.E. The effect of sex and age on isokinetic hip-abduction torques. *J Sport Rehabil* **2013**, *22*, 41-46, doi:10.1123/jsr.22.1.41.

76. Briem, K.; Jonsdottir, K.V.; Arnason, A.; Sveinsson, T. Effects of Sex and Fatigue on Biomechanical Measures During the Drop-Jump Task in Children. *Orthop J Sports Med* **2017**, *5*, 2325967116679640, doi:10.1177/2325967116679640.

77. Knapik, J.J.; Bauman, C.L.; Jones, B.H.; Harris, J.M.; Vaughan, L. Preseason strength and flexibility imbalances associated with athletic injuries in female collegiate athletes. *Am J Sports Med* **1991**, *19*, 76-81, doi:10.1177/036354659101900113.

78. Nilstad, A.; Andersen, T.E.; Bahr, R.; Holme, I.; Steffen, K. Risk factors for lower extremity injuries in elite female soccer players. *Am J Sports Med* **2014**, *42*, 940-948, doi:10.1177/0363546513518741.

79. DeMorat, G.; Weinhold, P.; Blackburn, T.; Chudik, S.; Garrett, W. Aggressive quadriceps loading can induce noncontact anterior cruciate ligament injury. *Am J Sports Med* **2004**, *32*, 477-483, doi:10.1177/0363546503258928.

80. Lipps, D.B.; Oh, Y.K.; Ashton-Miller, J.A.; Wojtys, E.M. Effect of increased quadriceps tensile stiffness on peak anterior cruciate ligament strain during a simulated pivot landing. *J Orthop Res* **2014**, *32*, 423-430, doi:10.1002/jor.22531.

81. Lipps, D.B.; Wojtys, E.M.; Ashton-Miller, J.A. Anterior cruciate ligament fatigue failures in knees subjected to repeated simulated pivot landings. *Am J Sports Med* **2013**, *41*, 1058-1066, doi:10.1177/0363546513477836.

82. Asuero, A.G.; Sayago, A.; Gonzales, A.G. The Correlation Coefficent: An Overview. *Critical Reviews in Analytical Chemistry* **2007**, 10.1080/10408340500526766, 41-59, doi:10.1080/10408340500526766.

83. Altman, D.G.; Bland, J.M. Assessing Agreement between Methods of Measurement. *Clin Chem* **2017**, *63*, 1653-1654, doi:10.1373/clinchem.2016.268870.

84. Bland, J.M.; Altman, D.G. Statistical methods for assessing agreement between two methods of clinical measurement. *Lancet* **1986**, *1*, 307-310.

85. Bland, J.M.; Altman, D.G. Agreed statistics: measurement method comparison. *Anesthesiology* **2012**, *116*, 182-185, doi:10.1097/ALN.0b013e31823d7784.

86. Giavarina, D. Understanding Bland Altman analysis. *Biochem Med (Zagreb)* **2015**, *25*, 141-151, doi:10.11613/BM.2015.015.

87. Meyer, U.; Ernst, D.; Schott, S.; Riera, C.; Hattendorf, J.; Romkes, J.; Granacher, U.; Gopfert, B.; Kriemler, S. Validation of two accelerometers to determine mechanical loading of physical activities in children. *J Sports Sci* **2015**, *33*, 1702-1709, doi:10.1080/02640414.2015.1004638.

88. Markolf, K.L.; Burchfield, D.M.; Shapiro, M.M.; Shepard, M.F.; Finerman, G.A.; Slauterbeck, J.L. Combined knee loading states that generate high anterior cruciate ligament forces. *J Orthop Res* **1995**, *13*, 930-935, doi:10.1002/jor.1100130618.

89. Yu, B.; Garrett, W.E. Mechanisms of non-contact ACL injuries. *Br J Sports Med* **2007**, *41 Suppl 1*, i47-51, doi:10.1136/bjsm.2007.037192.

90. Andriacchi, T.P.; Alexander, E.J.; Toney, M.K.; Dyrby, C.; Sum, J. A point cluster method for in vivo motion analysis: applied to a study of knee kinematics. *J Biomech Eng* **1998**, *120*, 743-749, doi:10.1115/1.2834888.

91. Shin, C.S.; Chaudhari, A.M.; Andriacchi, T.P. Valgus plus internal rotation moments increase anterior cruciate ligament strain more than either alone. *Med Sci Sports Exerc* **2011**, *43*, 1484-1491, doi:10.1249/MSS.0b013e31820f8395.

92. McLean, S.G.; Lipfert, S.W.; van den Bogert, A.J. Effect of gender and defensive opponent on the biomechanics of sidestep cutting. *Med Sci Sports Exerc* **2004**, *36*, 1008-1016, doi:10.1249/01.mss.0000128180.51443.83.

93. Sigward, S.M.; Powers, C.M. Loading characteristics of females exhibiting excessive valgus moments during cutting. *Clin Biomech (Bristol, Avon)* **2007**, *22*, 827-833, doi:10.1016/j.clinbiomech.2007.04.003.

94. Karatsidis, A.; Jung, M.; Schepers, H.M.; Bellusci, G.; Zee, M.d.; Veltink, P.H.; Andersen, M.S. Predicting kinetics using musculoskeletal modeling and inertial motion capture.

95. Malinzak, R.A.; Colby, S.M.; Kirkendall, D.T.; Yu, B.; Garrett, W.E. A comparison of knee joint motion patterns between men and women in selected athletic tasks. *Clin Biomech (Bristol, Avon)* **2001**, *16*, 438-445, doi:10.1016/s0268-0033(01)00019-5.

96. Withrow, T.J.; Huston, L.J.; Wojtys, E.M.; Ashton-Miller, J.A. The relationship between quadriceps muscle force, knee flexion, and anterior cruciate ligament strain in an in vitro simulated jump landing. *Am J Sports Med* **2006**, *34*, 269-274, doi:10.1177/0363546505280906.

97. Keizer, M.N.J.; Otten, E. Passive anterior tibia translation in anterior cruciate ligament-injured, anterior cruciate ligament-reconstructed and healthy knees: a systematic review. *Musculoskelet Surg* **2019**, *103*, 121-130, doi:10.1007/s12306-018-0572-6.

98. Rosene, J.M.; Fogarty, T.D. Anterior tibial translation in collegiate athletes with normal anterior cruciate ligament integrity. *J Athl Train* **1999**, *34*, 93-98.

99. Ahlden, M.; Sernert, N.; Karlsson, J.; Kartus, J. Outcome of anterior cruciate ligament reconstruction with emphasis on sex-related differences. *Scand J Med Sci Sports* **2012**, *22*, 618-626, doi:10.1111/j.1600-0838.2011.01306.x.

100. Lindstrom, M.; Strandberg, S.; Wredmark, T.; Fellander-Tsai, L.; Henriksson, M. Functional and muscle morphometric effects of ACL reconstruction. A prospective CT study with 1 year follow-up. *Scand J Med Sci Sports* **2013**, *23*, 431-442, doi:10.1111/j.1600-0838.2011.01417.x.

101. Teitsma, X.M.; van der Hoeven, H.; Tamminga, R.; de Bie, R.A. Impact of Patient Sex on Clinical Outcomes: Data From an Anterior Cruciate Ligament Reconstruction Registry, 2008-2013. *Orthop J Sports Med* **2014**, *2*, 2325967114550638, doi:10.1177/2325967114550638.

102. Peters, A.; Galna, B.; Sangeux, M.; Morris, M.; Baker, R. Quantification of soft tissue artifact in lower limb human motion analysis: a systematic review. *Gait Posture* **2010**, *31*, 1-8, doi:10.1016/j.gaitpost.2009.09.004.

103. Tsai, T.Y.; Lu, T.W.; Kuo, M.Y.; Lin, C.C. Effects of soft tissue artifacts on the calculated kinematics and kinetics of the knee during stair-ascent. *J Biomech* **2011**, *44*, 1182-1188, doi:10.1016/j.jbiomech.2011.01.009.

104. Chen, X.; Wnag, M.; Zhang, Y.; Feng, Y.; Wu, Z.; Huang, N.E. Detecting Signals from Data with Noise: Theory and Applications. *Journal of the Atmospheric Sciences* **2013**, *70*, 1489-1504.

105. Wood, L.B.; Asada, H. Low variance adaptive filter for cancelling motion artifact in wearable photoplethysmogram sensor signals. *Conf Proc IEEE Eng Med Biol Soc* **2007**, *2007*, 652-655, doi:10.1109/IEMBS.2007.4352374.

Appendix

A1: MATLAB Script 1

```
force=rstData.bndForce(:,:);

a1_tibial_force=force(:,1);
a2_tibial_force=force(:,2);
a3_tibial_force=force(:,3);
a4_tibial_force=force(:,4);

a5_femoral_force=force(:,5);
a6_femoral_force=force(:,6);
a7_femoral_force=force(:,7);
a8_femoral_force=force(:,8);

aa_max_tibial_x(z,:)=max(a1_tibial_force);
ab_max_tibial_y(z,:)=max(a2_tibial_force);
ac_max_tibial_z(z,:)=max(a3_tibial_force);
ad_max_tibial_resultant(z,:)=max(a4_tibial_force);
ae_max_femoral_x(z,:)=max(a5_femoral_force);
af_max_femoral_y(z,:)=max(a6_femoral_force);
ag_max_femoral_z(z,:)=max(a7_femoral_force);
ah_max_femoral_resultant(z,:)=max(a8_femoral_force);

clear 'vertical_tibial'
clear 'vertical_femoral'
clear 'vertical_resultant_tibial'
clear 'vertical_resultant_femoral'
clear 'force'

moment=rstData.bndTorque(:,:);

tibial_moment_x=moment(:,1);
tibial_moment_y=moment(:,2);
tibial_moment_z=moment(:,3);
femoral_moment_x=moment(:,4);
femoral_moment_y=moment(:,5);
femoral_moment_z=moment(:,6);

e_max_moment_tibial_x(z,:)=max(tibial_moment_x);
f_min_moment_tibial_x(z,:)=min(tibial_moment_x);
g_max_moment_tibial_y(z,:)=max(tibial_moment_y);
h_min_moment_tibial_y(z,:)=min(tibial_moment_y);
i_max_moment_tibial_z(z,:)=max(tibial_moment_z);
```

```
j_min_moment_tibial_z(z,:)=min(tibial_moment_z);
k_max_femoral_moment_x(z,:)=max(femoral_moment_x);
l_min_femoral_moment_x(z,:)=min(femoral_moment_x);
l_max_femoral_moment_y(z,:)=max(femoral_moment_y);
m_min_femoral_moment_y(z,:)=min(femoral_moment_y);
n_max_femoral_moment_z(z,:)=max(femoral_moment_z);
o_min_femoral_moment_z(z,:)=min(femoral_moment_z);

quad=rstData.mtuForce(:,6);
p_max_quad_force(z,:)=max(quad);

z=z+1;
```

A2: MATLAB Script 2

```
prompt = {'Enter the name of the file'};
title = 'File Name';
definput = {'name.h5'};
opts.Interpreter = 'tex';
answer = inputdlg(prompt,title,[1 50],definput,opts);
name=char(answer);
clear 'prompt';
clear 'title';
clear 'definput';
clear 'opts';
clear 'answer';

m=0;
a=name(end-2:end);
switch a
   case '.h5'
      m=1;
end
if(m==0)
   file='.h5';
   name={name,file};
   name=strjoin(name);
   name=name(~isspace(name));
end
clear 'a'
clear 'file'
clear 'm';

e=0;
a=name(1:5);
switch a
```

```
    case 'Left_'
        e=1;
    case 'Right'
        e=2;
end
switch e
    case 1
        b=name(6:10);
    case 2
        b=name(7:11);
end
clear 'a'
clear 'e';

info=h5info(name);

sensor_number=getfield(info, 'Groups',{2}, 'Groups', 'Name');
clear 'info';

location=which(name);
str_acc=('/Accelerometer');
str_gyo=('/Gyroscope');

acceleration={sensor_number,str_acc};
acceleration=strjoin(acceleration);
acceleration=acceleration(~isspace(acceleration));

gyroscope={sensor_number,str_gyo};
gyroscope=strjoin(gyroscope);
gyroscope=gyroscope(~isspace(gyroscope));

acc= h5read(location,acceleration);
gyro= h5read(location,gyroscope);

clear 'acceleration';
clear 'gyroscope';
clear 'location';
clear 'name';
clear 'sensor_number';
clear 'str_acc';
clear 'str_gyo';

linear=transpose(acc);
angular=transpose(gyro);

clear 'acc';
```

```
clear 'gyro';

plot(linear(:,1));
title('Preview of the Data');

question=questdlg('Please select the range you wish to analyze', 'Selecting a Range',
'Okay','defbtn');

clear 'question'

plot(linear(:,1));
[x]=ginput(2);
begin=x(1,1);
finish=x(2,1);
begin=sprintf('%.0f',begin);
finish=sprintf('%.0f',finish);
begin=str2double(begin);
finish=str2double(finish);

x=begin;
j=1;
while (x<=finish)
   range(j,1)=linear(x,1);
   x=x+1;
   j=j+1;
end

range=range;
plot(range);

w=1;
while (w==1)
   question=questdlg('Is this the correct span you wish to analyze?', 'Checking Span', 'Yes', 'No',
'defbtn');
   switch question
      case 'Yes'
         w=0;
      case 'No'
         clear 'question';
         clear 'range';
         clear 'begin';
         clear 'finish';

         statment=questdlg('Please select again', 'Selecting Span', 'Okay', 'defbtn');
         clear 'statment';
```

```
            plot(linear(:,1));
            [x]=ginput(2);
            begin=x(1,1);
            finish=x(2,1);
            begin=sprintf('%.0f',begin);
            finish=sprintf('%.0f',finish);
            begin=str2double(begin);
            finish=str2double(finish);

            x=begin;
            j=1;
            while (x<=finish)
               range(j,1)=angular(x,1);
               x=x+1;
               j=j+1;
            end
           range=range;
           plot(range);
        end
end

clear 'j';
clear 'question';
clear 'x';
clear 'w';

pks=findpeaks(range);
ave=2*mean(range);

x=1;
j=1;
while (x<=length(pks))
   if(pks(x)>ave)
      value(j,1)=pks(x);
      loc(j,1)=find(range==pks(x));
      j=j+1;
   end
   x=x+1;
end

clear 'x';
clear 'j';
clear 'pks';
clear 'finish';
clear 'e';
clear 'ave';
```

```
clear 'find';

plot(range);
title('Determine the Peaks');
hold on;
scatter(loc,value,'g*');
hold off;

f=length(value);
f=num2str(f);
phrase= 'You currently have';
pharse= ', is this correct?';

str={phrase,f,pharse};
str=strjoin(str);

question=questdlg(str, 'Number of Points', 'Yes', 'No', 'defbtn');

clear 'str';
clear 'f';
clear 'phrase';
clear 'pharse';

switch question
   case 'Yes'
      s=0;
   case 'No'
      s=1;
end

clear 'question';

while (s==1)
   list={'Add Points', 'Remove Points', 'Change Limiting Value', 'Removal of Specific Point',
'Current Count'};
   prompt='Please select an option from the list below in order to correct the data';
   choice=listdlg('ListSize', [250
250],'PromptString',prompt,'SelectionMode','single','Name','Data Point
Selection','ListString',list);

   clear 'prompt';
   clear 'list';

   switch choice
      case 1
```

```
question=questdlg('Please hold the "Shift" key and select the points you wish to add, then right click and select "Export Cursor Data". The variable name should be "cursor_info". Press "ENTER" when you finished.','Add Points','Okay','Go Back','defbtn');
switch question
   case 'Okay'
      clear 'question';
      plot(range);
      title('Current Selection');
      hold on
      scatter(loc,value,'g*');
      hold off;
      datacursormode('on');

      p=1;
      while(p==1)
      waitforbuttonpress;
      key=get(gcf,'CurrentKey');
         if strcmp(key,'return')
            w=struct2table(cursor_info);
            p=0;
         end
      end
      clear 'p';
      clear 'key';

      p=w(:,2);
      p=table2array(p);
      clear 'w';

      w=1;
      while(w<=length(p(:,1)))
         d=1;
         if(p(d,1)>=loc(end))
            loc=[loc; p(d,1)];
            value=[value; p(d,2)];
            d=length(loc)+1;
         end
         while(d<=length(loc))
            if(loc(d)>p(w,1))
               sub_begin=loc(1:d-1);
               sub_end=loc(d:end);
               sub_begin_2=value(1:d-1);
               sub_end_2=value(d:end);
               g=p(w,1);
               k=p(w,2);
               clear 'loc';
```

```
            clear 'value';
            loc=[sub_begin; g; sub_end];
            value=[sub_begin_2; k; sub_end_2];
            d=length(loc);
        end
    d=d+1;
    end
    w=w+1;
end

plot(range);
title('Determine the Peaks');
hold on;
scatter(loc,value,'g*');
hold off;

f=length(value);
f=num2str(f);
phrase= 'You currently have';
pharse= ', is this correct? Or do you wish to continue to edit?';

str={phrase,f,pharse};
str=strjoin(str);

question=questdlg(str, 'Number of Points', 'Continue', 'Finished', 'defbtn');

clear 'str';
clear 'f';
clear 'phrase';
clear 'pharse';

switch question
    case 'Finished'
        s=0;
end
clear 'question';
clear 'p';
clear 'sub_begin';
clear 'sub_begin_2';
clear 'sub_end';
clear 'sub_end_2';
clear 'w';
clear 'd';
clear 'g';
clear 'h';
clear 'k';
```

```
            clear 'choice';
            clear 'j';
        end
    case 2
        question=questdlg('Please hold the "Shift" key and select the points you wish to delete, then right click and select "Export Cursor Data". The variable name should be "cursor_info". Press "ENTER" when you finished.','Delete Points','Okay','Go Back','defbtn');
        switch question
            case 'Okay'
            clear 'question';
            plot(range);
            title('Current Selection');
            hold on
            scatter(loc,value,'g*');
            hold off;
            datacursormode('on');

            p=1;
            while(p==1)
            waitforbuttonpress;
            key=get(gcf,'CurrentKey');
                if strcmp(key,'return')
                    w=struct2table(cursor_info);
                    p=0;
                end
            end
            clear 'p';
            clear 'key';

            p=w(:,2);
            p=table2array(p);
            clear 'w';

            w=1;
            while(w<=length(p(:,1)))
                d=1;
                while(d<=length(loc))
                    if(loc(d)==p(w,1))
                        loc(d)=[];
                        value(d)=[];
                        d=length(loc);
                    end
                d=d+1;

                end
                w=w+1;
```

```
            if(w==length(p(:,1)))
                break;
            end
        end

        plot(range);
        title('Determine the Peaks');
        hold on;
        scatter(loc,value,'g*');
        hold off;

        f=length(value);
        f=num2str(f);
        phrase= 'You currently have';
        pharse= ', is this correct? Or do you wish to continue to edit?';

        str={phrase,f,pharse};
        str=strjoin(str);

        question=questdlg(str, 'Number of Points', 'Continue', 'Finished', 'defbtn');

        clear 'str';
        clear 'f';
        clear 'phrase';
        clear 'pharse';

        switch question
            case 'Finished'
                s=0;
        end
        clear 'question';
        clear 'p';
        clear 'sub_begin';
        clear 'sub_begin_2';
        clear 'sub_end';
        clear 'sub_end_2';
        clear 'w';
        clear 'd';
        clear 'g';
        clear 'h';
        clear 'k';
        clear 'choice';
        clear 'j';
    end
case 3
  prompt = {'Please enter the new limiting value'};
```

```
title = 'Limiting Value';
definput = {'2'};
opts.Interpreter = 'tex';
limiter = inputdlg(prompt,title,[1 50],definput,opts);
limiter=str2double(limiter);

clear 'prompt';
clear 'title';
clear 'definput';
clear 'opts';
clear 'loc';
clear 'value';

x=1;
j=1;
ave=limiter*mean(range);
pks=findpeaks(range);
while (x<=length(pks))
   if(pks(x)>ave)
      value(j,1)=pks(x);
      loc(j,1)=find(range==pks(x));
      j=j+1;
   end
   x=x+1;
end

plot(range);
title('Determine the Peaks');
hold on;
scatter(loc,value,'g*');
hold off;

f=length(value);
f=num2str(f);
phrase= 'You currently have';
pharse= ', is this correct? Or do you wish to continue to edit?';

str={phrase,f,pharse};
str=strjoin(str);

question=questdlg(str, 'Number of Points', 'Continue', 'Finished', 'defbtn');

clear 'str';
clear 'f';
clear 'phrase';
clear 'pharse';
```

```
        switch question
          case 'Finished'
             s=0;
        end
        clear 'question';
       case 4
        a=1;
        e=1;
        while (a==1)
          prompt = {'Please enter the number of which point you wish to remove'};
          title = 'Specific Point';
          definput = {'1'};
          opts.Interpreter = 'tex';
          point = inputdlg(prompt,title,[1 50],definput,opts);
          point=str2double(point);

          if(point<=length(loc(:,1)))
             a=0;
          else
             question=questdlg('The point you have selected does not exist, please choose again',
'Invalid Point', 'Okay', 'Cancel', 'defbtn');
             switch question
                case 'Cancel'
                   a=0;
                   e=0;
             end
          end
        end

        clear 'prompt';
        clear 'title';
        clear 'definput';
        clear 'opts';

        if (e==1)
          loc(point)=[];
          value(point)=[];
        end

        f=length(value);
        f=num2str(f);
        phrase= 'You currently have';
        pharse= ', is this correct? Or do you wish to continue to edit?';

        str={phrase,f,pharse};
```

```
        str=strjoin(str);

        question=questdlg(str, 'Number of Points', 'Continue', 'Finished', 'defbtn');

        clear 'str';
        clear 'f';
        clear 'phrase';
        clear 'pharse';

        switch question
           case 'Finished'
              s=0;
        end
       case 5
        f=length(value);
        f=num2str(f);
        phrase= 'You currently have';
        pharse= ', is this correct? Or do you wish to continue to edit?';

        str={phrase,f,pharse};
        str=strjoin(str);

        question=questdlg(str, 'Number of Points', 'Continue', 'Finished', 'defbtn');

        clear 'str';
        clear 'f';
        clear 'phrase';
        clear 'pharse';

        switch question
           case 'Finished'
              s=0;
        end
        clear 'question';
    end
end

clear 's';
clear 'cursor_info';

x=1;
j=1;
while (x<=length(loc))
    before_peak=(loc(x,1)-49)+begin;
    after_peak=(loc(x,1)+50)+begin;
```

```
   while(before_peak<=after_peak)
      m=1;
      while(m<4)
         linear_acceleration(j,m)=linear(before_peak,m);
         angular_velocity(j,m)=angular(before_peak,m);
         m=m+1;
      end
      j=j+1;
      before_peak=before_peak+1;
   end
   x=x+1;
end

clear 'begin';
clear 'after_peak';
clear 'before_peak';
clear 'm';

d=1;
k=100;
j=1;
x=1;
while(x<=length(loc))
  sub(:,1)=1:100;
  sub(:,2)=angular_velocity(d:k,1);
  sub(:,3)=angular_velocity(d:k,2);
  sub(:,4)=angular_velocity(d:k,3);
  m=1;
  first=1;
  second=2;
  fourth=4;
  fifth=5;
  l=1;

  while(l<=length(sub))
     if(sub(l,1)==1||sub(l,1)==2)
        while(m<4)
           angular_acceleration(j,m)=0;
           m=m+1;
        end
        j=j+1;
        m=1;
     end
     if(sub(l,1)>=3 && sub(l,1)<=98)
       while(m<4)
          step_one=(sub(first,m+1)-(8*sub(second,m+1))+(8*sub(fourth,m+1))-(sub(fifth,m+1)));
```

```
            step_two=(step_one)/(12*(1/256));
            angular_acceleration(j,m)=(step_two);
            m=m+1;
          end
          j=j+1;
          first=first+1;
          second=second+1;
          fourth=fourth+1;
          fifth=fifth+1;
          m=1;
        end
        if(sub(l,1)==99||sub(l,1)==100)
           while(m<4)
              angular_acceleration(j,m)=0;
              m=m+1;
           end
           j=j+1;
           m=1;
        end
        l=l+1;
    end
    x=x+1;
    d=d+100;
    k=k+100;
end

clear 'angular';
clear 'fifth';
clear 'first';
clear 'fourth';
clear 'l';
clear 'linear';
clear 'loc';
clear 'm';
clear 'range';
clear 'second';
clear 'step_one';
clear 'step_two';
clear 'sub';
clear 'value';
clear 'x';

d=1;
k=100;
j=1;
s=0;
```

```
while(k<=length(linear_acceleration))
   sub(:,1)=linear_acceleration(d:k,1);
   sub(:,2)=linear_acceleration(d:k,2);
   sub(:,3)=linear_acceleration(d:k,3);
   sub(:,4)=angular_velocity(d:k,1);
   sub(:,5)=angular_velocity(d:k,2);
   sub(:,6)=angular_velocity(d:k,3);
   sub(:,7)=angular_acceleration(d:k,1);
   sub(:,8)=angular_acceleration(d:k,2);
   sub(:,9)=angular_acceleration(d:k,3);

   l_1=max(sub(:,1));
   o_1=find(sub(:,1)==l_1);
      loc_max(j,1)=o_1+(100*s);
   l_2=max(sub(:,2));
   o_2=find(sub(:,2)==l_2);
      loc_max(j,2)=o_2+(100*s);
   l_3=max(sub(:,3));
   o_3=find(sub(:,3)==l_3);
      loc_max(j,3)=o_3+(100*s);

      max_linear_acceleration(j,1)=l_1;
      max_linear_acceleration(j,2)=l_2;
      max_linear_acceleration(j,3)=l_3;

   v_1=max(sub(:,4));
   o_4=find(sub(:,4)==v_1);
      loc_max(j,4)=o_4+(100*s);
   v_2=max(sub(:,5));
   o_5=find(sub(:,5)==v_2);
      loc_max(j,5)=o_5+(100*s);
   v_3=max(sub(:,6));
   o_6=find(sub(:,6)==v_3);
      loc_max(j,6)=o_6(1,1)+(100*s);

      max_angular_velocity(j,1)=v_1;
      max_angular_velocity(j,2)=v_2;
      max_angular_velocity(j,3)=v_3;

   a_1=max(sub(:,7));
   o_7=find(sub(:,7)==a_1);
      loc_max(j,7)=o_7+(100*s);
   a_2=max(sub(:,8));
   o_8=find(sub(:,8)==a_2);
      loc_max(j,8)=o_8+(100*s);
```

```
a_3=max(sub(:,9));
o_9=find(sub(:,9)==a_3);
   loc_max(j,9)=o_9+(100*s);

   max_angular_acceleration(j,1)=a_1;
   max_angular_acceleration(j,2)=a_2;
   max_angular_acceleration(j,3)=a_3;

l_1=min(sub(:,1));
o_1=find(sub(:,1)==l_1);
   loc_min(j,1)=o_1+(100*s);
l_2=min(sub(:,2));
o_2=find(sub(:,2)==l_2);
   loc_min(j,2)=o_2+(100*s);
l_3=min(sub(:,3));
o_3=find(sub(:,3)==l_3);
   loc_min(j,3)=o_3+(100*s);

   min_linear_acceleration(j,1)=l_1;
   min_linear_acceleration(j,2)=l_2;
   min_linear_acceleration(j,3)=l_3;

v_1=min(sub(:,4));
o_4=find(sub(:,4)==v_1);
   loc_min(j,4)=o_4+(100*s);
v_2=min(sub(:,5));
o_5=find(sub(:,5)==v_2);
   loc_min(j,5)=o_5+(100*s);
v_3=min(sub(:,6));
o_6=find(sub(:,6)==v_3);
   loc_min(j,6)=o_6+(100*s);

   min_angular_velocity(j,1)=v_1;
   min_angular_velocity(j,2)=v_2;
   min_angular_velocity(j,3)=v_3;

a_1=min(sub(:,7));
o_7=find(sub(:,7)==a_1);
   loc_min(j,7)=o_7+(100*s);
a_2=min(sub(:,8));
o_8=find(sub(:,8)==a_2);
   loc_min(j,8)=o_8+(100*s);
a_3=min(sub(:,9));
o_9=find(sub(:,9)==a_3);
   loc_min(j,9)=o_9+(100*s);
```

```
        min_angular_acceleration(j,1)=a_1;
        min_angular_acceleration(j,2)=a_2;
        min_angular_acceleration(j,3)=a_3;

    j=j+1;
    s=s+1;
    k=k+100;
    d=d+100;
end

clear 'd';
clear 'g';
clear 'h';
clear 'j';
clear 'k';
clear 'm';
clear 'o';
clear 'p';
clear 'sub';

figure ('Name','Linear Acceleration');
subplot(3,1,1)
plot(linear_acceleration(:,1),'c');
ylabel('m/s');
title('X-Direction');
hold on
scatter(loc_max(:,1),max_linear_acceleration(:,1),'g*');
scatter(loc_min(:,1),min_linear_acceleration(:,1),'r*');
hold off;
subplot(3,1,2)
subplot(3,1,2)
plot(linear_acceleration(:,2),'b');
ylabel('m/s');
title('Y-Direction');
hold on
scatter(loc_max(:,2),max_linear_acceleration(:,2),'g*');
scatter(loc_min(:,2),min_linear_acceleration(:,2),'r*');
hold off;
subplot(3,1,3)
plot(linear_acceleration(:,3),'m')
ylabel('m/s');
title('Z-Direction');
hold on
scatter(loc_max(:,3),max_linear_acceleration(:,3),'g*');
scatter(loc_min(:,3),min_linear_acceleration(:,3),'r*');
hold off;
```

```
figure('Name','Angular Velocity');
subplot(3,1,1);
plot(angular_velocity(:,1),'c');
ylabel('rad/s');
title('X-Direction');
hold on
scatter(loc_max(:,4),max_angular_velocity(:,1),'g*');
scatter(loc_min(:,4),min_angular_velocity(:,1),'r*');
hold off;
subplot(3,1,2)
plot(angular_velocity(:,2),'b');
ylabel('rad/s');
title('Y-Direction');
hold on
scatter(loc_max(:,5),max_angular_velocity(:,2),'g*');
scatter(loc_min(:,5),min_angular_velocity(:,2),'r*');
hold off;
subplot(3,1,3)
plot(angular_velocity(:,3),'m');
ylabel('rad/s');
title('Z-Direction');
hold on
scatter(loc_max(:,6),max_angular_velocity(:,3),'g*');
scatter(loc_min(:,6),min_angular_velocity(:,3),'r*');
hold off;

figure('Name','Angular Acceleration');
subplot(3,1,1)
plot(angular_acceleration(:,1),'c');
ylabel('rad/s^2')
title('X-Direction');
hold on
scatter(loc_max(:,7),max_angular_acceleration(:,1),'g*');
scatter(loc_min(:,7),min_angular_acceleration(:,1),'r*');
hold off;
subplot(3,1,2)
plot(angular_acceleration(:,2),'b');
ylabel('rad/s^2');
title('Y-Direction');
hold on
scatter(loc_max(:,8),max_angular_acceleration(:,2),'g*');
scatter(loc_min(:,8),min_angular_acceleration(:,2),'r*');
hold off;
subplot(3,1,3)
plot(angular_acceleration(:,3),'m');
```

```
ylabel('rad/s^2');
title('Z-Direction');
hold on
scatter(loc_max(:,9),max_angular_acceleration(:,3),'g*');
scatter(loc_min(:,9),min_angular_acceleration(:,3),'*r');
hold off;

clear 'loc_max';
clear 'loc_min';
clear 's';

question=questdlg('Are you creating a new excel file for this data or are you adding to an already
existing file?', 'File Writing', 'New','Adding to an existing file','defbtn');
switch question
   case 'New'
      s=0;
   case 'Adding to an existing file'
      s=1;
end

if(s==0)
   prompt={'Please enter the name of the file you wish to create'};
   title='Creating the File';
   definput={'Left_Leg_01-01-00'};
   opts.Interpreter='tex';
   answer=inputdlg(prompt,title,[1 50],definput,opts);
   name=char(answer);

   clear 'prompt';
   clear 'title';
   clear 'definput';
   clear 'answer';

   d='.xlsx';

   filename={name,d};
   filename=strjoin(filename);
   filename=filename(~isspace(filename));

   clear 'name';
   clear 'question';
   clear 'd';
   switch b
      case 'Upper'
         all_linear=array2table(linear_acceleration,'VariableNames',{'X','Y','Z'});
         writetable(all_linear,filename,'Sheet',1,'Range','M3');
```

```
a= 'Linear Acceleration';
c=cellstr(a);
t=cell2table(c,'VariableNames',{'Upper'});
writetable(t,filename,'Sheet',1,'Range','M1')
clear 'a';
clear 'c';
clear 't';
all_velocity=array2table(angular_velocity,'VariableNames',{'wX','wY','wZ'});
writetable(all_velocity,filename,'Sheet',1,'Range','Q3');
a= 'Angular Velocity';
c=cellstr(a);
t=cell2table(c,'VariableNames',{'Upper'});
writetable(t,filename,'Sheet',1,'Range','Q1')
clear 'a';
clear 'c';
clear 't';
all_acceleration=array2table(angular_acceleration,'VariableNames',{'aX','aY','aZ'});
writetable(all_acceleration,filename,'Sheet',1,'Range','U3');
a= 'Angular Acceleration';
c=cellstr(a);
t=cell2table(c,'VariableNames',{'Upper'});
writetable(t,filename,'Sheet',1,'Range','U1')
clear 'a';
clear 'c';
clear 't';

max_linear=array2table(max_linear_acceleration,'VariableNames',{'X','Y','Z'});
writetable(max_linear,filename,'Sheet',2,'Range','AA3');
a= 'Max Linear Acceleration';
c=cellstr(a);
t=cell2table(c,'VariableNames',{'Upper'});
writetable(t,filename,'Sheet',2,'Range','AA1')
clear 'a';
clear 'c';
clear 't';
max_velocity=array2table(max_angular_velocity,'VariableName',{'wX','wY','wZ'});
writetable(max_velocity,filename,'Sheet',2,'Range','AE3');
a= 'Max Angular Velocity';
c=cellstr(a);
t=cell2table(c,'VariableNames',{'Upper'});
writetable(t,filename,'Sheet',2,'Range','AE1')
clear 'a';
clear 'c';
clear 't';

max_acceleration=array2table(max_angular_acceleration,'VariableName',{'aX','aY','aZ'});
```

```
        writetable(max_acceleration,filename,'Sheet',2,'Range','AI3');
        a= 'Max Angular Acceleration';
        c=cellstr(a);
        t=cell2table(c,'VariableNames',{'Upper'});
        writetable(t,filename,'Sheet',2,'Range','AI1')
        clear 'a';
        clear 'c';
        clear 't';

        min_linear=array2table(min_linear_acceleration,'VariableNames',{'X','Y','Z'});
        writetable(min_linear,filename,'Sheet',2,'Range','AM3');
        a= 'Min Linear Acceleration';
        c=cellstr(a);
        t=cell2table(c,'VariableNames',{'Upper'});
        writetable(t,filename,'Sheet',2,'Range','AM1')
        clear 'a';
        clear 'c';
        clear 't';
        min_velocity=array2table(min_angular_velocity,'VariableNames',{'wX','wY','wZ'});
        writetable(min_velocity,filename,'Sheet',2,'Range','AQ3');
        a= 'Min Angular Velocity';
        c=cellstr(a);
        t=cell2table(c,'VariableNames',{'Upper'});
        writetable(t,filename,'Sheet',2,'Range','AQ1')
        clear 'a';
        clear 'c';
        clear 't';

min_acceleration=array2table(min_angular_acceleration,'VariableNames',{'aX','aY','aZ'});
        writetable(min_acceleration,filename,'Sheet',2,'Range','AU3');
        a= 'Min Angular Acceleration';
        c=cellstr(a);
        t=cell2table(c,'VariableNames',{'Upper'});
        writetable(t,filename,'Sheet',2,'Range','AU1')
        clear 'a';
        clear 'c';
        clear 't';
        type filename
    case 'Lower'
        all_linear=array2table(linear_acceleration,'VariableNames',{'X','Y','Z'});
        writetable(all_linear,filename,'Sheet',1,'Range','A3');
        a= 'Linear Acceleration';
        c=cellstr(a);
        t=cell2table(c,'VariableNames',{'Lower'});
        writetable(t,filename,'Sheet',1,'Range','A1')
        clear 'a';
```

```
clear 'c';
clear 't';
all_velocity=array2table(angular_velocity,'VariableNames',{'wX','wY','wZ'});
writetable(all_velocity,filename,'Sheet',1,'Range','E3');
a= 'Angular Velocity';
c=cellstr(a);
t=cell2table(c,'VariableNames',{'Lower'});
writetable(t,filename,'Sheet',1,'Range','E1')
clear 'a';
clear 'c';
clear 't';
all_acceleration=array2table(angular_acceleration,'VariableNames',{'aX','aY','aZ'});
writetable(all_acceleration,filename,'Sheet',1,'Range','I3');
a= 'Angular Acceleration';
c=cellstr(a);
t=cell2table(c,'VariableNames',{'Lower'});
writetable(t,filename,'Sheet',1,'Range','I1')
clear 'a';
clear 'c';
clear 't';

max_linear=array2table(max_linear_acceleration,'VariableNames',{'X','Y','Z'});
writetable(max_linear,filename,'Sheet',2,'Range','C3');
a= 'Max Linear Acceleration';
c=cellstr(a);
t=cell2table(c,'VariableNames',{'Lower'});
writetable(t,filename,'Sheet',2,'Range','C1')
clear 'a';
clear 'c';
clear 't';
max_velocity=array2table(max_angular_velocity,'VariableName',{'wX','wY','wZ'});
writetable(max_velocity,filename,'Sheet',2,'Range','G3');
a= 'Max Angular Velocity';
c=cellstr(a);
t=cell2table(c,'VariableNames',{'Lower'});
writetable(t,filename,'Sheet',2,'Range','G1')
clear 'a';
clear 'c';
clear 't';

max_acceleration=array2table(max_angular_acceleration,'VariableName',{'aX','aY','aZ'});
writetable(max_acceleration,filename,'Sheet',2,'Range','K3');
a= 'Max Angular Acceleration';
c=cellstr(a);
t=cell2table(c,'VariableNames',{'Lower'});
writetable(t,filename,'Sheet',2,'Range','K1')
```

```
        clear 'a';
        clear 'c';
        clear 't';

        min_linear=array2table(min_linear_acceleration,'VariableNames',{'X','Y','Z'});
        writetable(min_linear,filename,'Sheet',2,'Range','O3');
        a= 'Min Linear Acceleration';
        c=cellstr(a);
        t=cell2table(c,'VariableNames',{'Lower'});
        writetable(t,filename,'Sheet',2,'Range','O1')
        clear 'a';
        clear 'c';
        clear 't';
        min_velocity=array2table(min_angular_velocity,'VariableNames',{'wX','wY','wZ'});
        writetable(min_velocity,filename,'Sheet',2,'Range','S3');
        a= 'Min Angular Velocity';
        c=cellstr(a);
        t=cell2table(c,'VariableNames',{'Lower'});
        writetable(t,filename,'Sheet',2,'Range','S1')
        clear 'a';
        clear 'c';
        clear 't';

min_acceleration=array2table(min_angular_acceleration,'VariableNames',{'aX','aY','aZ'});
        writetable(min_acceleration,filename,'Sheet',2,'Range','W3');
        a= 'Min Angular Acceleration';
        c=cellstr(a);
        t=cell2table(c,'VariableNames',{'Lower'});
        writetable(t,filename,'Sheet',2,'Range','W1')
        clear 'a';
        clear 'c';
        clear 't';
        type filename
   end
   selpath=uigetdir;
   copyfile(filename,'time_remnant.xlsx');
   movefile(filename,selpath);
end

if (s==1)
   check=isfile('time_remnant.xlsx');
   switch check
      case 1
         name='time_remnant.xlsx';
         prompt = {'Enter the name of the Excel file'};
         title = 'File Name';
```

```
        definput = {'Left_Leg_01-01-00'};
        opts.Interpreter = 'tex';
        answer = inputdlg(prompt,title,[1 50],definput,opts);
        sub_name=char(answer);
        d='.xlsx';

        true_name={sub_name,d};
        true_name=strjoin(true_name);
        true_name=true_name(~isspace(true_name));
    case 0
        question=questdlg('The file you wish to pull does not currently have a time remnant in
the folder. In order to continue, please move the file you wish to add data to, into the folder.
Once done, press "Enter". Afterwhich, you will prompted to enter the name of the file','Add
File','Okay','defbtn');
        p=1;
        while(p==1)
            waitforbuttonpress;
            key=get(gcf,'CurrentKey');
                if strcmp(key,'return')
                    p=0;
                end
        end
        clear 'p';
        clear 'key';
        prompt = {'Enter the name of the Excel file'};
        title = 'File Name';
        definput = {'Left_Leg_01-01-00'};
        opts.Interpreter = 'tex';
        answer = inputdlg(prompt,title,[1 50],definput,opts);
        sub_name=char(answer);
        d='.xlsx';

        name={sub_name,d};
        name=strjoin(name);
        name=name(~isspace(name));
end
switch b
    case 'Upper'
        sheet=1;
        xlRange='A4:C10004';
        all_linear_sub=xlsread(name,sheet,xlRange);
        all_linear_current=array2table(all_linear_sub,'VariableNames',{'X','Y','Z'});
        clear 'xlRange';
        xlRange='E4:G10004';
        all_velocity_sub=xlsread(name,sheet,xlRange);
        all_velocity_current=array2table(all_velocity_sub,'VariableNames',{'wX','wY','Wz'});
```

```
clear 'xlRange';
xlRange='I4:K10004';
all_acceleration_sub=xlsread(name,sheet,xlRange);

all_acceleration_current=array2table(all_acceleration_sub,'VariableNames',{'aX','aY','aZ'});
clear 'xlRange';
clear 'sheet';

sheet=2;
xlRange='C4:E104';
max_linear_sub=xlsread(name,sheet,xlRange);
max_linear_current=array2table(max_linear_sub,'VariableNames',{'X','Y','Z'});
clear 'xlRange';
xlRange='G4:I104';
max_velocity_sub=xlsread(name,sheet,xlRange);
max_velocity_current=array2table(max_velocity_sub,'VariableNames',{'wX','wY','wZ'});
clear 'xlRange';
xlRange='K4:M104';
max_acceleration_sub=xlsread(name,sheet,xlRange);

max_acceleration_current=array2table(max_acceleration_sub,'VariableNames',{'aX','aY','aZ'});
clear 'xlRange';
xlRange='O4:Q104';
min_linear_sub=xlsread(name,sheet,xlRange);
min_linear_current=array2table(min_linear_sub,'VariableNames',{'X','Y','Z'});
clear 'xlRange';
xlRange='S4:U104';
min_velocity_sub=xlsread(name,sheet,xlRange);
min_velocity_current=array2table(min_velocity_sub,'VariableNames',{'X','Y','Z'});
clear 'xlRange';
xlRange='W4:Y104';
min_acceleration_sub=xlsread(name,sheet,xlRange);

min_acceleration_current=array2table(min_acceleration_sub,'VariableNames',{'X','Y','Z'});
clear 'xlRange'
clear 'sheet';

writetable(all_linear_current,name,'Sheet',1,'Range','A3');
a= 'Linear Acceleration';
c=cellstr(a);
t=cell2table(c,'VariableNames',{'Lower'});
writetable(t,name,'Sheet',1,'Range','A1')
clear 'a';
clear 'c';
clear 't';
all_linear=array2table(linear_acceleration,'VariableNames',{'X','Y','Z'});
```

```
writetable(all_linear,name,'Sheet',1,'Range','M3');
a= 'Linear Acceleration';
c=cellstr(a);
t=cell2table(c,'VariableNames',{'Upper'});
writetable(t,name,'Sheet',1,'Range','M1')
clear 'a';
clear 'c';
clear 't';

writetable(all_velocity_current,name,'Sheet',1,'Range','E3');
a= 'Angular Velocity';
c=cellstr(a);
t=cell2table(c,'VariableNames',{'Lower'});
writetable(t,name,'Sheet',1,'Range','E1')
clear 'a';
clear 'c';
clear 't';
all_velocity=array2table(angular_velocity,'VariableNames',{'wX','wY','wZ'});
writetable(all_velocity,name,'Sheet',1,'Range','Q3');
a= 'Angular Velocity';
c=cellstr(a);
t=cell2table(c,'VariableNames',{'Upper'});
writetable(t,name,'Sheet',1,'Range','Q1')
clear 'a';
clear 'c';
clear 't';

writetable(all_acceleration_current,name,'Sheet',1,'Range','I3');
a= 'Angular Acceleration';
c=cellstr(a);
t=cell2table(c,'VariableNames',{'Lower'});
writetable(t,name,'Sheet',1,'Range','I1')
clear 'a';
clear 'c';
clear 't';
all_acceleration=array2table(angular_acceleration,'VariableNames',{'aX','aY','aZ'});
writetable(all_acceleration,name,'Sheet',1,'Range','U3');
a= 'Angular Acceleration';
c=cellstr(a);
t=cell2table(c,'VariableNames',{'Upper'});
writetable(t,name,'Sheet',1,'Range','U1')
clear 'a';
clear 'c';
clear 't';

writetable(max_linear_current,name,'Sheet',2,'Range','C3');
```

```
a= 'Max Linear Acceleration';
c=cellstr(a);
t=cell2table(c,'VariableNames',{'Lower'});
writetable(t,name,'Sheet',2,'Range','C1')
clear 'a';
clear 'c';
clear 't';
max_linear=array2table(max_linear_acceleration,'VariableNames',{'X','Y','Z'});
writetable(max_linear,name,'Sheet',2,'Range','AA3');
a= 'Max Linear Acceleration';
c=cellstr(a);
t=cell2table(c,'VariableNames',{'Upper'});
writetable(t,name,'Sheet',2,'Range','AA1')
clear 'a';
clear 'c';
clear 't';

writetable(max_velocity_current,name,'Sheet',2,'Range','G3');
a= 'Max Angular Velocity';
c=cellstr(a);
t=cell2table(c,'VariableNames',{'Lower'});
writetable(t,name,'Sheet',2,'Range','G1')
clear 'a';
clear 'c';
clear 't';
max_velocity=array2table(max_angular_velocity,'VariableName',{'wX','wY','wZ'});
writetable(max_velocity,name,'Sheet',2,'Range','AE3');
a= 'Max Angular Velocity';
c=cellstr(a);
t=cell2table(c,'VariableNames',{'Upper'});
writetable(t,name,'Sheet',2,'Range','AE1')
clear 'a';
clear 'c';
clear 't';

writetable(max_acceleration_current,name,'Sheet',2,'Range','K3');
a= 'Max Angular Acceleration';
c=cellstr(a);
t=cell2table(c,'VariableNames',{'Lower'});
writetable(t,name,'Sheet',2,'Range','K1')
clear 'a';
clear 'c';
clear 't';

max_acceleration=array2table(max_angular_acceleration,'VariableName',{'aX','aY','aZ'});
writetable(max_acceleration,name,'Sheet',2,'Range','AI3');
```

```
a= 'Max Angular Acceleration';
c=cellstr(a);
t=cell2table(c,'VariableNames',{'Upper'});
writetable(t,name,'Sheet',2,'Range','AI1')
clear 'a';
clear 'c';
clear 't';

writetable(min_linear_current,name,'Sheet',2,'Range','O3');
a= 'Min Linear Acceleration';
c=cellstr(a);
t=cell2table(c,'VariableNames',{'Lower'});
writetable(t,name,'Sheet',2,'Range','O1')
clear 'a';
clear 'c';
clear 't';
min_linear=array2table(min_linear_acceleration,'VariableNames',{'X','Y','Z'});
writetable(min_linear,name,'Sheet',2,'Range','AM3');
a= 'Min Linear Acceleration';
c=cellstr(a);
t=cell2table(c,'VariableNames',{'Upper'});
writetable(t,name,'Sheet',2,'Range','AM1')
clear 'a';
clear 'c';
clear 't';

writetable(min_velocity_current,name,'Sheet',2,'Range','S3');
a= 'Min Angular Velocity';
c=cellstr(a);
t=cell2table(c,'VariableNames',{'Lower'});
writetable(t,name,'Sheet',2,'Range','S1')
clear 'a';
clear 'c';
clear 't';
min_velocity=array2table(min_angular_velocity,'VariableNames',{'wX','wY','wZ'});
writetable(min_velocity,name,'Sheet',2,'Range','AQ3');
a= 'Min Angular Velocity';
c=cellstr(a);
t=cell2table(c,'VariableNames',{'Upper'});
writetable(t,name,'Sheet',2,'Range','AQ1')
clear 'a';
clear 'c';
clear 't';

writetable(min_acceleration_current,name,'Sheet',2,'Range','W3');
a= 'Min Angular Acceleration';
```

```
        c=cellstr(a);
        t=cell2table(c,'VariableNames',{'Lower'});
        writetable(t,name,'Sheet',2,'Range','W1')
        clear 'a';
        clear 'c';
        clear 't';

min_acceleration=array2table(min_angular_acceleration,'VariableNames',{'aX','aY','aZ'});
        writetable(min_acceleration,name,'Sheet',2,'Range','AU3');
        a= 'Min Angular Acceleration';
        c=cellstr(a);
        t=cell2table(c,'VariableNames',{'Upper'});
        writetable(t,name,'Sheet',2,'Range','AU1')
        clear 'a';
        clear 'c';
        clear 't';
        type name
      case 'Lower'
        sheet=1;
        xlRange='M4:O10004';
        all_linear_sub=xlsread(name,sheet,xlRange);
        all_linear_current=array2table(all_linear_sub,'VariableNames',{'X','Y','Z'});
        clear 'xlRange';
        xlRange='Q4:S10004';
        all_velocity_sub=xlsread(name,sheet,xlRange);
        all_velocity_current=array2table(all_velocity_sub,'VariableNames',{'wX','wY','Wz'});
        clear 'xlRange';
        xlRange='U4:W10004';
        all_acceleration_sub=xlsread(name,sheet,xlRange);

all_acceleration_current=array2table(all_acceleration_sub,'VariableNames',{'aX','aY','aZ'});
        clear 'xlRange';
        clear 'sheet';

        sheet=2;
        xlRange='AA4:AC104';
        max_linear_sub=xlsread(name,sheet,xlRange);
        max_linear_current=array2table(max_linear_sub,'VariableNames',{'X','Y','Z'});
        clear 'xlRange';
        xlRange='AE4:AG104';
        max_velocity_sub=xlsread(name,sheet,xlRange);
        max_velocity_current=array2table(max_velocity_sub,'VariableNames',{'wX','wY','wZ'});
        clear 'xlRange';
        xlRange='AI4:AK104';
        max_acceleration_sub=xlsread(name,sheet,xlRange);
```

```
max_acceleration_current=array2table(max_acceleration_sub,'VariableNames',{'aX','aY','aZ'});
        clear 'xlRange';
        xlRange='AM4:AO104';
        min_linear_sub=xlsread(name,sheet,xlRange);
        min_linear_current=array2table(min_linear_sub,'VariableNames',{'X','Y','Z'});
        clear 'xlRange';
        xlRange='AQ4:AS104';
        min_velocity_sub=xlsread(name,sheet,xlRange);
        min_velocity_current=array2table(min_velocity_sub,'VariableNames',{'wX','wY','wZ'});
        clear 'xlRange';
        xlRange='AU4:AW104';
        min_acceleration_sub=xlsread(name,sheet,xlRange);

min_acceleration_current=array2table(min_accleration_sub,'VariableNames',{'aX','aY','aZ'});
        clear 'xlRange'
        clear 'sheet';

        writetable(all_linear_current,name,'Sheet',1,'Range','M3');
        a= 'Linear Acceleration';
        c=cellstr(a);
        t=cell2table(c,'VariableNames',{'Upper'});
        writetable(t,name,'Sheet',1,'Range','M1')
        clear 'a';
        clear 'c';
        clear 't';
        all_linear=array2table(linear_acceleration,'VariableNames',{'X','Y','Z'});
        writetable(all_linear,name,'Sheet',1,'Range','A3');
        a= 'Linear Acceleration';
        c=cellstr(a);
        t=cell2table(c,'VariableNames',{'Lower'});
        writetable(t,name,'Sheet',1,'Range','A1')
        clear 'a';
        clear 'c';
        clear 't';

        writetable(all_velocity_current,name,'Sheet',1,'Range','Q3');
        a= 'Linear Acceleration';
        c=cellstr(a);
        t=cell2table(c,'VariableNames',{'Upper'});
        writetable(t,name,'Sheet',1,'Range','Q1')
        clear 'a';
        clear 'c';
        clear 't';
        all_velocity=array2table(angular_velocity,'VariableNames',{'wX','wY','wZ'});
        writetable(all_velocity,name,'Sheet',1,'Range','E3');
```

```
a= 'Angular Velocity';
c=cellstr(a);
t=cell2table(c,'VariableNames',{'Lower'});
writetable(t,name,'Sheet',1,'Range','E1')
clear 'a';
clear 'c';
clear 't';

writetable(all_acceleration_current,name,'Sheet',1,'Range','U3');
a= 'Angualar Acceleration';
c=cellstr(a);
t=cell2table(c,'VariableNames',{'Upper'});
writetable(t,name,'Sheet',1,'Range','U1')
clear 'a';
clear 'c';
clear 't';
all_acceleration=array2table(angular_acceleration,'VariableNames',{'aX','aY','aZ'});
writetable(all_acceleration,name,'Sheet',1,'Range','I3');
a= 'Angular Acceleration';
c=cellstr(a);
t=cell2table(c,'VariableNames',{'Lower'});
writetable(t,name,'Sheet',1,'Range','I1')
clear 'a';
clear 'c';
clear 't';

writetable(max_linear_current,name,'Sheet',2,'Range','AA3');
a= 'Max Linear Acceleration';
c=cellstr(a);
t=cell2table(c,'VariableNames',{'Upper'});
writetable(t,name,'Sheet',2,'Range','AA1')
clear 'a';
clear 'c';
clear 't';
max_linear=array2table(max_linear_acceleration,'VariableNames',{'X','Y','Z'});
writetable(max_linear,name,'Sheet',2,'Range','C3');
a= 'Max Linear Acceleration';
c=cellstr(a);
t=cell2table(c,'VariableNames',{'Lower'});
writetable(t,name,'Sheet',2,'Range','C1')
clear 'a';
clear 'c';
clear 't';

writetable(max_velocity_current,name,'Sheet',2,'Range','AE3');
a= 'Max Angular Velocity';
```

```
c=cellstr(a);
t=cell2table(c,'VariableNames',{'Upper'});
writetable(t,name,'Sheet',2,'Range','AE1')
clear 'a';
clear 'c';
clear 't';
max_velocity=array2table(max_angular_velocity,'VariableName',{'wX','wY','wZ'});
writetable(max_velocity,name,'Sheet',2,'Range','G3');
a= 'Max Angular Velocity';
c=cellstr(a);
t=cell2table(c,'VariableNames',{'Lower'});
writetable(t,name,'Sheet',2,'Range','G1')
clear 'a';
clear 'c';
clear 't';

writetable(max_acceleration_current,name,'Sheet',2,'Range','AI3');
a= 'Max Angular Acceleration';
c=cellstr(a);
t=cell2table(c,'VariableNames',{'Upper'});
writetable(t,name,'Sheet',2,'Range','AI1')
clear 'a';
clear 'c';
clear 't';

max_acceleration=array2table(max_angular_acceleration,'VariableName',{'aX','aY','aZ'});
writetable(max_acceleration,name,'Sheet',2,'Range','K3');
a= 'Max Angular Acceleration';
c=cellstr(a);
t=cell2table(c,'VariableNames',{'Lower'});
writetable(t,name,'Sheet',2,'Range','K1')
clear 'a';
clear 'c';
clear 't';

writetable(min_linear_current,name,'Sheet',2,'Range','AM3');
a= 'Min Linear Acceleration';
c=cellstr(a);
t=cell2table(c,'VariableNames',{'Upper'});
writetable(t,name,'Sheet',2,'Range','AM1')
clear 'a';
clear 'c';
clear 't';
min_linear=array2table(min_linear_acceleration,'VariableNames',{'X','Y','Z'});
writetable(min_linear,name,'Sheet',2,'Range','O3');
a= 'Min Linear Acceleration';
```

```
        c=cellstr(a);
        t=cell2table(c,'VariableNames',{'Lower'});
        writetable(t,name,'Sheet',2,'Range','O1')
        clear 'a';
        clear 'c';
        clear 't';

        writetable(min_velocity_current,name,'Sheet',2,'Range','AQ3');
        a= 'Min Angular Velocity';
        c=cellstr(a);
        t=cell2table(c,'VariableNames',{'Upper'});
        writetable(t,name,'Sheet',2,'Range','AQ1')
        clear 'a';
        clear 'c';
        clear 't';
        min_velocity=array2table(min_angular_velocity,'VariableNames',{'wX','wY','wZ'});
        writetable(min_velocity,name,'Sheet',2,'Range','S3');
        a= 'Min Angular Velocity';
        c=cellstr(a);
        t=cell2table(c,'VariableNames',{'Lower'});
        writetable(t,name,'Sheet',2,'Range','S1')
        clear 'a';
        clear 'c';
        clear 't';

        writetable(min_acceleration_current,name,'Sheet',2,'Range','AU3');
        a= 'Min Angular Acceleration';
        c=cellstr(a);
        t=cell2table(c,'VariableNames',{'Upper'});
        writetable(t,name,'Sheet',2,'Range','AU1')
        clear 'a';
        clear 'c';
        clear 't';

min_acceleration=array2table(min_angular_acceleration,'VariableNames',{'aX','aY','aZ'});
        writetable(min_acceleration,name,'Sheet',2,'Range','W3');
        a= 'Min Angular Acceleration';
        c=cellstr(a);
        t=cell2table(c,'VariableNames',{'Lower'});
        writetable(t,name,'Sheet',2,'Range','W1')
        clear 'a';
        clear 'c';
        clear 't';
        type name
    end
    if (check==1)
```

```
        movefile(name,true_name);
        name=true_name;
    end
    selpath=uigetdir;
    movefile(name,selpath);
end
```

A3: MATLAB Script 3

```
x = [ones(size(LA)) LA AV LA.*AV];
[b,~,r,rint] = regress(Moment,x);
contain0 = (rint(:,1)<0 & rint(:,2)>0);
idx = find(contain0 == false);

x=1;
j=1;
m=1;

while(x<=length(LA))
    if (x ~= idx(m))
        LA_clean(j,:)=LA(x,:);
        AV_clean(j,:)=AV(x,:);
        Moment_clean(j,:)=Moment(x,:);
        j=j+1;
    end
    if (x == idx(m))
        m=m+1;
        if (m > length(idx))
            m=length(idx);
        end
    end
    x=x+1;
end

p = [ones(size(LA_clean)) LA_clean AV_clean LA_clean.*AV_clean];
[l,~,~,~,stats] = regress(Moment_clean,p);



scatter3(LA_clean,AV_clean,Moment_clean,'filled','b')
hold on
scatter3(LA(idx),AV(idx),Moment(idx),'r');

x1fit = min(LA_clean):.1:max(LA_clean);
x2fit = min(AV_clean):.11:max(AV_clean);
[X1FIT,X2FIT] = meshgrid(x1fit,x2fit);
```

```
YFIT = b(1) + b(2)*X1FIT + b(3)*X2FIT + b(4)*X1FIT.*X2FIT;
mesh(X1FIT,X2FIT,YFIT)

title('F(Femoral AV, Tibial AV) = Max Quad Force','FontSize',30);
xlabel('Femoral Angular Velocity','FontSize',25);
ylabel('Tibial Angular Velocity','FontSize',25);
zlabel('Maximum Quadriceps Force','FontSize',25)
```